

Montana Tech Library

Digital Commons @ Montana Tech

Graduate Theses & Non-Theses

Student Scholarship

Spring 2021

PROTEIN EXPRESSION IN MAMMALIAN CELL LINES AFTER LOWLEVEL METAL EXPOSURE

Sydney Jennings

Follow this and additional works at: https://digitalcommons.mtech.edu/grad_rsch

PROTEIN EXPRESSION IN MAMMALIAN CELL LINES AFTER LOW- LEVEL METAL EXPOSURE

by
Sydney Jennings

A thesis submitted in partial fulfillment of the
requirements for the degree of

Interdisciplinary Masters of Science

Montana Tech
2021



Abstract

Mining in Butte, Montana has been ongoing since the mid-19th century. The US Environmental Protection Agency (EPA) added the Butte Area to the National Priority List in 1983, designating it a Superfund site. Butte is currently part of the largest EPA Superfund site in the United States. The EPA lists arsenic (As), cadmium (Cd), lead (Pb), and mercury (Hg) as metal contaminants of concern for residents living in proximity to the Butte Area Superfund site. However, very limited human biomonitoring has been conducted in Butte and studies that have been published focus on Pb and, to a lesser extent, As. No synergistic, antagonistic, or additive studies have been conducted, even though it is widely accepted that the exposure in Butte is a metal mixture scenario, rather than single element exposure. Metals that are trace micronutrients, such as copper (Cu), manganese (Mn), and zinc (Zn) have been largely unrecognized as possibly having negative health effects on residents of Butte, despite the fact the metals have been historically released into the soil, water, and air through active blasting and crushing of ore and are known to be potential neurotoxins. This study aims to gather data on metal distribution in soil and dust samples from a neighborhood near active mining operations, determine the bioavailability of the metals present, extract and quantify proteins and inflammatory markers from meconium samples, and investigate metal mixture interactions in human bronchial epithelial cells (BEAS-2B) and human embryonic kidney cells (HEK-293). A physiological-based extraction test (PBET), inductively coupled plasma mass spectrometry (ICP-MS), and inductively coupled plasma optical emission spectrometry (ICP-OES) were employed to assess metal distribution and bioavailability. To determine a link between metal exposure and possible health effects, inflammatory markers were measured by enzyme-linked immunoassays (ELISA), and metal-specific proteins were quantified by western blot assays. Metal distribution results showed that As, Mn, and Pb levels were highest in the soil samples, whereas levels of the Cd, Cu, and Zn were highest in the dust samples. The bioavailability of the metals was determined to be highest in the stomach phase for the dust samples and highest in the intestinal phase for the soil samples. Furthermore, expression of the mammalian proteins and cytokines of interest was affected differently by exposure to metal mixtures compared to single metal exposures.

Keywords: Butte, Montana, Environmental Protection Agency, Superfund Site, Heavy Metals, Trace Micronutrients, Human Biomonitoring

Dedication

I would like to express my love and gratitude to my amazing parents, Mark and Sheri, my siblings, Jolynn, Ryan, Whitney, and Shelby, and my grandma Joyce. Each of them has shaped me into the person I am proud to be today and have supported me every step of the way during my education. Additionally, I would like to deeply thank the rest of my family and friends for all their love, support, and encouragement during my time at Montana Technological University.

Acknowledgements

First and foremost, I wish to pay my sincerest appreciation to my advisor and committee chair, **Dr. Katie Hailer** for the time and effort she devoted towards assisting me with this project and my graduate education, as well as her invaluable encouragement, guidance, and knowledge throughout my time at Montana Technological University. I would also like to thank Dr. Hailer for her unwavering friendship and support, which was crucial towards my success and personal growth.

I would like to extend my deepest appreciation to the rest of my committee members who devoted their time and knowledge towards helping me succeed. Specifically, **Dr. Alysia Cox** for her constant enthusiasm and geochemical knowledge, **Dr. Julie Hart** for her extensive toxicological knowledge and words of reassurance throughout my project, and **Dr. Karen Wesenberg** for her knowledge of chemistry and statistics and willingness to serve on my committee.

Special recognition to **Dr. Beverly Hartline**, the Dean of the Graduate School, for providing funding for the preliminary bioavailability study for this project as well as the extensive scientific knowledge and support she provided during my time at Montana Technological University.

A special thank you to **Matt Young** at the University of Montana for his assistance, expertise, and time he devoted towards analyzing the soil and dust samples that were collected for this project.

I would also like to acknowledge the Montana Technological University Research office for awarding me Graduate Research Assistantship funding for my final semester. The Montana Technological University Chemistry and Geochemistry Department for offering me Graduate Teaching Positions for my first three semesters as a graduate student and providing funding and support for my project. Lastly, the Chemistry and Geochemistry and Biology Departments for allowing me to use lab spaces and equipment to carry out my research.

Table of Contents

ABSTRACT	II
DEDICATION	III
ACKNOWLEDGEMENTS	IV
LIST OF TABLES	IX
LIST OF FIGURES.....	XI
LIST OF EQUATIONS	XIV
GLOSSARY OF TERMS.....	XV
 1. BACKGROUND.....	 1
1.1. <i>Previous Work</i>	2
2. INTRODUCTION	6
2.1. <i>General Heavy Metal Details</i>	6
2.2. <i>Essential and Nonessential Heavy Metals and Metalloids</i>	7
2.3. <i>Heavy Metal Interactions</i>	10
2.4. <i>Arsenic</i>	12
2.4.1. Arsenic General Information	12
2.4.2. Arsenic and Neurological Disorders	14
2.4.3. Arsenic Metabolism.....	15
2.4.4. Arsenic and Oxidative Stress	17
2.4.5. Arsenic Protein of Interest	18
2.4.6. Arsenic Conclusions.....	19
2.5. <i>Copper</i>	19
2.5.1. Copper General Information	19
2.5.2. Copper Metabolism.....	20
2.5.3. Copper and Neurological Disorders.....	21

2.5.4.	Copper and Oxidative Damage	24
2.5.5.	Copper Protein of Interest.....	25
2.5.6.	Copper Conclusions	26
2.6.	<i>Manganese</i>	26
2.6.1.	Manganese General Information	26
2.6.2.	Manganese Metabolism	28
2.6.3.	Manganese and Neurological Disorders.....	28
2.6.4.	Manganese and Oxidative Damage.....	30
2.6.5.	Manganese Protein of Interest.....	31
2.6.6.	Manganese Conclusions	32
2.7.	<i>Zinc</i>	32
2.7.1.	Zinc General Information	32
2.7.2.	Zinc Metabolism	33
2.7.3.	Zinc and Neurological Disorders.....	34
2.7.4.	Zinc and Oxidative Damage	36
2.7.5.	Zinc Protein of Interest.....	36
2.7.6.	Zinc Conclusions	37
2.8.	<i>Meconium</i>	37
2.9.	<i>Inflammatory Markers</i>	40
2.9.1.	Interleukin 6	40
2.9.2.	Tumor Necrosis Factor alpha.....	40
3.	RESEARCH GOALS	42
4.	RESEARCH METHODS	44
4.1.	<i>Preliminary Bioavailability Study</i>	44
4.1.1.	Trace Metal Cleaning Protocol	44
4.1.2.	Sample Collection	44
4.1.3.	Preparation and Digest for Total Metal Content	45
4.1.4.	Preparation and Digest of Stomach Samples	46
4.1.5.	Preparation and Digest of Intestinal Samples	46

4.1.6.	Bioavailability Determination	47
4.2.	<i>Biological Experiments</i>	47
4.2.1.	Mammalian Cell Line Metal-Exposure Determination	47
4.2.2.	Cell Culture Preparation	48
4.2.3.	Protein Extraction Process	49
4.2.3.1.	Mammalian Cell Cultures	49
4.2.3.2.	Meconium Samples	50
4.2.4.	Determination of Sample Protein Concentration(s)	50
4.2.5.	Western Blot Analysis	53
4.2.6.	Enzyme-Linked Immunoassay Analysis	56
5.	RESULTS	57
5.1.	<i>Preliminary Bioavailability Study</i>	57
5.2.	<i>Biological Experiments</i>	62
5.2.1.	Meconium Protein Determination	62
5.2.2.	Arsenic Protein Expression Analysis	63
5.2.2.1.	Meconium Western Blots	63
5.2.2.2.	HEK293 Western Blot	64
5.2.2.3.	BEAS-2B Western Blot	67
5.2.3.	Copper Protein Expression Analysis	69
5.2.3.1.	Meconium Western Blots	69
5.2.3.2.	HEK 293 Western Blot	71
5.2.3.3.	BEAS-2B Western Blot	73
5.2.4.	Manganese Protein Expression Analysis	74
5.2.4.1.	Meconium Western Blots	74
5.2.4.2.	HEK293 and BEAS-2B Western Blots	76
5.2.5.	Zinc Protein Expression Analysis	77
5.2.5.1.	Meconium Western Blots	77
5.2.5.2.	HEK293 and BEAS-2B Western Blots	79
5.2.6.	Tumor Necrosis Factor alpha Analysis	80

5.2.6.1.	HEK293 ELISA	80
5.2.6.2.	BEAS-2B ELISA	82
5.2.6.3.	Meconium ELISA	83
5.2.7.	Interleukin 6 Analysis	84
5.2.7.1.	HEK293 ELISA	84
5.2.7.2.	BEAS-2B ELISA	85
6.	DISCUSSION.....	87
6.1.	<i>Preliminary Bioavailability Study</i>	87
6.2.	<i>Meconium Protein Expression</i>	88
6.3.	<i>Arsenic Exposure Protein Expression</i>	90
6.4.	<i>Copper Exposure Protein Expression</i>	91
6.5.	<i>Manganese Exposure Protein Expression</i>	93
6.6.	<i>Zinc Exposure Protein Expression</i>	93
6.7.	<i>Cytokine Expression</i>	94
7.	CONCLUSIONS.....	95
8.	RECOMMENDATIONS AND FUTURE DIRECTIONS	98
9.	REFERENCES CITED.....	100
10.	APPENDIX A: BCA ASSAY DILUTION TABLES AND CALCULATIONS	122
11.	APPENDIX B: SAMPLE PROTEIN CONCENTRATIONS AND SDS-PAGE GEL LOADING VOLUMES	123
12.	APPENDIX C: RAW DATA USED TO GENERATE METAL BOX PLOTS.....	124
13.	APPENDIX D: AVERAGE STOMACH AND INTESTINAL DIGEST METAL CONCENTRATIONS.....	126
14.	APPENDIX E: NORMALIZED WESTERN BLOT PROTEIN DATA	127
15.	APPENDIX F: TUMOR NECROSIS FACTOR ELISA DATA	129
16.	APPENDIX G: INTERLEUKIN 6 ELISA DATA.....	131

List of Tables

Table I: ICP-MS Hair Analysis Median ppm Concentration.....	3
Table II: ICP-MS Whole Blood Analysis Median ppb Concentration	4
Table III: Meconium Metal Detection (Units: $\mu\text{g kg}^{-1}$) in Newborns in Butte Montana (MT) and Columbia South Carolina (SC).....	5
Table IV: Calculated Metal Exposure Concentrations	48
Table V: Mammalian Cell Line Metal Exposures	49
Table VI: Bioavailability Analysis of Dust Samples	61
Table VII: Bioavailability Analysis of Soil Samples.....	61
Table VIII: Metal Exposure Ratios for Study Elements of Concern	62
Table IX: Standard Mixture Volumes Needed	122
Table X: Dilution Factors to Determine Unknown Protein Concentration	122
Table XI: BCA Assay Values for SDS-PAGE Sample Loading.....	123
Table XII: Raw Arsenic Data Used to Generate Box Plot.....	124
Table XIII: Raw Cadmium Data Used to Generate Box Plot.....	124
Table XIV: Raw Copper Data Used to Generate Box Plot.....	124
Table XV: Raw Manganese Data Used to Generate Box Plot.....	125
Table XVI: Raw Lead Data Used to Generate Box Plot	125
Table XVII: Raw Zinc Data Used to Generate Box Plot.....	125
Table XVIII: Average Stomach Digest Concentrations	126
Table XIX: Average Intestinal Digest Concentrations	126
Table XX: As Exposure Normalized Densitometric AS3MT Values in HEK293 Cells.....	127

Table XXI: As Exposure Normalized Densitometric AS3MT Values in BEAS-2B Cells ...	
.....	127
Table XXII: Cu Exposure Normalized Densitometric CTR1 Values in HEK293 Cells .	128
Table XXIII: Cu Exposure Normalized Densitometric CTR1 Values in BEAS-2B Cells....	
.....	128
Table XXIV: HEK293 TNF- α ELISA Concentration Data.....	129
Table XXV: BEAS-2B TNF- α ELISA Concentration Data	129
Table XXVI: Meconium TNF- α ELISA Concentration Data	130
Table XXVII: HEK293 IL6 ELISA Concentration Data	131
Table XXVIII: BEAS-2B IL6 ELISA Concentration Data	131

List of Figures

Figure 1: Butte, MT Study Area	3
Figure 2: Periodic Table Indicating Essential Elements for Humans	8
Figure 3: Essential Element Dose-Response Curve.....	8
Figure 4: Dose-Response Curve for a Nonessential Element with a Threshold Dose.....	9
Figure 5: Reaction Between Two Glutathione Molecules and a Metal Ion.....	11
Figure 6: Arsenic Transport Mechanisms and Reactions	14
Figure 7: Arsenic Metabolism	16
Figure 8: Brain Copper Homeostasis	22
Figure 9: Fenton/Haber-Weiss Reactions Involving Copper.....	23
Figure 10: Copper Transport and Association with Alzheimer's Disease.....	24
Figure 11: Cellular Manganese Transport	31
Figure 12: Zinc Transport in Mammalian cells	34
Figure 13: Zinc Transport and Association with Alzheimer's Disease	35
Figure 14: Map of Sampling Location for Preliminary Bioavailability Study	42
Figure 15: Meconium Sample BCA Analysis (450 nm).....	52
Figure 16: Arsenic Total Metal and Bioavailability Data.....	57
Figure 17: Cadmium Total Metal and Bioavailability Data	58
Figure 18: Copper Total Metal and Bioavailability Data	58
Figure 19: Lead Total Metal and Bioavailability Data	59
Figure 20: Manganese Total Metal and Bioavailability Data.....	59
Figure 21: Zinc Total Metal and Bioavailability Data.....	60

Figure 22: Ponceau S-Stained Nitrocellulose Membrane Containing Meconium Samples ..	
.....	62
Figure 23: AS3MT Western Blot Analysis of Meconium Samples 1-3 and 7-10.....	63
Figure 24: AS3MT Western Blot Analysis of Meconium samples 11-16.....	64
Figure 25: AS3MT Western Blot Analysis of Varying Metal Exposures in HEK293 Cells.	
.....	65
Figure 26: AS3MT Expression in Arsenic-Treated HEK293 Cells.....	66
Figure 27: AS3MT Western Blot Analysis of Varying Metal Exposures in BEAS-2B Cells	
.....	67
Figure 28: AS3MT Expression in Arsenic-Treated BEAS-2B Cells.....	68
Figure 29: CTR1 Western Blot Analysis of Meconium Samples 1-3 and 7-10	69
Figure 30: CTR1 Western Blot Analysis of Meconium samples 11-16	70
Figure 31: CTR1 Western Blot Analysis of Varying Metal Exposures in HEK293 Cells	71
Figure 32: CTR1 Expression in Copper-Treated HEK293 Cells.....	72
Figure 33: CTR1 Western Blot Analysis of Varying Metal Exposures in BEAS-2B Cells..	
.....	73
Figure 34: CTR1 Expression in Copper-Treated BEAS-2B Cells.....	74
Figure 35: ZNT10 Western Blot Analysis of Meconium Samples 1-3 and 7-9	75
Figure 36: ZNT10 Western Blot Analysis of Meconium Samples 10-16	75
Figure 37: ZNT10 Western Blot Analysis of Varying Metal Exposures in HEK293 Cells..	
.....	76
Figure 38: ZNT10 Western Blot Analysis of Varying Metal Exposures in BEAS-2B Cells	
.....	77

Figure 39: ZNT1 Western Blot Analysis of Meconium Samples 1-3 and 7-9	78
Figure 40: ZNT1 Western Blot Analysis of Meconium Samples 10-16	78
Figure 41: ZNT1 Western Blot Analysis of Varying Metal Exposures in HEK293 Cells ..	79
Figure 42: ZNT1 Western Blot Analysis of Varying Metal Exposures in BEAS-2B Cells	80
Figure 43: TNF- α ELISA Plate Results in HEK293 Cells	81
Figure 44: TNF- α ELISA Plate Results in BEAS-2B Cells	82
Figure 45: TNF- α ELISA Plate Results of the Meconium Samples.....	83
Figure 46: IL-6 ELISA Plate Results in HEK293 Cells	84
Figure 47: IL-6 ELISA Plate Results in BEAS-2B Cells	85

List of Equations

Equation

(1)	47
(2)	47
(3)	48
(4)	51
(5)	52
(6)	52
(7)	122
(8)	122
(9)	122

Glossary of Terms

Term	Definition
AD	Alzheimer's Disease
ADL	Above detection limit
A β	Amyloid beta peptide
APP	Amyloid precursor protein
AS3MT	Arsenic (+3 oxidation state) methyltransferase
ATSDR	Agency for Toxic Substances and Disease Registry
BBB	Blood brain barrier
BCB	Blood-cerebrospinal fluid barrier
BDL	Below detection limit
BEAS-2B	Human bronchial epithelial cells
CTR1	Copper transport protein 1
ELISA	Enzyme-linked immunoassay
GSH	Glutathione
HEK293	Human embryonic kidney cells
IARC	International Agency for Research on Cancer
ICP-MS	Inductively coupled plasms mass spectrometry
ICP-OES	Inductively coupled optical emission spectrometry
<LoD	Below limit of detection
MTs	Metallothioneins
MTDEQ	Montana Department of Environmental Quality
PBET	Physiological-based extraction test
PD	Parkinson's Disease
SOD	Superoxide dismutase
U.S. EPA	United States Environmental Protection Agency
ZNT1	Zinc transporter protein 1
ZNT10	Zinc transporter protein 10

1. Background

Butte, Montana has been designated one of the largest Superfund sites in the U.S. due to 150 years of historic mining and smelting (The City-County of Butte Silver Bow, n.d). Superfund sites are designated by the United States Environmental Protection Agency (U.S. EPA) as contaminated waste areas that require long-term cleanup due to the introduction of hazardous material through a variety of agricultural processes including manufacturing facilities, processing plants, landfills, and mining sites (US EPA, 2015). Cleanup of these locations is necessary due to the risks presented to human or environmental health (McDermott *et al.*, 2020). About 15 million people, including approximately 3.5 million children live within one mile of a federal Superfund site in the U.S. (US EPA, 2015). Exposure to metals occurs mainly through inhalation, dermal absorption, and ingestion of contaminated foods, soil, and dust (Imperato *et al.*, 2003). The U.S. EPA reports that the general population ingests soil and dust particles at a rate of 100 mg/day and 50 mg/day for children and adults respectively (Hong *et al.*, 2016).

Mining for Cu has been occurring in Butte since the late-19th century, which has introduced large quantities of waste into the surrounding air, water, and soils, from mining, milling, blasting, and smelting processes (The City-County of Butte Silver Bow, n.d.; SILVER BOW CREEK/BUTTE AREA Site Profile, n.d.). Due to this contamination, Butte was officially designated a U.S. EPA Superfund site in 1983, with As, Cd, Pb, and Hg being listed as contaminants of concern for those residing within the Butte Area Superfund site (SILVER BOW CREEK/BUTTE AREA Site Profile, n.d). Limited biomonitoring has been performed for Butte residents, and most studies have focused on the historical waste concerns in the area, but little is known about the effects of the current surface mining within city limits (Hailer *et al.*, 2017). The restricted studies that have been performed have included testing of Pb blood levels in children

and to a much lesser extent, urine As levels of residents from Anaconda, MT. Anaconda is a town 25 miles northwest of Butte, in Deer Lodge County, with a population of approximately 3,500 that is part of the area designated as the mining Superfund site in combination with the Butte area (ATSDR, 2019).

Additionally, all published studies that have been performed investigate only single-metal exposure scenarios, even though contaminant exposure in Butte is widely accepted to be a metal mixture scenario. Yet, no published synergistic, antagonistic, or additive studies have been conducted in Butte. Furthermore, the trace micronutrients, Cu, Mn, and Zn, that are present in the soil, and dust of Butte have been largely unrecognized as possibly having negative health impacts on the residents, even though these are metals known to be potential neurotoxins, especially upon chronic exposure (Turker *et al.*, 2013; Karri *et al.*, 2016; Lucchini *et al.*, 2017). By furthering human biomonitoring studies in the Butte area, the impact of environmental chemical elements and their metabolites on living organisms can be assessed by measuring biomarkers in body fluids or tissues (WHO, 2015; Iwata *et al.*, 2018).

1.1.Previous Work

In a previous study, 116 volunteers from Butte and 86 volunteers from Bozeman, Montana submitted hair and blood samples and a complete lifestyle survey (Hailer *et al.*, 2017). Blood samples were representative of short-term exposure levels, while hair samples provided insight into long-term exposure levels. In addition to the biological samples, three air monitors were stationed around Butte to collect air particulate throughout four summer months and soil samples from 32 volunteers were also obtained (Hailer *et al.*, 2017) (Figure 1). Inductively coupled mass spectrometry (ICP-MS) was used for elemental analysis of all sample types collected (Hailer *et al.*, 2017). The results of this study showed that aluminum (Al), As, Cd, Cu,

Mn, Mo, and uranium (U) were statistically elevated in hair samples, while As was statistically elevated in blood samples (Hailer *et al.*, 2017) (Table II and Table III). Additionally, detectable levels of As, Pb, Cu, Mn, and Cd were found in the soil samples with As and Cu being elevated in some samples, and air sampling analysis revealed elevated levels of As and Mn (Hailer *et al.*, 2017).

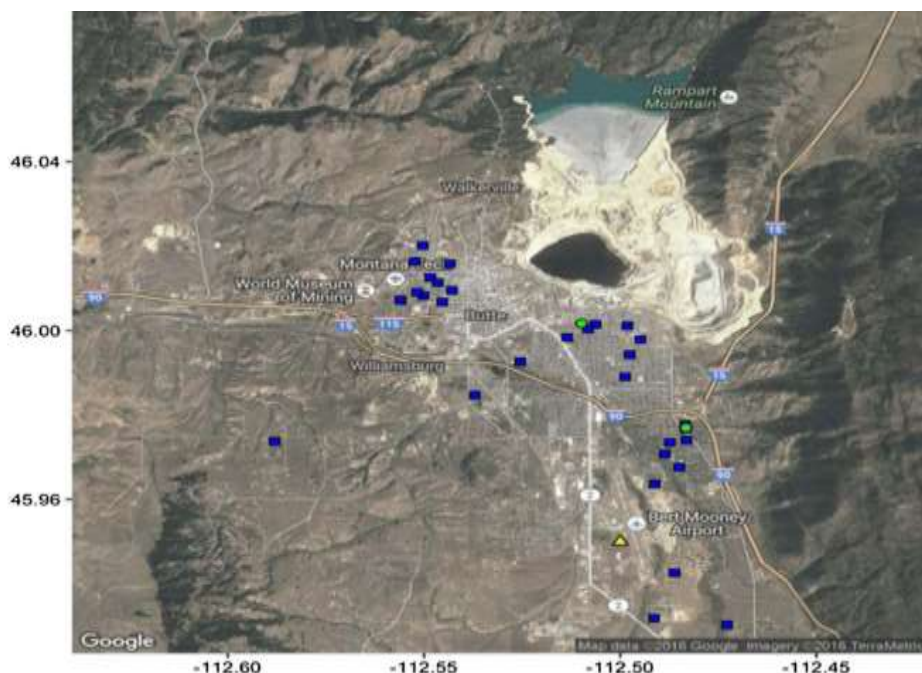


Figure 1: Butte, MT Study Area

Soil (blue squares) and air (green circles) samples were collected. Soil samples were collected once and air samples were collected weekly from May through October 2015. Weather information was collected at Bert Mooney Airport weather station (yellow triangle) (Hailer *et al.*, 2017).

Table I: ICP-MS Hair Analysis Median ppm Concentration

Element	Butte	Bozeman
Aluminum*	5	3
Arsenic*	0.07	0.05
Cadmium*	0.03	0.02
Copper*	22	18
Lead	1	1
Manganese*	0.53	0.17
Molybdenum*	0.05	0.04
Strontium	2.1	2.4
Uranium*	0.07	0.04
Zinc	170	180

ICP-MS analysis of 202 hair samples, 116 from Butte and 86 from Bozeman. Results are represented in average ppm between groups. “*” indicates the distribution of element concentrations are statistically significant by Wilcoxon rank-sum test (Hailer *et al.*, 2017).

Table II: ICP-MS Whole Blood Analysis Median ppb Concentration

Element	Butte	Bozeman	U.S. Avg
Aluminum	217.8	190.6	NA
Arsenic*	14.2	9.2	0-12
Cadmium	nd	nd	0.33
Copper	814.9	800.8	802.4
Lead (µg/dL)	1.2	1	1.30
Manganese	12.5	14.8	9.4
Molybdenum*	6.2	5.8	1.2-4.8
Selenium	197.8	211.9	192
Strontium	38.5	37.6	NA
Uranium	5.7	6.2	NA
Zinc	4911	5330	4665

ICP-MS analysis of 141 blood samples, 69 from Butte and 72 from Bozeman. Results are represented in average ppb between groups. *As was found to be significant by Wilcoxon Rank Sum analysis. NA = Published average for whole blood is unavailable (Hailer *et al.*, 2017).

In a published epidemiological study that compared the rates of brain and other nervous system cancers for Silver Bow and Deer Lodge Counties to rates in other counties of Montana and the US, it was identified that there was a significant increase in the rate ratio (IRR) of cancer in the brain and nervous system for residents ages 0 - 4 years and 30 - 34 years of Silver Bow and Deer Lodge counties compared to the remaining 54 counties in Montana (Zhang *et al.*, 2020). Cancers of the brain and nervous system are the 13th most common types of cancer in Montana and represent approximately 2% of all new cancer cases in the state (Montana Department of Public Health and Human Services, 2019). Increased risk for brain cancer and other nervous system cancers was also found in adults 30 -34 years of age who were born before the declaration of superfund sites (1981-1985), but it is not known how many of these individuals continuously resided in Silver Bow or Deer Lodge County (Zhang *et al.*, 2020). Overall, this study suggested that the elevated risk of brain cancer and other cancers of the nervous system in very young children and adults is cause for concern for resident of Silver Bow and Deer Lodge Counties (Zhang *et al.*, 2020).

More recently, a pilot study was performed to assess intrauterine metal exposure of fetuses from mothers living in Butte, Montana (McDermott *et al.*, 2020). Meconium samples

were collected from 17 infants in Columbia, South Carolina as a comparison population and 15 infants from Butte (McDermott *et al.*, 2020). The metal concentrations found in the Columbia samples were similar to low levels identified in other meconium studies however, in comparison, the Butte samples were found to be 1792-fold higher for Cu, 1650-fold higher for Mn, 1883-fold higher for Zn, and 23-fold higher for As (McDermott *et al.*, 2020) (Table III). Metals were quantified via ICP-MS and a t-test and Wilcoxon rank-sum test were used to determine statistical differences between the Butte and Columbia samples (McDermott *et al.*, 2020).

Table III: Meconium Metal Detection (Units: $\mu\text{g kg}^{-1}$) in Newborns in Butte Montana (MT) and Columbia South Carolina (SC)

	As ($\mu\text{g kg}^{-1}$)	Cu ($\mu\text{g kg}^{-1}$)	Mn ($\mu\text{g kg}^{-1}$)	Mo ($\mu\text{g kg}^{-1}$)	Pb ($\mu\text{g kg}^{-1}$)	Zn ($\mu\text{g kg}^{-1}$)
Butte N=15	Median:32 Min:16 Max:49 Mean:35 Std. Dev:10	Median:26,311 Min: 1,006 Max:47,270 Mean:28,134 Std. Dev:10,411	Median:5,364 Min:388 Max:18,120 Mean:6,870 Std. Dev:5,726	Median:32 Min:16 Max:49 Mean:35 Std. Dev:13	Median:# Mean:5 Std. Dev:5	Median:81,642 Min:22,120 Max:312,695 Mean:109,154 Std. Dev:82,772
Columbia N=17	<LoD	Median: 14.68 Min: 2.40 Max: 27.42 Mean: 14.75 Std. Dev: 7.68	Median: 3.25 Min: 0.20 Max: 27.42 Mean: 4.67 Std. Dev: 4.48	< LoD	< LoD	Median:43.34 Min:12.17 Max:117.25 Mean:53.74 Std. Dev:36.16

ICP-MS Analysis of Metal Meconium Concentrations from Newborns in Butte, MT and Columbia SC. LoD for MT samples: As = 5.0, Cu = 5.0, Mn = 5.0, Mo = 0.1, Pb = 0.1, Zn = 5.0. LoD for SC samples: As = 1.4, Cu = 0.5, Mn = 0.5, Mo = 0.7, Pb = 0.6, Zn = 1.8. #sample was above LoD. (McDermott *et al.*, 2020).

2. Introduction

2.1. General Heavy Metal Details

The term “heavy metals” is often used to describe metals and metalloids that have been associated with contamination and potential toxicity or ecotoxicity (Duffus, 2002). Typically, heavy metals have a specific density above 5 g/cm^3 with an atomic weight greater than 40.04 g/mol (Engwa *et al.*, 2019). These metals are ubiquitous environmental elements that are non-biodegradable, environmentally persistent, bioaccumulative in nature, and have varying toxic effects on living systems. (Engwa *et al.*, 2019; Ali and Khan, 2019). Bioaccumulation is defined as the amount of a contaminant accumulated in an organism as a result of its uptake from both the surrounding abiotic environment and its diet (Ali and Khan, 2019). Once metals are accumulated in the body and its tissues, elimination can be difficult, especially in the context of non-essential metals (Kalay and Canli, 2000).

Natural sources of heavy metals in the environment include weathering of metal-bearing rocks and volcanic eruptions (Ali and Khan, 2019). The major anthropogenic sources include natural emissions, burning of fossil fuels, mining, smelting, and other agricultural and industrial activities (Ali and Kahn, 2019). Environmentally, the most relevant and hazardous heavy metals and metalloids include chromium (Cr), nickel (Ni), Cu, Zn, Pb, Hg, and As (Barakat, 2011). The usage and subsequent concentrations of these elements within the environment are increasing, leading to greater toxic effects on biological systems (Wongsasuluk *et al.*, 2014). Depending on the dose absorbed, and route and duration of exposure to these toxicants, negative effects can eventually be seen in the organs and tissues of living organisms. Exposure can be acute, meaning that contact with the toxicant is short-term, whereas chronic exposure refers to contact that is continuous or repetitive over a long period. Generally, these contaminants are more toxic as

cations or organic species, and some can cross the blood-brain and placental barriers, which increases the negative effects these toxicants can cause since they may be able to have a direct effect on the brain or placenta (Zheng *et al.*, 2003)

2.2. Essential and Nonessential Heavy Metals and Metalloids

Typically, these heavy metals are trace elements, meaning that they are found in small amounts in the environment. Additionally, some play important roles in pathways of biological systems and are further characterized as trace micronutrients or essential elements. Too low and too high of a concentration of essential elements can lead to varying health effects for humans (Ali and Kahn 2019). Three of the four metals investigated in this study, Cu, Mn, and Zn, are well-known human trace micronutrients (Figure 2), meaning that a certain concentration of each metal is needed within the human body for important biological functions. When bound to proteins, essential metals facilitate catalytic reactions and stabilize structural domains, or can also serve as intracellular secondary messengers and modulators of synaptic transmissions (Schlief *et al.*, 2005; Yamasaki *et al.*, 2007; Dodani *et al.*, 2014; Que *et al.*, 2015). Because of these biological requirements, dose-response curves for essential elements indicate areas of deficiency and excess that can result in negative health effects (Figure 3) (Klaassen, 2019). Furthermore, metals that are not required for biological functions are referred to as “non-essential”. Of the 6 metals investigated in the preliminary bioavailability study, As, Pb, and Cd, are considered to be nonessential for humans.

Periodic Table of the Elements

Essential for Humans

Suggested to be Essential

1 H 1.01																	18 He 4.00			
3 Li 6.94	4 Be 9.01																	10 Ne 20.18		
11 Na 22.99	12 Mg 24.31																	16 S 32.07	17 Cl 35.45	18 Ar 39.95
19 K 39.10	20 Ca 40.08	21 Sc 44.96	22 Ti 47.87	23 V 50.94	24 Cr 51.99	25 Mn 54.94	26 Fe 55.85	27 Co 58.93	28 Ni 58.69	29 Cu 63.55	30 Zn 65.38	31 Ga 69.72	32 Ge 72.63	33 As 74.92	34 Se 78.97	35 Br 79.90	36 Kr 84.80			
37 Rb 84.47	38 Sr 87.62	39 Y 88.91	40 Zr 91.22	41 Nb 92.91	42 Mo 95.94	43 Tc 98.91	44 Ru 101.07	45 Rh 102.91	46 Pd 106.42	47 Ag 107.87	48 Cd 112.41	49 In 114.82	50 Sn 118.71	51 Sb 121.76	52 Te 127.6	53 I 126.90	54 Xe 131.29			
55 Cs 132.91	56 Ba 137.33	57-71 La 138.91	72 Hf 178.49	73 Ta 180.95	74 W 183.84	75 Re 186.21	76 Os 190.23	77 Ir 192.22	78 Pt 195.08	79 Au 196.97	80 Hg 200.59	81 Tl 204.38	82 Pb 207.2	83 Bi 208.98	84 Po [209]	85 At [209.98]	86 Rn 222.02			
87 Fr 223.02	88 Ra 226.03	89-103 Ac 227.03	104 Rf [261]	105 Db [262]	106 Sg [266]	107 Bh [264]	108 Hs [269]	109 Mt [268]	110 Ds [271]	111 Rg [272]	112 Cn [277]	113 Uut unknown	114 Fl [289]	115 Uup unknown	116 Lv [290]	117 Uus unknown	118 Uuo unknown			

57 La 138.91	58 Ce 140.12	59 Pr 140.91	60 Nd 144.24	61 Pm 144.91	62 Sm 150.36	63 Eu 151.96	64 Gd 157.25	65 Tb 158.93	66 Dy 162.50	67 Ho 164.93	68 Er 167.26	69 Tm 168.93	70 Yb 173.06	71 Lu 174.97
89 Ac 227.03	90 Th 232.04	91 Pa 231.04	92 U 238.03	93 Np 237.05	94 Pu 244.06	95 Am 243.06	96 Cm 247.07	97 Bk 247.07	98 Cf 251.08	99 Es [254]	100 Fm 257.10	101 Md 258.1	102 No 259.10	103 Lr [262]

Figure 2: Periodic Table Indicating Essential Elements for Humans
 Periodic table indicated the metals that are known to be essential for humans (blue), those that are suggested to be essential for humans (green), and those that are not known to be required for any biological processes in humans. The metals and metalloids of interest for the bioavailability study are indicated by a bold, black box (modified from Essential Elements for Life, n.d.)

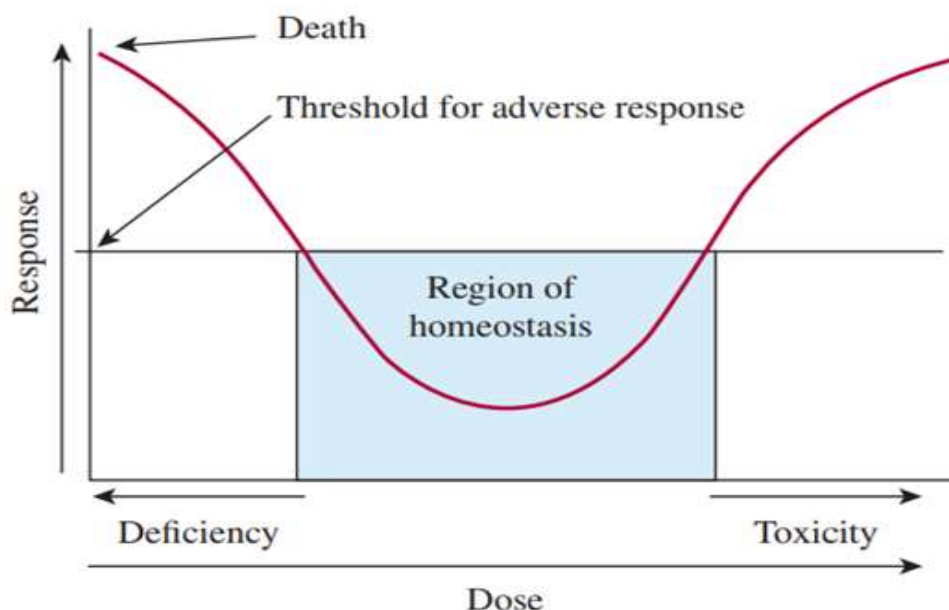


Figure 3: Essential Element Dose-Response Curve
 Figure depicting a dose-response curve of an essential metal in which it can be observed that too low and too high of a dose of an essential element can become toxic for biological systems (Klaassen, 2019).

Non-essential metal toxicants with threshold concentrations will remain nontoxic to humans until a certain concentration is surpassed, whereas those without a threshold level are toxic to humans even at very low concentrations (Klassen, 2019) (Figure 4). The toxicity curves for metal mixtures are relatively unknown, but it is assumed that threshold and toxicity levels are different from single-metal exposure curves.

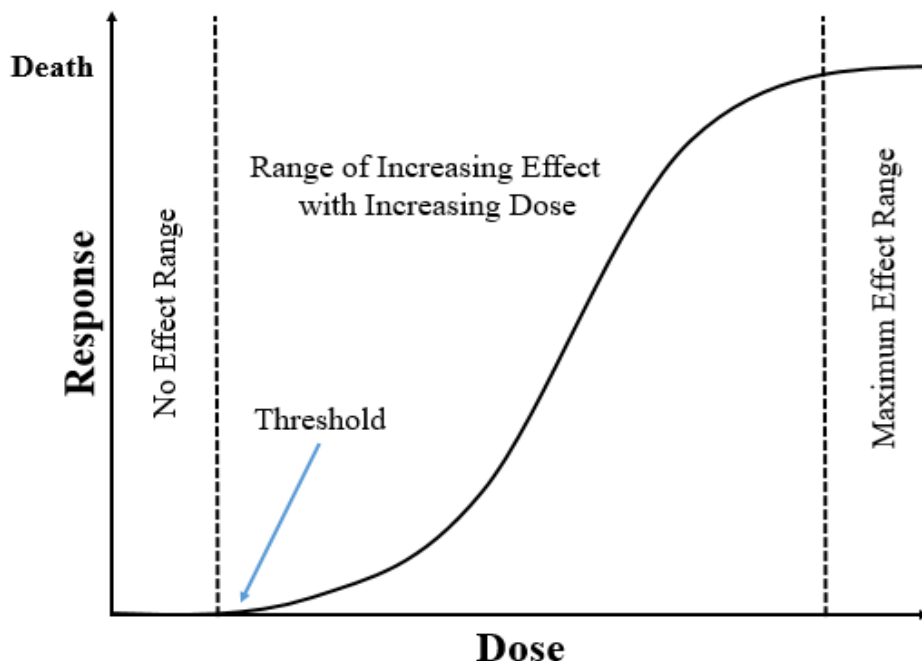


Figure 4: Dose-Response Curve for a Nonessential Element with a Threshold Dose
Figure depicting a dose-response curve for a non-essential element possessing a toxicity threshold dose in a biological system. Once the threshold dose is reached, a response will be encountered and will increase until the maximum effect dose is reached, typically resulting in death (adapted from Klaassen, 2019).

The retention of these toxicants in organisms greatly depends on the metal speciation and physiological mechanisms developed by the organisms to maintain homeostasis and detoxify the heavy metal (Ali and Khan, 2019). In eukaryotes, regulation mechanisms typically involve changes in expressions of genes needed for transport of these micronutrients (Bird, 2015). This is because fact that living systems do not have the means to degrade heavy metals, which plays a major role in the accumulation of these species to harmful levels (Beyersmann and Hartwig, 2008). Continual heavy metal exposure can result in an internal imbalance, which can result in

the body using the accumulated metals as substitutes for essential elements (Rehman *et al.*, 2018). These stored toxicants destroy major metabolic processes and create antioxidant imbalances as well as influence the activity of various hormones and essential enzymes and increase the body's susceptibility toward infection due to alterations in carbohydrate, protein, and lipid metabolism (Safty *et al.*, 2009; Mukke and Chinte, 2012).

2.3. Heavy Metal Interactions

There is a substantial evidence base indicating that metal mixtures can cause significantly increased effects on mammalian models and human health when compared to single metals. Currently, few studies investigate the effect of low-dose, toxic metals and the effect that they have on essential metals in an organism (Cobbina *et al.*, 2015a). Most toxic metals are found in low concentrations within the environment; however, it has been established that there is the potential for interaction with essential elements even under low-level exposure to toxic metals (Cobbina *et al.*, 2015a).

The interactions of these elements can also lead to the generation of reactive oxygen species (ROS), such as the hydroxide radical (HO^\bullet), superoxide radical ($\text{O}_2^{\bullet-}$), and hydrogen peroxide (H_2O_2) (Wang and Fowler, 2008). This can increase the overall oxidative stress in the organism and possibly deplete antioxidant reserves (Wang and Fowler, 2008). Interactions with sulfhydryl macromolecules may result in inhibition of the enzymes involved in cellular energy production and depletion of major antioxidants of cells, particularly those that include a thiol group (Jadhav *et al.*, 2007; Wang and Fowler, 2008). In excess concentrations, some heavy metals can bind to glutathione (GSH), leading to the depletion of this major antioxidant molecule and possible subsequent health effects (Figure 5).

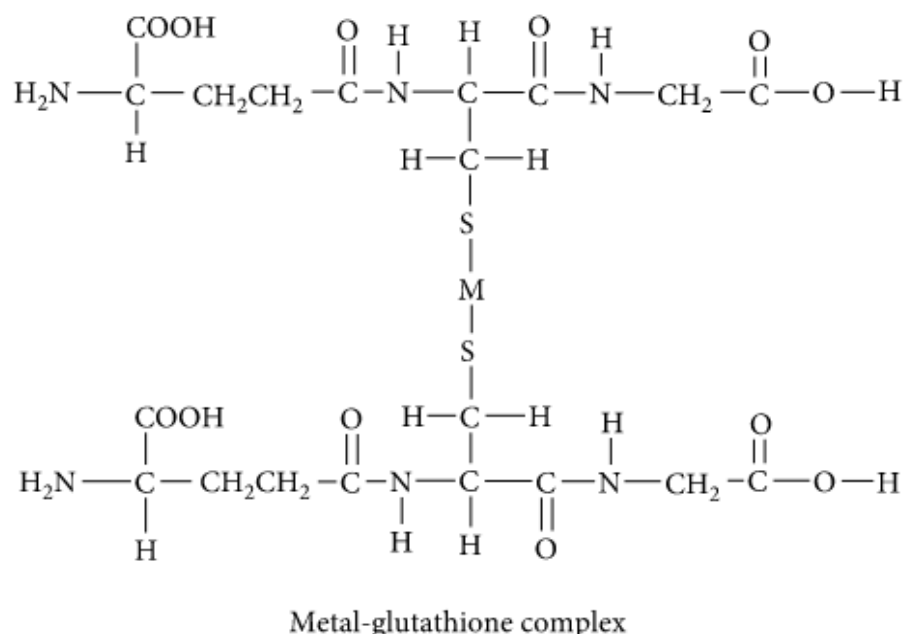


Figure 5: Reaction Between Two Glutathione Molecules and a Metal Ion
 Depiction of two glutathione molecules reacting with and sequestering a metal ion, through the replacement of a hydrogen molecule from each thiol group in the compound (Ali *et al.*, 2019).

Micronutrients with similar physical and chemical properties and shared absorption pathways are known to compete with transport proteins (Sandström, 2001). Metals typically associate with protein metal-binding sites according to the Irving-Williams series in which the relative stability of complexes formed with essential metals is: Mn (II) < Fe (II) < Ni (II) < Co (II) < Cu (II) > Zn (II), indicating that Cu (II) and Zn (II) are bound preferentially over other ions such as Mn (II) (Bird, 2015). The major question surrounding toxic heavy metal interactions has been whether or not the interactions are synergistic, antagonistic, or additive. A recent toxicity study on low dose exposures to these toxicants suggested that these interactions were synergistic and that heavy metal mixtures showed higher toxicities than single metal exposures (Cobbina *et al.*, 2015b)

2.4.Arsenic

2.4.1. Arsenic General Information

Arsenic (As) is a metalloid, possessing both metal and non-metal properties, that is released into the atmosphere as a byproduct of soil/rock erosion and industrialization or agricultural processes (Garza-Lombó *et al.*, 2019). This metalloid is present in the soil, air, and water and is the 12th most abundant element in the human body (Garza-Lombó *et al.*, 2019). Typically, the most common route of exposure to As is through contaminated food and water, and once in circulation, As can affect virtually every organ and tissue in the body (Garza-Lombó *et al.*, 2019). Due to the prevalence of As in the atmosphere, the numerous anthropogenic processes that release it into the environment, potential for human exposure, and the magnitude and severity of possible As-induced health problems, the United States Agency for Toxic Substances and Disease Registry (ATSDR) has ranked As at the top of its priority list (Shen *et al.*, 2013). Arsenic is also classified as a human carcinogen by the International Agency for Research on Cancer (IARC) and the U.S. Environmental Protection Agency (EPA) (Shen *et al.*, 2013).

The oxidation state of As can vary greatly depending on the redox status, biological activities, and pH of the environment it is in (Shen *et al.*, 2013). The environmental behavior, physical and chemical properties, toxicity, mobility, and biotransformation are extremely different between each species (Cullen and Reimer, 1989). When in combination with elements such as oxygen, sulfur, and chlorine, As is referred to as inorganic As (*iAs*), and when combined with hydrogen or carbon, it is referred to as organic As (Jomova *et al.*, 2011). There are two oxidations states in which *iAs* can occur, which are arsenite +3 (*iAs*III) and arsenate +5 (*iAs*V) (Garza-Lombó *et al.*, 2019). These species can be monomethylated to form monomethylarsonic acid (MMAV) or dimethylated to form dimethylarsinic acid (DMAV) by a protein known as

arsenic (+3 oxidation state) methyltransferase (AS3MT) (Jomova *et al.*, 2011). Biomethylation, involving reductases and methyltransferases, is the major metabolic pathway for *iAs* in humans and most animals (Stýblo *et al.*, 2002)

Inorganic As can cross the blood-brain barrier (BBB) through the use of aqua(glycerol)porins (AQP), organic anion transporters, and glucose transporters (GLUT) for *iAsIII* and phosphate transporters for *iAsV*, which is quickly reduced to *iAsIII* after transport into the cells (Liu *et al.*, 2002; Torres-Avila *et al.*, 2010; Calatayud *et al.*, 2012) (Figure 6). Methylation of *iAs* can also occur via enzymatic or nonenzymatic conjugation with GSH, generating As triglutathione (As(GS)₃) (Garza-Lombó *et al.*, 2019). Once inside the brain, *iAs* is methylated by AS3MT in areas that express this protein (Sánchez-Peña *et al.*, 2010). Additionally, *iAsIII* and *iAsV* are suggested to accumulate in the brain more readily during development when the BBB is not fully developed (Garza-Lombó *et al.*, 2019). Inorganic As has also been reported to alter the BBB gap junction, which could allow for other toxic heavy metals to more easily cross the BBB and have increased deleterious effects (Manthari *et al.*, 2018; Golmohammadi *et al.*, 2019).

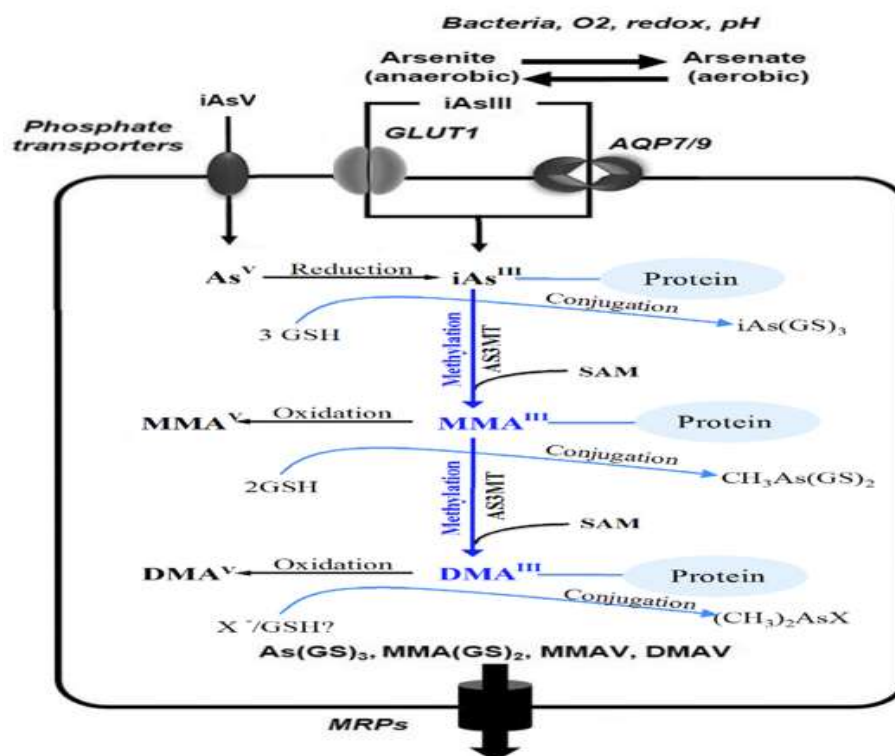


Figure 6: Arsenic Transport Mechanisms and Reactions
 Arsenic transport across the blood-brain barrier via various transporters and the subsequent reactions that occur once As enters mammalian cells (derived from Khairul *et al.*, 2017; Garza-Lombó *et al.*, 2019).

2.4.2. Arsenic and Neurological Disorders

There are numerous mechanisms in which As can alter human cellular function, most of which are related to its neurotoxic nature (Garza-Lombó *et al.*, 2019). Based on clinical observations, it has been concluded that *iAs* can have a serious impact on the neurological system after inhalation and/or oral exposure (Lagerkvist and Zetterlund, 1994; Calderón *et al.*, 2001; Uede and Furukawa, 2003). Ingestion of *iAs* can cause nervous system damage, with exposure levels of 2 mg/kg As per day leading to encephalopathy, headaches, mental confusion, seizures, and a coma (Bartolome *et al.*, 1999; Jomova *et al.*, 2011). Chronic exposure to lower levels of *iAs* around 0.03–0.1 mg/kg As per day typically results in symmetrical peripheral neuropathy (Foy *et al.*, 1992; Chakraborti *et al.*, 2003; Jomova *et al.*, 2011).

Upon exposure to the central nervous system (CNS), induction of cognitive delay, reductions in full-scale intelligence quotients (IQ) and memory, neurodevelopmental alterations, and neurodegenerative disorders may be observed (Garza-Lombó *et al.*, 2019). It has been determined that high levels of urinary *i*As and low levels of dimethylarsinic acid (DMAV) are associated with an increased risk of developing Alzheimer's disease (AD) (Yang *et al.*, 2018). Additionally, rat brains treated with *i*As showed increased levels of pro-inflammatory cytokines, indicating a strong inflammatory response, which plays a part in increasing the levels of amyloid precursor protein (APP) (Escudero-Lourdes *et al.*, 2016; Mao *et al.*, 2016; Firdaus *et al.*, 2018; Niño *et al.*, 2018; Garza-Lombó *et al.*, 2019). Inorganic As is also known to increase proteotoxic stress, synergize with dopamine to trigger neurotoxicity, and induce the accumulation and oligomerization of α -synuclein, which is the pathological biomarker of Parkinson's disease (PD) (Shavali and Sens, 2008; Cholanians *et al.*, 2016). The molecular mechanisms and complete metabolism of As can be used to explain how As damages the CNS by way of oxidative stress, energy failure, mitochondrial dysfunction, epigenetics, neurotransmitter and synaptic transmitter homeostasis alterations, cell death pathways, and inflammation (Garza-Lombó *et al.*, 2019).

2.4.3. Arsenic Metabolism

The common form of As that enters the body is *i*AsIII, which does so via a simple diffusion mechanism (Cohen *et al.*, 2006; Jomova *et al.*, 2011). A small amount of *i*AsV can cross the cell membrane via an energy-dependent transport system but is immediately reduced to *i*AsIII (Cohen *et al.*, 2006; Jomova *et al.*, 2011). The toxicity of *i*AsV is partially accounted for by its conversion to *i*AsIII in many metabolic pathways (Garza-Lombó *et al.*, 2019). Metabolism of *i*As, which tends to be far more toxic than organic As, involves a two-electron reduction of *i*AsV to *i*AsIII, mediated by glutathione, followed by oxidative methylation by AS3MT, using S-

adenosylmethionine (SAM) as a co-substrate (Hughes, 2002; Shi *et al.*, 2004; Valko *et al.*, 2005; Garza-Lombó *et al.*, 2019).

The protein, AS3MT, methylates *iAsIII* to monomethylarsonic acid or arsenate (*MMAV*) which is reduced further to monomethylarsonous acid (*MMAIII*), to be dimethylated to dimethylarsinic acid (*DMAV*), which can then be reduced to dimethylarsinous acid (*DMAIII*) (Toxicological Profile for Arsenic, 2007; Watanabe and Hirano, 2013; Garza-Lombó *et al.*, 2019) (Figure 7). Most end products of these biomethylation reactions are excreted through the urine (Jaishankar *et al.*, 2014). However, *MMAIII*, which is highly toxic, is not excreted and remains in the cells as an intermediate product and has been linked to As-carcinogenesis (Singh *et al.*, 2007; Jaishankar *et al.*, 2014).

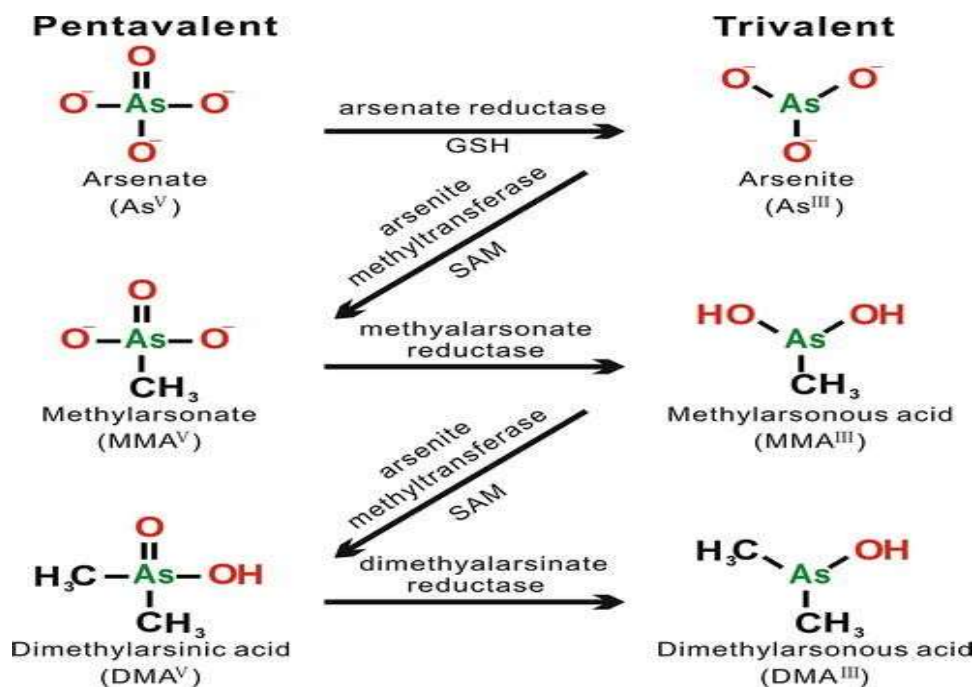


Figure 7: Arsenic Metabolism

Arsenic methylation and reduction reactions involved in the metabolism of the metal within the human body (Chen *et al.*, 2013).

2.4.4. Arsenic and Oxidative Stress

Some of the deleterious effects of As are due to the ability of the element to bind to thiol groups in proteins, leading to disruption of catalytic activity and overall inhibition of enzymes, many of which are important for cellular energy metabolism (Jomova *et al.*, 2011). It has been shown that, at biologically relevant concentrations, all three trivalent arsenic species (*i*AsIII, MMAIII, and DMAIII) can inhibit the Pyruvate Dehydrogenase (PDH) complex, resulting in an overall decrease in citric acid cycle activity and cellular adenosine triphosphate (ATP) production (Petrick *et al.*, 2001; Bergquist *et al.*, 2009; Shen *et al.*, 2013). It is suggested that inorganic arsenate (HAsO_4^{2-}), a molecular analog of phosphate (HPO_4^{2-}), can compete for phosphate anion transporters and mimic inorganic phosphate in the generation of adenosine triphosphate (ATP) during oxidative phosphorylation, creating adenosine diphosphate-arsenate instead of ATP (Hughes, 2002; Jomova *et al.*, 2011). This mimicry results in the replacement of ATP by ADP-arsenate in glycolysis and cellular respiration and an overall uncoupling of oxidative phosphorylation due to the absence of high-energy phosphate bonds (Hughes, 2002; Jomova *et al.*, 2011). Inhibition of cellular glucose uptake, gluconeogenesis, fatty acid oxidation, and further production of acetyl CoA, and subsequent cell death can also be resultant of As-induced enzyme inactivation (Miller *et al.*, 2002).

Oxidative damage mediated by ROS, as well as morphological changes to mitochondrial integrity that lead to a rapid decline of mitochondrial membrane potential are key traits in As pathogenesis (Jomova *et al.*, 2011). Upon As exposure, both animals and humans experience an increase in ROS/reactive nitrogen species (RNS) formation, including peroxy radicals (ROO^\bullet), the superoxide anion radical (O_2^\bullet), singlet oxygen ($^1\text{O}_2$), hydroxyl radical (OH^\bullet), hydrogen peroxide (H_2O_2), the dimethylarsenic radical ($((\text{CH}_3)_2\text{As}^\bullet)$), and the dimethylarsenic peroxy radical ($((\text{CH}_3)_2\text{AsOO}^\bullet)$) during metabolism of the element (Jomova *et al.*, 2011).

Monomethylated and dimethylated *i*As are suggested to be the most potent due to their ability to produce such radicals (Zamora *et al.*, 2014). Mitochondria are a primary source of *i*As-induced ROS formation due to the inhibition of certain enzymes, which leads to a depletion of the mitochondrial NADH pool, resulting in oxidative stress, and an imbalance in ROS (Shen *et al.*, 2013). Additionally, a major contributor to the overall increase in oxidative stress is the prevention of GSH production, limiting the amount of the antioxidant available to protect cells against oxidative damage by *i*AsIII (Miller *et al.*, 2002). Cascade mechanisms of these free radical formations, combined with glutathione-depleting agents, increase the sensitivity of cells to As and other heavy metal toxicity (Garza-Lombó *et al.*, 2019).

2.4.5. Arsenic Protein of Interest

The major methyltransferase responsible for As biomethylation in humans is As (+3 oxidation state) methyltransferase (AS3MT), which is also referred to as Cyt 19 (Shen *et al.*, 2013). Little information is known about AS3MT in the context of human metabolism, but it has been established that it catalyzes the transfer of the methyl group of S-adenosylmethionine (SAM) to trivalent As (Cullen and Reimer, 1989; Marapakala *et al.*, 2012; Stýblo *et al.*, 2002; Ajees *et al.*, 2012). Since AS3MT requires SAM as a co-substrate, excessive As exposure and the resulting AS3MT activity is thought to lead to a depletion of SAM levels (Zhao *et al.*, 1997; Reichard *et al.*, 2007; Coppin *et al.*, 2008). This depletion then leads to high S-adenosylhomocysteine (SAH) levels, which can in turn negatively regulate the activity of SAM-dependent methyltransferases such as AS3MT (Zhao *et al.*, 1997; Reichard *et al.*, 2007; Coppin *et al.*, 2008). Due to these possible conflicting activities of AS3MT and its required co-substrate SAM, it is not clear whether the expression of the protein will increase or decrease in the presence of As. However, since AS3MT is the major protein responsible for the metabolism of

As in the human body, it is predicted that an increase of protein expression will occur in an environment where As is in excess.

2.4.6. Arsenic Conclusions

Arsenic is readily released into the atmosphere by a variety of anthropogenic activities as well as natural processes, which compound to steadily increase the amount of As an individual may be exposed to through the environment. Although it is prevalent in the human body, As is identified as a human carcinogen and can be highly toxic to humans through a variety of mechanisms. The toxicity of As depends majorly on the species and type of exposure, but overall, exposure to inorganic As species leads to more deleterious effects in humans than organic arsenic species. Arsenic exposure can cause a variety of neurological health effects, most of which are related to oxidative damage caused by As interactions in the body. This oxidative damage is linked mainly to the compound's affinity to bind to thiol groups in proteins, which can lead to the deactivation of enzymes involved in cellular glucose uptake, the citric acid cycle, and the production of glutathione and ATP. Overall, As itself has not been proven to be a direct neurotoxin, but rather exposure to As increases susceptibility to neurological disorders through many mechanisms, most of which are linked to oxidative damage.

2.5. Copper

2.5.1. Copper General Information

Copper is the third most abundant essential transition metal in humans with the highest Cu content in the body being found in the liver, followed closely by the brain (Szerdahelyi and Kása 1986; Lewińska-Preis *et al.* 2011). Natural sources of Cu include meats, vegetables, and cereals, but exposure occurs mainly due to industrialization processes such as mining (Bost *et al.*, 2016). Copper is essential as a cofactor and/or structural component for several biologically

important enzymes (Scheiber *et al.*, 2014). Cu acts as a major cofactor for Cytochrome C oxidase and proteins from the superoxide dismutase family (Davies *et al.*, 2013; Scheiber *et al.*, 2014). Cytochrome C oxidase is a member of the superfamily of heme-copper-containing oxidases and catalyzes the final step of the electron transport chain when cytochrome c is oxidized or reduced by dioxygen (Ferguson-Miller and Babcock 1996). Superoxide dismutase 1 and 3 are Cu-dependent and responsible for converting superoxide to oxygen and hydrogen peroxide, playing a major role in antioxidant defenses (Perry *et al.*, 2010).

Copper is also suggested to play a role in biological processes such as cellular respiration, free-radical defense, and neurotransmitter synthesis (Zatta and Frank, 2007; Desai and Kaler, 2008; Scheiber and Dringen, 2013). Homeostasis of Cu within the body is tightly regulated since it is an essential element, but the upper and lower limits of homeostatic regulation remain unclear (Araya *et al.*, 2006). In the case of neurodegenerative diseases, these homeostatic mechanisms may fail as a result of Cu deficiency or overload (Bulcke *et al.*, 2017).

2.5.2. Copper Metabolism

The absorption of Cu occurs by the small intestine and is then transferred to the liver via the portal vein from which it is further distributed to the muscle and brain through the bloodstream (de Romaña *et al.*, 2011). Copper transport protein 1 (CTR1) is essential for the absorption of Cu via the small intestine, making it clear that CTR1 is required for Cu to be bioavailable (Nose *et al.*, 2006). Accumulation of Cu in the cytosol of cells may result in toxicity, but under physiological conditions, Cu concentrations within cells are kept around 10^{-8} M, by the binding of Cu to metallothioneins (MTs) and GSH (Rae *et al.*, 1999; Scheiber *et al.*, 2014). Approximately 90% of Cu found in the serum is bound to ceruloplasmin, a major copper-binding protein, as well as albumin and transcuprein proteins (Prohaska, 2008; van den Berghe

and Klomp, 2009; Lutsenko, 2016;). Cells work to keep cytosolic Cu levels low by utilizing chaperone and Cu-binding proteins, because when in excess, free, unbound Cu can drive the production of ROS due to its chemical redox capabilities and its potential to displace other metals in metalloproteins (Robinson and Winge, 2010; Palumaa, 2013; Bird, 2015).

2.5.3. Copper and Neurological Disorders

The brain contains approximately 7.0% of the body's Cu content, yet a disproportionately low level of antioxidants, increasing the brain's susceptibility to oxidative stress induced by Cu and its high redox activity (Hung *et al.*, 2010; Hung *et al.*, 2013). Brain Cu homeostasis is regulated by the blood-brain barrier (BBB) and blood-cerebrospinal fluid barrier (BCB), with the main entry route of Cu into active brain tissues being the BBB, through the combined action of CTR1 and ATP7A (Choi and Zheng 2009; Monnot *et al.*, 2011; Zheng and Monnot 2012; Fu *et al.*, 2014) (Figure 9). It has been suggested that the BCB's role in Cu homeostasis is to remove Cu from the cerebrospinal fluid (CSF) into the blood (Andrade *et al.*, 2017). However, in developing brains, the BCB has been indicated to be the main route of Cu entry (Donsante *et al.*, 2010).

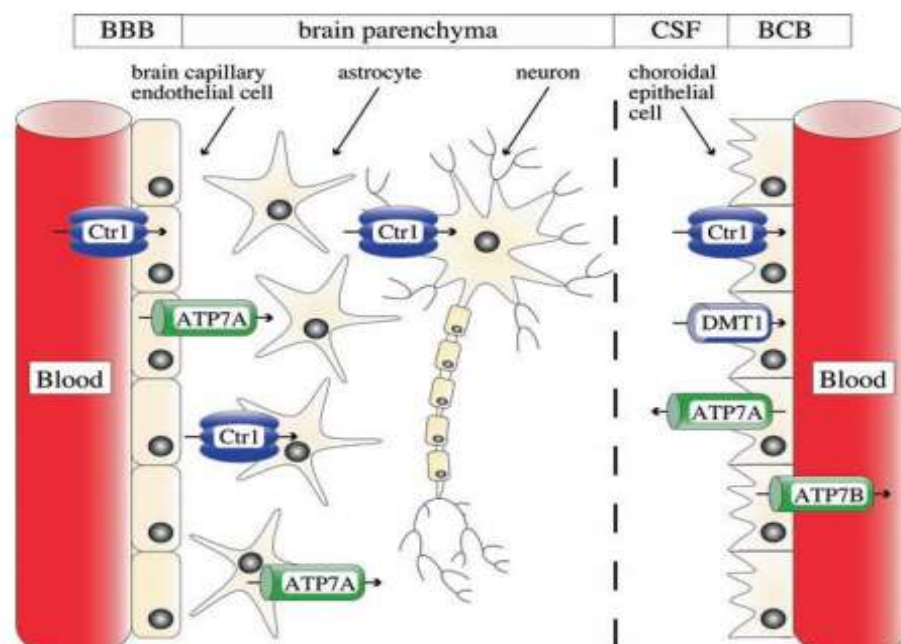


Figure 8: Brain Copper Homeostasis
Mechanisms of Cu transport into the brain and the proteins that play a role in maintaining brain Cu homeostasis (Bulcke *et al.*, 2017).

Total brain Cu content has been estimated to be 3.1 $\mu\text{g/g}$ wet weight in humans, but the brain has many anatomically and physiologically different regions which vary in specific Cu content (Lech and Sadlik 2007; Davies *et al.*, 2012; Krebs *et al.*, 2014; Ramos *et al.*, 2014). Altered homeostasis and mislocation of brain Cu are commonly linked to AD and other neurodegenerative disorders (Mathys and White, 2017). Alzheimer's disease is the most common form of adult neurodegeneration characterized by a progressive loss of cognitive function and eventual death (Mathys and White, 2017). Amyloid plaque and tau neurofibrillary tangle formation, chronic neuroinflammation, oxidative stress, and disruption in essential metal homeostasis are the major neuropathological hallmarks of this disease (Mathys and White, 2017). Major changes in the levels and localization of Cu have been identified in the brains of people with AD, with Cu accumulation being seen in the amyloid deposits and subsequent Cu deficiency being observed in other brain regions (Mathys and White, 2017).

Furthermore, Cu binding sites are present in the amyloid precursor protein (APP) and amyloid beta (A β) peptide, which can lead to possible Cu interactions that may result in the formation of ROS and potential neurotoxic outcomes (Mathys and White, 2017). Specifically, it is suggested that the Cu⁺² reductase activity that is present within the Cu binding domain of APP contributes majorly to free radical formation that is sufficient enough to promote Cu-mediated neurotoxicity (Hung *et al.*, 2010). Extracellular Cu in the brain may also activate the Fenton/Haber-Weiss reactions, leading to an overall increase in the brain oxidative stress load (Brewer, 2008; Gybina *et al.*, 2009) (Figure 9).

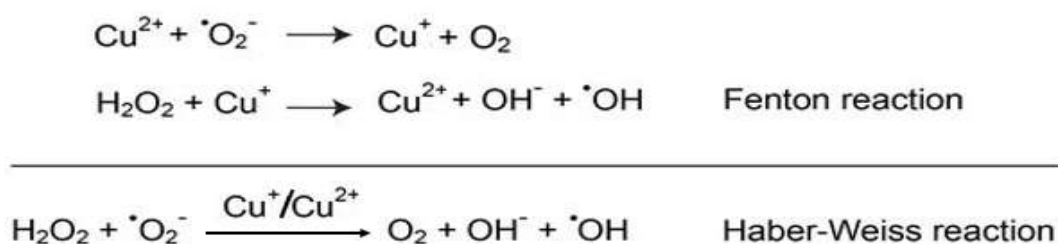


Figure 9: Fenton/Haber-Weiss Reactions Involving Copper
 Depiction of the generation of reactive oxygen species through the participation of Cu in the Fenton/Haber-Weiss reactions (derived from Mathys and White, 2017).

The mechanisms involved in this mis-location of Cu are not fully understood, however CTR1 and ATP7A and ATP7B are the main transporters involved in the regulation of Cu⁺¹ in the brain, while the Divalent Metal Transporter 1 (DMT1) is thought to play a major role in the delivery of Cu⁺² in the brain (Kuo *et al.*, 2006; Zheng and Monnot 2012; Yu *et al.*, 2017) (Figure 10). Additionally, molecular chaperones of Cu, such as antioxidant protein-1 (ATOX1), cytochrome oxidase c copper chaperone (COX17), and copper chaperone protein for superoxide dismutase (SOD), are all thought to play a part in brain Cu localization (Harris, 2001; Zheng and Monnot 2012). Divalent Cu is also involved in the expression of the matrix metalloproteinases (MMP) responsible for the degradation of A β , the major components of amyloid plaques, by

activating a glycogen synthase pathway, which also contributes to tau hyper-phosphorylation (Li *et al.*, 2017). In the synaptic cleft, Cu also can bind to A β and facilitate the formation of senile plaques (Li *et al.*, 2017).

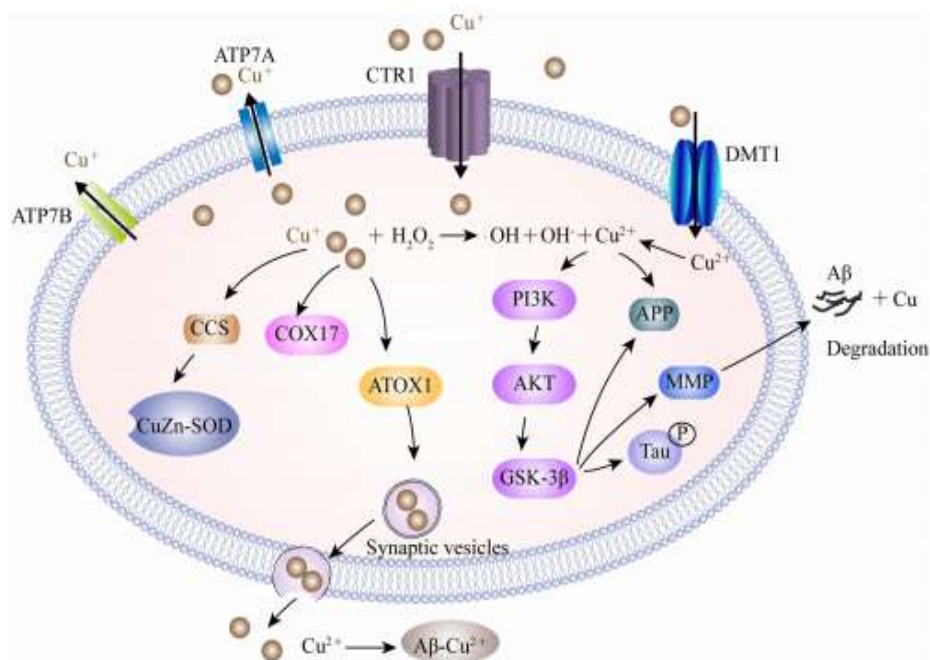


Figure 10: Copper Transport and Association with Alzheimer's Disease
Proteins involved in Cu transport into and out of the brain as well as the proteins that are associated with Cu and its association with Alzheimer's Disease (Li *et al.*, 2017).

2.5.4. Copper and Oxidative Damage

The redox activity of Cu occurs as it cycles between the Cu⁺¹ and Cu⁺² states. The role of Cu in the pathology of neurodegenerative disorders such as AD and Parkinson's Disease (PD) is largely due to its redox capabilities, as well as its ability to bind with molecular oxygen (McCord and Fridovich, 1969). The mitochondria are one of the major targets for Cu-induced oxidative damage (Bulcke *et al.*, 2017). However, this redox capacity is important for biological energy metabolism performed by cytochrome C oxidase, ceruloplasmin-driven iron metabolism, antioxidant activity controlled by Cu and Zn superoxide dismutase (SOD1), and neurotransmitter synthesis by dopamine- β -monooxygenase (Davies *et al.*, 2013; Scheiber *et al.*, 2014).

The oxidative damage caused by Cu and/or Cu-induced oxidative stress may also lead to activation of the tumor suppressor protein P53, which triggers apoptosis (Wang *et al.*, 2014; Phatak and Muller, 2015). Inflammation is normally a protective response for the brain to prevent cell injury, but during periods of Cu dis-homeostasis in AD, inflammation can be triggered by abnormal protein aggregation or by pro- and anti-inflammatory cytokine imbalances (Wyss-Coray and Mucke, 2002; Minghetti, 2005; Mathys and White, 2017). Copper is known to play a major role in both toxic and protective inflammatory reactions, and it is well established that Cu induces peripheral secretion of IL-6 and IL-8 (Kennedy *et al.*, 1998; Schmalz *et al.*, 1998; Choo *et al.*, 2013).

2.5.5. Copper Protein of Interest

The high-affinity copper transport protein 1 (CTR1), coded by the gene SLC31A11, is known to be ubiquitously expressed in all tissue types (Kuo *et al.*, 2001). Most importantly, CTR1 is responsible for making Cu bioavailable so it can be used by proteins for proper functioning (Gupta and Lutsenko, 2009). It has been found CTR1 is expressed in the placenta, aiding in the transport of Cu between fetal and maternal circulation (Kuo *et al.*, 2001; Michelsen-Correa *et al.*, 2021). This Cu transport protein is controlled at the post-transcriptional level based on the Cu concentration of the cells (Petrus *et al.*, 2003). The protein is localized in a stable form on plasma membranes under Cu-depleted conditions, but loses stability in the presence of excess Cu levels (Molloy and Kaplan, 2009). Additionally, in an experiment with cultured HEK cells, it was observed that high levels of Cu induce CTR1 endocytosis and degradation (Guo *et al.*, 2004). It is hypothesized that CTR1 expression will be decreased under high Cu conditions. This is expected to prevent the uptake of excessive Cu, which could lead to detrimental health

effects. There may also be an increased presence of a precursor protein in the presence of excess Cu, as an indicator of CTR1 inactivity.

2.5.6. Copper Conclusions

Copper is an essential element required for a wide array of biological processes ranging from cellular respiration to free radical synthesis. It also acts as an essential cofactor for proteins that play a role in antioxidant defenses. Even though Cu is an essential element, excessive concentrations in humans can result in negative health effects, so tight homeostatic regulation exists. Copper is majorly absorbed through the small intestine and the copper transport protein (CTR1) is partially responsible for the bioavailability of Cu in the human body as well as Cu transport into the brain. Altered Cu homeostasis in the brain is the key factor in AD, which involves Cu mis-locations rather than excess or deficiency. However, excess Cu may exacerbate some health conditions, leading to loss of Cu function in certain cell types and Cu-mediated toxicity in others. The ability of Cu to easily cycle between Cu^{+1} and Cu^{+2} states results in the generation of reactive oxygen species, leading to oxidative stress-induced damage in mammalian cells, one of the major contributing factors to the toxic nature of Cu.

2.6. Manganese

2.6.1. Manganese General Information

Manganese (Mn) is one of the most abundant naturally occurring metals in the earth's crust (Soares *et al.*, 2017). Manganese can transition between 5 valence states but is majorly found as Mn^{2+} or Mn^{3+} (Aschner *et al.*, 2007). There are many environmental sources of Mn, which include erosion of metal-bearing rocks and soils, decomposed plants, use of fungicides, mining and smelting, and combustion of Mn-containing emissions (O'Neal and Zheng, 2015). Manganese exposure can occur in a variety of environmental settings, and through the ingestion

of contaminated food and water, contact with contaminated soils, or inhalation of contaminated dust (O'Neal and Zheng, 2015). In the environment, Mn is majorly found in an oxidized form as MnO_2 or Mn_3O_4 (Post, 1999).

In the human body, Mn primarily exists as Mn^{2+} or Mn^{3+} , of which Mn^{2+} in the blood is bound to albumin and β -globulin (Harris and Chen, 1994; Reaney *et al.*, 2002; O'Neal and Zheng, 2015). Meanwhile, virtually all Mn^{3+} is bound to transferrin (Tf) to form a stable complex (Michalke and Fernsebner, 2014). In the tissues of bones and major organs, Mn exists primarily as Mn^{2+} (Crossgrove and Zheng, 2004). Manganese is absorbed quickly by the human body via oral and inhalation exposures but has a much shorter half-life in the blood compared to the tissues once inside the body (O'Neal and Zheng, 2015). Data has suggested that Mn accumulates extensively in human bone with a half-life of 8-9 years (O'Neal and Zheng, 2015).

Manganese is essential to human health, as it acts as an active site co-factor for many enzymes required for overall development, brain development and functioning, maintenance of nerve and immune cell functions, and regulation of blood sugar and vitamins (Aschner *et al.*, 2007; Crossgrove and Zheng, 2004; Guilarte, 2010). However, overexposure to Mn can be toxic to the human body. In human tissues, normal Mn concentrations should be around 1 mg/kg in bone, 1.04 mg/kg in the pancreas, 0.98 mg/kg in the kidney, and 4-15 $\mu\text{g/L}$ overall in the human body (Rahil-Khazen *et al.*, 2002; Liu *et al.*, 2014; Manganese | Toxicological Profile | ATSDR, n.d.). Manganese in the human body is transported and regulated by many macromolecules such as zinc transport protein 10 (ZNT10), MT, DMT1, Cp, and SOD1 (Gibbons *et al.*, 1976; Au *et al.*, 2008; Sheng *et al.*, 2012; DeWitt *et al.*, 2013).

2.6.2. Manganese Metabolism

Manganese absorption occurs primarily through the gastrointestinal tract, but also can occur in the lungs following inhalation of contaminated materials, or through oral exposure (Nadaska *et al.*, 2012). Gastrointestinal absorption is influenced by Fe metabolism; therefore, an Fe deficiency increases the absorption of Mn through transport proteins shared by the metals (DeWitt *et al.*, 2013). The highest Mn uptake occurs in the liver, second only to the brain, but inhaled Mn can bypass the liver, entering directly into the bloodstream and then into the brain via the olfactory tract, allowing it to bypass the BBB (Chua and Morgan, 1997; Lucchini *et al.*, 2012; Zoni *et al.*, 2012).

Once Mn enters the circulation, it accumulates mainly in the liver, brain, and bone (Subramanian and Meranger, 1985; Rahil-Khazen *et al.*, 2002; Krebs *et al.*, 2014; Liu *et al.*, 2014). The liver is known to store high amounts of Mn and hepatobiliary excretion accounts for 80% of Mn elimination (Chua and Morgan, 1997; O'Neal and Zheng, 2015). Due to the high excretion responsibility of the liver, damage to this organ can result in excessive accumulation of brain Mn and an increased risk of neurodegeneration with continued Mn exposure (Long *et al.*, 2009; Squitti *et al.*, 2009).

2.6.3. Manganese and Neurological Disorders

The brain is said to be the target organ of Mn toxicity, with Mn accumulating in regions of the brain that have high Fe concentrations (Robison *et al.*, 2013; O'Neal and Zheng, 2015). Divalent Mn (Mn^{2+}) is thought to be transported into the brain mainly by DMT1, but citrate transporters, and a Zn transport protein (ZIP8), are also suggested to play a role in its delivery (Chua and Morgan, 1997; Aschner *et al.*, 2007; Yokel, 2009; Michalke and Fernsebner, 2014). Trivalent Mn (Mn^{3+}), is thought to enter the brain primarily through complexation with Tf via a

transferrin receptor (Tfr)-mediated process (Zheng and Chodobski, 2005). Once inside the brain tissues, Mn accumulates in certain brain structures and has a half-life of about 5-7 days (Grünecker *et al.*, 2013; O'Neal and Zheng, 2015). Elimination of Mn from the brain is much slower than that of other organs, which is thought to be caused by slow eliminations from the CSF or that redistribution from bone to the CNS may occur (Crossgrove and Zheng, 2004; O'Neal *et al.*, 2014; O'Neal and Zheng, 2015).

It has been demonstrated that pregnant women accumulate Mn at increased levels compared to others, and since Mn is transported through the placenta, elevated maternal Mn exposure can lead to fetal overload (Takser *et al.*, 2004; Erikson *et al.*, 2007; Oulhote *et al.*, 2014). As a result, there may be accumulation in the developing brain as well as changes in neurological structures, which may cause motor, cognitive, and behavioral impairments (Lucchini *et al.*, 2017). Children also accumulate higher levels of Mn and eliminate less Mn than adults, making them more susceptible to Mn toxicity (O'Neal and Zheng, 2015). Inhalation of airborne particles is one of the primary sources of early-life exposure, and those living near industrialization processes may be at higher risk for child developmental issues (Lucchini *et al.*, 2017).

Exposure to Mn has been proven to result in clinical signs and symptoms similar to PD with notable variations (O'Neal and Zheng, 2015). Similar clinical observations are thought to lie within changes in neurotransmission rather than massive dopamine neuronal cell loss which are selectively lesioned in PD, but remain intact following excessive Mn exposure (Guilarte, 2010; O'Neal and Zheng, 2015). Once the signs and symptoms of Mn neurotoxicity appear, they are typically irreversible and progress despite removal from the exposure environment (O'Neal and Zheng, 2015). It has been shown that Mn may alter neuron repair processes by competing

with Cu for transport, intracellular storage, and trafficking, which may contribute overall to the non-motor symptoms seen in Mn-induced Parkinsonian disorder (O'Neal and Zheng, 2015). Additionally, interactions with Mn and Pb or As are known to lead to severe neurodevelopmental deficiencies compared to single-metal exposures (Claus Henn *et al.*, 2012; Rodrigues *et al.*, 2016).

2.6.4. Manganese and Oxidative Damage

Manganese-induced neurotoxicity is regulated by many factors such as oxidative injury, mitochondrial dysfunction, protein misfolding, and neuroinflammation (Harischandra *et al.*, 2019). Since Mn is a redox-active element possessing a high reduction potential, accumulation of Mn under altered homeostatic conditions can lead to the formation of ROS, and an overall increase in the oxidative stress load in an organism (Harischandra *et al.*, 2019). Manganese can also impair cellular antioxidant machinery, leading to an imbalance between ROS generation and its elimination, which plays a major role in Mn-induced neurodegenerative processes (Harischandra *et al.*, 2019). In the brains of humans exposed to Mn, glial cell activation occurs, which plays an important role in increasing Mn-induced neurotoxicity by causing the release of ROS and pro-inflammatory cytokines (Harischandra *et al.*, 2019). It is suggested Mn accumulation can occur in many organelles under acute exposure, however, under chronic exposures, Mn is found majorly in the mitochondria, leading to mitochondrial dysfunction (Morello *et al.*, 2008). Manganese transport into cells and organelles is controlled but a wide variety of transporters (Figure 11)

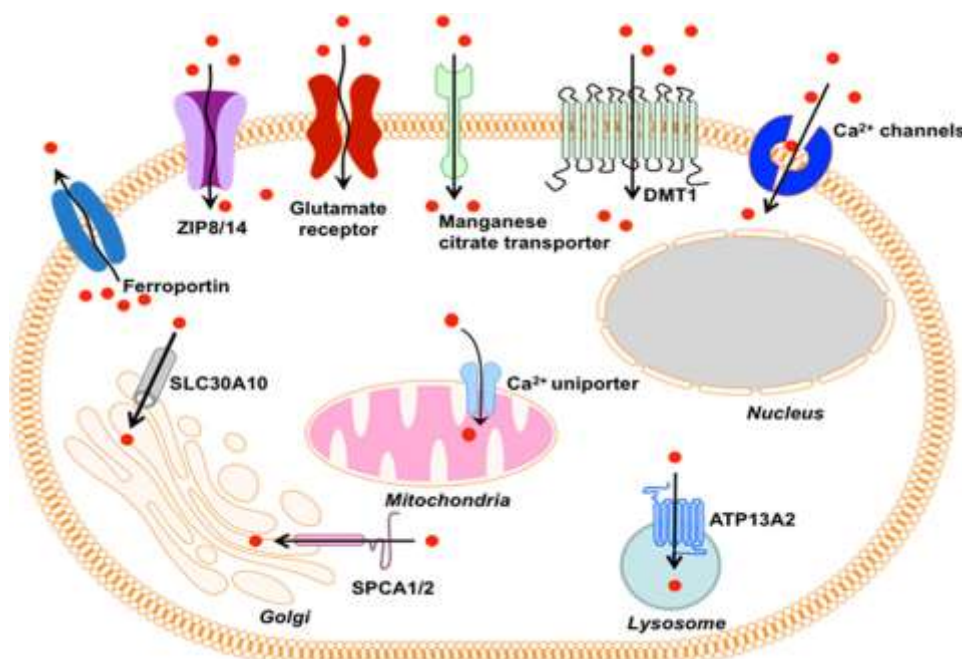


Figure 11: Cellular Manganese Transport
 Depiction of the different proteins involved in manganese transport into mammalian cells (Harishchandra *et al.*, 2019)

2.6.5. Manganese Protein of Interest

The solute carrier, ZNT10, coded by the gene SLC30A10, has been suggested to regulate Mn export from cells and play a protective role against Mn toxicity (O'Neal and Zheng, 2015; Zogzas and Mukhopadhyay, 2017). This protein is highly expressed in the liver and possesses a higher specificity for Mn over Zn (O'Neal and Zheng, 2015). An autosomal-recessive mutation that blocks the Mn efflux activity of this protein results in increased Mn accumulation in cells, which can lead to adult-onset Parkinsonism (Quadri *et al.*, 2012). In a study of a patient harboring a homozygous mutation in SLC30A10, approximately a 10-fold increase was seen in blood Mn levels and the patient developed difficulty walking and conducting fine hand motor movements (Tuschl *et al.*, 2008). It is hypothesized that ZNT10 will be upregulated in the presence of high Mn concentrations to export excess Mn out of the cells to avoid Mn-induced toxicity.

2.6.6. Manganese Conclusions

Manganese is an essential trace element that acts as an active site co-factor for many enzymes and is also required for brain development and functioning. In excess, Mn can become harmful to the human body, so there is a strict homeostatic mechanism to control the levels of Mn within the cells. This homeostatic mechanism involves the transport of Mn by zinc transport protein 10 (ZNT10), as well as other metal transporters. Manganese absorption into the human body occurs mainly via the gastrointestinal tract and once in circulation, the brain is one of the major organs in which Mn accumulates. Manganese can also cross the BBB and placental barrier, increasing its toxicity since it can bypass these two major protective barriers. Excessive Mn exposure has been proven to result in Manganese-induced Parkinsonism, which presents with symptoms similar to PD.

2.7. Zinc

2.7.1. Zinc General Information

Zinc is the second most abundant transition metal after Fe in living organisms and is the only metal cofactor found in more than 300 enzymes (Rink, 2000; VasÅik, 2000). The major role of Zn in biological systems is to stabilize the structure of proteins, including signaling enzymes that are part of signal transduction and transcription factors (Beyersmann, 2002). Zinc is an essential catalyst and co-catalyst in enzymes that control DNA synthesis, normal growth, brain development, membrane stability, bone formation, and wound healing (Barceloux, 1999; Mocchegiani *et al.*, 2000). Zinc is also considered to be crucial for immune responses, as it influences and interacts with many components of the immune system (Chasapis *et al.*, 2012).

Around 85% of Zn within the human body is localized in bone and muscle and 11% in the skin, liver, and remaining tissues (Chasapis *et al.*, 2012). Daily dietary intake of Zn is

recommended to be 15 mg/day, and the tolerable upper intake level of Zn is listed at 25 mg/day (MacDonald, 2000; Tapiero and Tew, 2003). The effect of Zn on the body depends majorly on the dose and length of exposure, where long periods or high exposure may provoke Zn accumulations with subsequent toxicity (Chasapis *et al.*, 2012). Zinc ions within the body are hydrophilic and are unable to cross membranes by passive diffusion, but rather transport has been described as possessing saturable and non-saturable components depending on the Zn concentration (Chasapis *et al.*, 2012).

2.7.2. Zinc Metabolism

Chronic and acute exposure can lead to Zn poisoning, so cellular levels of Zn are typically maintained in the range of 0.1 and 0.5 mM (Eide, 2006). To maintain this homeostatic range, eukaryotes possess MTs that control cellular Zn levels, as well as compartmentalization techniques (Maret, 2003). Metallothioneins play a major role in the detoxification of metals, specifically Zn and Cu due to high binding efficiencies for these metals (Chasapis *et al.*, 2012). This homeostatic control works to avoid excessive Zn accumulation and is controlled mainly by a Zn-importer (ZIP) family and a Zn-exporter family (ZNT) (Figure 12) (Lichten and Cousins 2009).

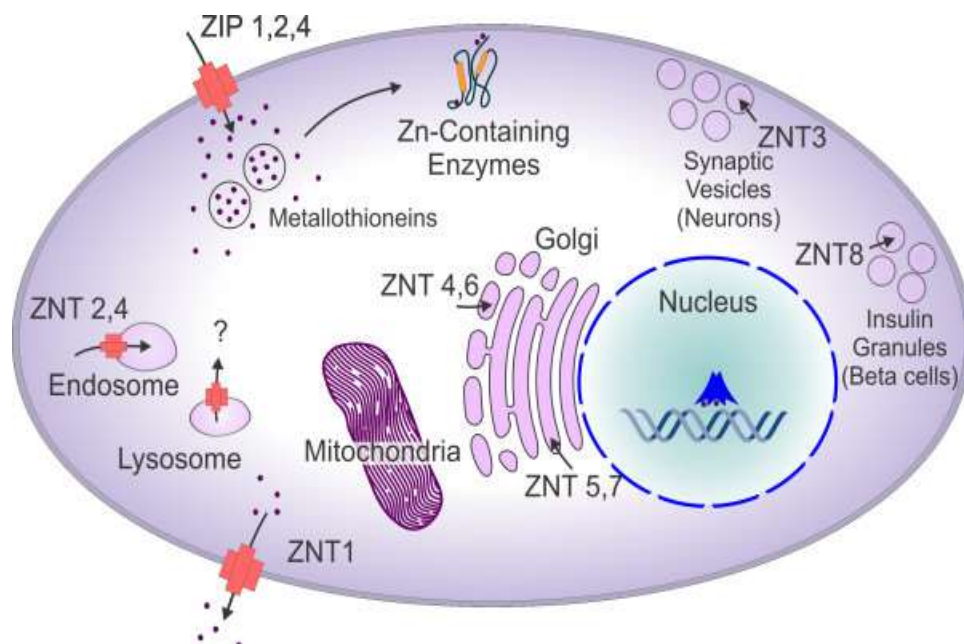


Figure 12: Zinc Transport in Mammalian cells
Cellular Zn localization within mammalian cells via ZNT and ZIP transporters (John *et al.*, 2010).

A disruption of Zn homeostasis in the brain is associated with altered expression of MTs and ZNT1 (Chasapis *et al.*, 2012). When MTs bind to Zn, they protect against oxidative stress and work to suppress cell death via apoptotic pathways by redistributing cellular Zn (Chasapis *et al.*, 2012). Additionally, MTs play an important regulatory role in the uptake, distribution, storage, and release of Zn and may also play a competing role in Zn absorption with the common transport proteins (VasÅik, 2000). When Zn is high, it can also reduce Cu bioavailability via MT induction (Michelsen-Correa *et al.*, 2021). Therefore, Zn excess may lead to Cu deficiency (Michelsen-Correa *et al.*, 2021).

2.7.3. Zinc and Neurological Disorders

Zinc-induced neurotoxicity has been indicated to play a role in neuronal damage often associated with stroke, seizures, and neurodegenerative disorders (Morris and Levenson, 2017). In addition to neuronal damage, the mechanisms that lead to Zn-induced neurotoxicity include mitochondrial and energy production dysfunction as well as the aggregation of A β peptides

found in AD (Morris and Levenson, 2017). One of the metal's major roles in neurodegenerative disorders is linked to its ability to modulate N-methyl-D-aspartate (NMDA) receptors, which are permeable to Zn ions (Inoue *et al.*, 2015; Morris and Levenson, 2017). Free, excess Zn ions not only modulate these receptors, but also act as intermediates in biochemical cascade events such as calcium dysregulation, ROS production, mitochondrial disruption, and excitotoxicity that leads to neuronal damage or death (Granzotto and Sensi 2015; Wang *et al.*, 2015; Morris and Levenson, 2017).

Several studies have shown that Zn metabolism is altered in AD and other neurodegenerative diseases (Aschner, 1996; Wang *et al.*, 2010). Post-mortem analyses have shown that there are marked accumulations of Zn in A β plaques, which is thought to be because the A β peptide has several Zn-binding sites (Dong *et al.*, 2003; Friedlich *et al.*, 2004; Stoltenberg *et al.*, 2005). Because of these binding sites, Zn is the only physiologically available metal can precipitate with A β plaques, so this observed enrichment indicates that Zn binding plays a role in the formation of the A β plaques (Faller, 2009) (Figure 13).

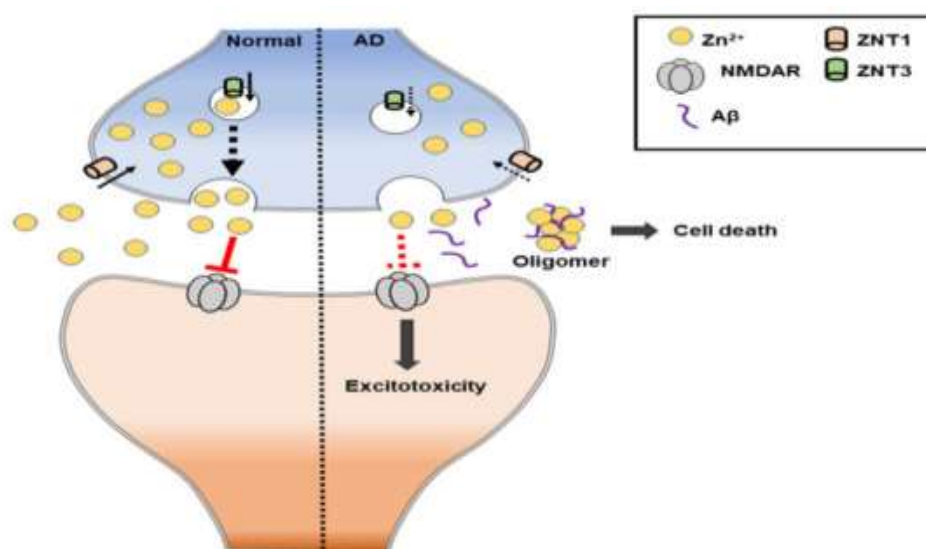


Figure 13: Zinc Transport and Association with Alzheimer's Disease
Interaction of Zn and beta-amyloid oligomers in AD after NMDAR-assisted influx into neurons (Choi *et al.*, 2020).

2.7.4. Zinc and Oxidative Damage

Excess Zn can easily become sequestered by the mitochondria, which triggers the generation of ROS by interfering with the activity of complex III of the electron transport chain (Frazzini *et al.*, 2006). This leads to mitochondrial dysfunction and neuronal death, which is a major link between Zn and a variety of neurodegenerative disorders (Frazzini *et al.*, 2006). Unlike other transition metals, Zn does not undergo redox reactions, due to the additional stability that the metal possesses with a fully occupied d shell (Chasapis *et al.*, 2012). Zinc is suggested to have a dual effect on the secretion of pro-inflammatory cytokines, as it is known to trigger as well as suppress the release of these molecules (Bao *et al.*, 2003). Supplementation of Zn in humans has been associated with decreases in IL-6 and TNF α (Zhou *et al.*, 2004; Chasapis *et al.*, 2012).

Even though excess Zn levels can lead to the induction of oxidative stress in some situations, Zn is known to play a major protective role against oxidative stress in the body (Marreiro *et al.*, 2017). Zinc can act as an anti-inflammatory agent by providing structural stability to cell membranes and induced metallothionein synthesis, which is involved in the reduction of hydroxyl radicals and the sequestration of ROS (Marreiro *et al.*, 2017). Additionally, Zn is a structural component of SOD, which plays a role in reducing the overall toxicity of the ROS within the cell (Marreiro *et al.*, 2017).

2.7.5. Zinc Protein of Interest

The protein, Zinc Transporter 1, (ZNT1), is the only member of the SLC30 family of proteins that transports the metal directly across the plasma membrane, whereas other members of the family employ vesicles known as zinosomes to aid in Zn sequestration (Haase and Maret 2003; Taylor *et al.*, 2008). This protein, coded by gene SLC30A1, is ubiquitously expressed in

all tissues and becomes upregulated in the intestine, brain, and placenta when dietary Zn intake increases (Andrews *et al.*, 2004; Chohanadisai *et al.*, 2005; Helston *et al.*, 2007; Huang and Tapaamorndech, 2013). In mice, it has been found that ZNT1 plays an essential role in embryonic development, maternal Zn transport to the embryo, and cellular Zn homeostatic maintenance (Andrews *et al.*, 2004). It is predicted that excess Zn levels will result in increased expression of ZNT1 in order to avoid accumulation of Zn in cells.

2.7.6. Zinc Conclusions

Zn is an essential element that is a metal co-factor in more than 300 enzymes, acting to stabilize protein structures. Since excess Zn can be toxic to humans, a homeostatic mechanism involving metallothioneins and two families of Zn transporters is used to maintain Zn levels in a desirable range. The transport protein ZNT1 is ubiquitously expressed in mammalian cells and is upregulated in most tissues in the presence of excess Zn. Disruption of Zn homeostasis has been linked to several neurodegenerative diseases, including AD. Even though excess Zn levels can be linked to the formation of reactive oxygen species and lead to neurological disorders, Zn is also known to play a protective role against oxidative stress in the human body.

2.8. Meconium

Meconium is the first stool secreted by a newborn and is made up of accumulated waste material ingested from the amniotic fluid beginning from the 12th week of gestation forward (Michelsen-Correa *et al.*, 2021). Meconium is normally excreted by the fetus in the first day or two after birth (Michelsen-Correa *et al.*, 2021). Since meconium indicates material accumulation over 6 months, analysis of meconium samples has been used to assess long-term exposure to heavy metals for gestating mothers living in highly polluted environments (Li *et al.*, 2008). Essential metals such as Zn, Fe, Cu, and Mn are needed for the synthesis of cofactors that

perform many functions during fetal development but are also detrimental if the fetus becomes exposed to excess concentrations (Michelsen-Correa *et al.*, 2021).

Exposure to Cu, Mn, Zn, As, and other metals through inhalation, dermal absorption, and ingestion of contaminated food, soil, and dust has been shown to significantly increase the risk for neurodevelopmental disabilities in children exposed in utero and/or during childhood (Liu *et al.*, 2010; McDermott *et al.*, 2011; Ciesielski *et al.*, 2012; McDermott *et al.*, 2013; Rodríguez-Barranco *et al.*, 2013; Al-Saleh *et al.*, 2014; Claus Henn *et al.*, 2017; Aschner and Costa, 2011–2018). Meconium provides an ideal matrix to assess pre-natal metal exposure for infants, as collection is non-invasive and easy to perform (McDermott *et al.*, 2020). However, even when metals are found to be present in meconium samples, it is difficult to differentiate between “background” metal exposure from anthropogenic source exposure or to determine what concentration will be detrimental to the fetus (Michelsen-Correa *et al.*, 2021).

During gestation, foreign substances, including metals, are predominantly deposited in meconium directly from bile secretion or the fetus swallowing amniotic fluid containing the toxicants (Ortega García *et al.*, 2006). Although maternal blood and hair, infant hair, and cord blood can be used to assess metal exposure, a higher percentage of metals has been detected through meconium analysis than the other sample matrices (Ostrea *et al.*, 2008). Additionally, metal analyses of maternal and cord blood only indicate recent exposures and fetal exposure around the time of birth, unless the metals have been mobilized from maternal stores (Michelsen-Correa *et al.*, 2021).

Meconium formed during development and passed by the neonate may contain proteins that provide a characterization of the intrauterine environment (Lisowska-Myjak *et al.*, 2018). However, meconium protein composition can vary throughout intrauterine development

(Lisowska-Myjak *et al.*, 2018). A wide variety of proteins have been identified in meconium samples, including proteolytic enzymes, protease inhibitors, enzymes involved in lipid and carbohydrate metabolism, immunoglobulins, and neutrophil-derived proteins (Lisowska-Myjak *et al.*, 2018).

Ionic metals and other elements may be transported from the mother to the fetus via simple diffusion at the placental interface (Michelsen-Correa *et al.*, 2021). Due to similarities of charge, size, and structure, some metals, such as Cd, can pass through channels that are biologically designated to actively transport essential metals such as Fe or Zn (Ballatori, 2002; Bridges and Zalups, 2005). The placenta plays a multi-level protective role against xenobiotic transfer to the fetus, with one of the major protective agents being proteins that are expressed by cells along with the placental interface that sequester, detoxify, or transfer toxic substances back to maternal circulation (Michelsen-Correa *et al.*, 2021). The ability of the placenta to control the transfer of essential and non-essential metals may differ throughout development (Mikheev *et al.*, 2008).

Metals that primarily undergo fecal excretion include Mn, Cu, and Zn, while As relies on both urinary and fecal excretion routes (Gregus and Klaassen, 1986). Metals may also accumulate in the liver and kidney or other fetal tissues in addition to deposition in meconium during gestation (Kuriwaki *et al.*, 2005; Thévenod and Wolff, 2016; Michelsen-Correa *et al.*, 2021). It is unknown whether metal mixture exposures have different depositions in meconium than single metal exposures (Michelsen-Correa *et al.*, 2021).

2.9. Inflammatory Markers

2.9.1. Interleukin 6

Interleukin-6 (IL-6) is a pro-inflammatory cytokine that plays major roles in host defense, inflammation, cancer, and cellular growth and hypertrophy (Hunter and Jones, 2015; Rose-John, 2015). Interleukin 6 is important for hepatocyte regulation and processes in the placenta, nervous system, and endocrine system (Kishimoto *et al.*, 1995). This cytokine is found to be activated in the CNS during neuroinflammation associated with CNS infection or injury as well as several other conditions (Erta *et al.*, 2012). This suggests that IL-6 plays a critical role in maintaining homeostasis of neuronal tissue, however, overproduction of this cytokine in the brain can result in neurodegeneration (Rothaug *et al.*, 2016).

Under physiological conditions, low levels of IL-6 are present, but a dramatic increase in IL-6 secretion and expression is observed in various neurological disorders such as AD and PD (Benveniste, 1998; Rothaug *et al.*, 2016). Additionally, IL-6 can exert neuroprotective properties by increasing MT I and II, which are both known to inhibit cell death and brain damage and promote tissue recovery (Penkowa, 2006). Many cytokines, such as Tumor Necrosis Factor alpha (TNF- α), inflammatory factors, neurotransmitters, and neuropeptides have been shown to change IL-6 regulation in brain cells, mainly driven by membrane depolarization (Sallmann *et al.*, 2000; Erta *et al.*, 2012). Since exposures to the metals of interest are known to increase ROS formation, it is expected that IL-6 expression will be increased to deal with the increased oxidative stress load caused by the exposures.

2.9.2. Tumor Necrosis Factor alpha

Tumor necrosis factor alpha (TNF- α) is a homotrimer protein of approximately 17 kDa subunits that is identified as a pro-inflammatory cytokine (Santello and Volterra, 2012). This

cytokine and its receptors regulate many physiological functions, including immune surveillance, immune reactions, induction of cell death, and play important roles in the CNS (Locksley *et al.*, 2001; Bradley, 2008; Incorvaia *et al.*, 2008; Clark *et al.*, 2010). Due to its participation in many physiological processes, the expression of TNF- α is tightly regulated at the transcriptional, post-transcriptional, and translational levels to maintain important homeostasis (Decourt *et al.*, 2017).

There has been increasing evidence suggesting that TNF- α , along with its receptors, are present in the normal brain and display various specificities of expression and action (Santello and Volterra, 2012). Signaling of TNF- α plays a role in many CNS conditions and diseases such as PD and AD, as these constitutively expressed levels likely undergo deleterious transformations during CNS pathologies (Santello and Volterra, 2012). Once chronic brain inflammation is initiated, an upward spiral occurs, maintaining excessive levels of TNF- α , which can stimulate A β synthesis and neuronal loss (Koenigsknecht-Talboo, 2005). It has also been indicated, through in vivo studies, that TNF- α signaling exacerbates A β and tau pathologies seen in AD (Decourt *et al.*, 2017). Expression of TNF- α is expected to be increased to manage the increased oxidative stress load caused by exposure to metals and metal mixtures.

3. Research Goals

A preliminary bioavailability study was performed to determine the average concentrations of As, Cd, Cu, Pb, Mn, and Zn from residential soil and household dust samples from houses near current and historic mining operations (Figure 14). The average overall concentrations of the metals present in the samples as well as concentrations obtained from a physiological based extraction test (PBET) performed on the same samples were used to determine the percent of the metals bioavailable in each sample type. These values were then identified as the baseline concentrations of which cultures of two mammalian cell lines would be exposed to in order to investigate single metal and metal-mixture effects on mammalian cells.



Figure 14: Map of Sampling Location for Preliminary Bioavailability Study
 Visualization of the large surface mining activities within city limits. Greely neighborhood, outlined in red, and the proximity to the mining concentrator, outlined in yellow. The red markers within the Greely neighborhood boundary indicate the locations from which samples were collected.

It has been hypothesized that exposure to single metals and metals mixture found in Butte Montana's mining contaminated environment will affect the expression of four select proteins and two inflammatory markers, which can lead to the development of numerous health issues, such as neurodevelopmental and neurodegenerative disorders. To determine a link between metal

exposure in Butte and possible health effects, the inflammatory cytokines, Tumor Necrosis Factor alpha (TNF- α) and Interleukin-6 (IL-6), were measured by enzyme-linked immunoassay (ELISA). The arsenic methyltransferase protein (AS3MT), copper transport protein (CTR1), zinc transporter protein (ZNT10), and zinc transporter protein (ZNT1), were analyzed by western blot experiments. Expression of these proteins was investigated from previously collected meconium samples, as well as cultures from a human bronchial epithelial cell line (BEAS- 2B), and a human embryonic kidney cell line (HEK-293), that were exposed to varying concentrations of single metals and metals mixtures to potentially mimic chronic, low-level exposure over two weeks.

There is a limited knowledge base about the impact of metal mixtures in humans. Information on the interactions of metals that are essential elements is even more limited. This research will attempt to provide information on the impact of metal mixtures, some of which are essential elements, in mammalian cells. This is the beginning step towards gaining an understanding of how these mixtures affect the complete organism. Furthermore, this study can be used to provide a framework for preventive interventions, including specific environmental monitoring requirements that can help to minimize adverse health impacts for populations at risk due to single metal and metal mixture contamination in their communities. Lastly, this research has the potential to define new metals and metal mixtures that should be considered by environmental and public health regulatory agencies to protect human health.

4. Research Methods

4.1. Preliminary Bioavailability Study

4.1.1. Trace Metal Cleaning Protocol

To trace metal clean the polypropylene bottles (Environmental Express, Ultimate Cup™-50mL) used for the bioavailability study, the bottles, lids and, digestion caps were submerged in a container filled with 10% nitric acid (v/v) (Fisher Chemical, nitric acid trace metal grade 67-70%) and placed in a clean hood for 24 hours. The bottles and other components were then removed from the 10% nitric acid, rinsed thoroughly with ultrapure water, then submerged in a container filled with ultrapure water and placed in the cleaned hood for 24 hours. The contents were then rinsed a final time and placed in the cleaned hood for two days to dry. If the tubes were not used immediately after drying, they were placed into a trace metal-cleaned Ziploc bag and stored for future use. The Ziploc bags were trace metal cleaned in the same manner, however, the bags were filled with the 10% nitric acid or water and then sealed rather than being submerged in the solutions.

4.1.2. Sample Collection

Ten volunteers were recruited by email through the Greely Neighborhood Coalition. The metals, As, Cd, Cu, Pb, Mn, and Zn were chosen based on a previous study by the PI (Hailer *et al.*, 2017). Researchers collected residential soil samples following a procedure outlined by the Montana Department of Environmental Quality (MTDEQ). Approximately one inch of undisturbed topsoil from 3 higher traffic locations was collected with a plastic hand trowel and placed into trace metal cleaned Ziploc bags (MTDEQ, 2013). Once collected, the soil samples were then allowed to air dry in a trace metal cleaned hood for a week.

Volunteers were asked to collect dust from the floors of at least three main rooms of the house by using a broom on hard flooring or a vacuum cleaner on carpet flooring. The sample was then placed in trace a metal cleaned Ziploc bag provided by the researchers. The volunteers were asked to provide at least 2.0 g of dust and were encouraged to perform more than one round of dust collection to provide researchers with an adequate amount of dust. An information collection sheet was also provided to the volunteers in which they provided the collection date(s), rooms from which the samples were collected from, and method in which they used to collect the samples. The dust and soil samples were cleaned of debris and standardized by sieving the contents to 149 μm with stainless steel sieves (U. S. Standard Sieve, ATM Corporation). The sieves were thoroughly cleaned with ultrapure water before and after each standardization.

4.1.3. Preparation and Digest for Total Metal Content

Approximately 0.1 g of standardized soil or dust was weighed out and placed in an acid-washed 50 mL polypropylene digestion tube to determine total metal concentrations. To each sample, 3 mL of nitric acid and 1.5 mL of ultra-pure water were added. The samples were then digested in a hot block set at 90°C for 4 hours. The samples were allowed to cool and 1 mL of 30% hydrogen peroxide (Sunlight Supply Inc., Hydrogen Peroxide Technical Grade 34%) was added to each sample. The samples were then placed in a hot block set to 70°C for 30 minutes. Once digested, the samples were diluted to 50 mL with ultra-pure water and filtered with 0.2 μm sterile nylon filters (Fisher Scientific, .20 μm) before ICP-OES analysis. This digest method was derived and modified from U.S. EPA method 3050A, Acid Digestion of Sediment, Sludges, and Soils (U.S. EPA, 1992).

4.1.4. Preparation and Digest of Stomach Samples

The bioavailability of metals present in both sample types was evaluated by first digesting the contents in conditions that mimicked those of the gastrointestinal tract. Gastric solution for the stomach and intestinal phase digestions was prepared following published protocols (Sialelli *et al.*, 2010). Approximately 0.4 g of soil or dust was added to 40 mL of gastric solution (pH=2.5, 1.25 g pepsin activity 800-2500 units/mg, 0.50 g citrate, 0.50 g malate, 420 μ L lactic acid, 500 μ L acetic acid) in an acid-washed 50 mL polypropylene bottle and placed in a shaker incubator set at 150 rpm and 37°C for 1 hour. The samples were subsequently centrifuged at 3000 rpm for 10 minutes and a 5 mL aliquot representing the stomach phase was removed from each sample and filtered with 0.2 μ m sterile nylon filters before ICP-MS analysis.

4.1.5. Preparation and Digest of Intestinal Samples

To the bottles containing the stomach samples, 5 mL of gastric solution was added to retain the solid: solution ratio of 0.4 g: 40 mL. The sample mixtures were then neutralized to a pH of 7.0 by adding solid sodium hydrogen carbonate (Puratronic®, sodium hydrogen carbonate 99.998%, metal basis). To the neutralized samples, 70 mg bile salts (Oxoid, bile salts, pH (2% solution) 6.0 at 25°C) and 20 mg of pancreatin (MP Biomedicals, Pancreatin USP) were added. The mixtures were then placed in a shaker incubator set to 150 rpm and 37°C for 2 hours and subsequently centrifuged at 3000 rpm for 10 minutes. A 10 mL aliquot was removed from each sample and filtered with 0.2 μ m sterile nylon filters. From the filtered 10 mL aliquots, 5 mL aliquots were then removed and diluted to 50 mL with a 5% nitric acid matrix. The diluted samples representing the intestinal phase were then analyzed using ICP-MS.

4.1.6. Bioavailability Determination

The bioavailability and distribution data collected were then used to determine the percent bioavailability of each metal in the stomach and intestinal digest phases as compared to the amount of metal found in the total digest (1).

$$\frac{\text{Metal concentration of PBET stomach or intestinal sample (ppm)}}{\text{Metal concentration from total digest of same sample (ppm)}} \times 100 \quad (1)$$

4.2. Biological Experiments

4.2.1. Mammalian Cell Line Metal-Exposure Determination

The average total metal concentrations from each sample type for each metal, determined during the preliminary bioavailability study, were used to calculate what concentration of each metal the mammalian cell cultures should be exposed to as to potentially represent chronic, low-level metal exposure in Butte (Table IV). Determination of exposure concentration for all metals was performed using the same calculation shown below for As (2). Determination of exposure volume for each metal was also performed following the calculation included for As below (3)

The standard solutions of As, Cu, Mn, and Zn were also the standards used for generation of spikes and controls for ICP-MS and ICP-OES analysis in the preliminary bioavailability study (all standards were purchased from CPI International, Single-Element Aqueous RM, 1000 $\mu\text{g/mL}$ concentrations and 2% HNO_3 matrix).

$$\begin{aligned} \text{Avg. soil and dust concentration} &= \frac{(19.81 \frac{\text{mg}}{\text{kg}} + 38.37 \frac{\text{mg}}{\text{kg}})}{2} = 29.09 \frac{\text{mg}}{\text{kg}} \quad (2) \\ &\approx 30.0 \frac{\text{mg}}{\text{kg}} \text{ As} \\ \frac{30.0 \text{ mg As}}{\text{kg sample}} \times \frac{0.00001 \text{ kg sample}}{50.0 \text{ mL Sample}} &= 6.00 \times 10^{-5} \frac{\text{mg}}{\text{mL}} \text{ As} \\ 6.00 \times 10^{-5} \frac{\text{mg}}{\text{mL}} \text{ As} \times \frac{1 \text{ g}}{1000 \text{ mg}} \times \frac{1000 \text{ mL}}{1 \text{ L}} \times \frac{1 \text{ mol As}}{74.92 \text{ g As}} &= 8.01 \times 10^{-7} \frac{\text{mol}}{\text{L}} \text{ As} \end{aligned}$$

where avg. is average, sample dilution is 50.0 mL, sample weight is 0.00001 kg, and 74.92 g is the molar mass of As.

Table IV: Calculated Metal Exposure Concentrations

	Arsenic	Copper	Manganese	Zinc
Concentration (mol/L)	8.01×10^{-7}	2.25×10^{-5}	1.84×10^{-5}	2.04×10^{-5}

$$\left(6.00 \times 10^{-5} \frac{mg}{mL} As\right) \times (20.0 mL media) = \left(\frac{0.1 mg}{mL} standard As solution\right) (x) \quad (3)$$

$$x = 0.001 mL As \approx 1 \mu L As Standard Solution$$

4.2.2. Cell Culture Preparation

Control flasks of two mammalian cell lines, human embryonic kidney cells (HEK-293) (ATCC, 293; Embryonic Kidney; Human (homo sapiens)) and human bronchial epithelial cells (BEAS-2B) (ATCC, BEAS-2B; Bronchial Epithelium; Human (Homo sapiens)), were prepared by seeding 1 mL of frozen stock of each cell type into 20 mL of DMEM growth media (Corning, Dulbecco's Modification of Eagle's Medium, 4.5 g/L, L-glutamine, and sodium pyruvate) containing 10% fetal bovine serum (FBS) (v/v) (Fisher Scientific, Research Grade Fetal Bovine Serum, 500 mL, Triple 0.1 μ m Sterile Filtered) and 1% Penicillin/Streptomycin (v/v) (Lonza, BioWhittaker® Penicillin/Streptomycin) and allowed to grow to 90% confluency in a tissue culture flask (Fisher Scientific, 75 cm², Vented cap, TC treated, Sterile).

Once the cells in the control flasks reached 90% confluency, the growth media was removed from the flasks and 5 mL of Trypsin was added to each flask (Corning 0.25% Trypsin, 2.21 mM EDTA, 1x [-] sodium bicarbonate) to dissociate the adherent cells from the bottom of the flasks. The 5 mL of Trypsin from each control flask of the same cell type was then removed from the flasks and combined in a sterile falcon tube to be re-aliquoted for preparation of culture flask for each exposure scenario (Table V).

Table V: Mammalian Cell Line Metal Exposures

	Arsenic (As)	Copper (Cu)	Manganese (Mn)	Zinc (Zn)
Exposure 1	Control	Control	Control	Control
Exposure 2	As	Cu	Mn	Zn
Exposure 3	As:Cu	Cu:As	Mn:As	Zn:As
Exposure 4	As:Mn	Cu:Mn	Mn:Cu	Zn:Cu
Exposure 5	As:Zn	Cu:Zn	Mn:Zn	Zn:Mn
Exposure 6	As:Cu:Mn:Zn	As:Cu:Mn:Zn	As:Cu:Mn:Zn	As:Cu:Mn:Zn

The flasks were maintained over a two-week period, during which, all flasks were split and re-fed on the same schedule. When the cells were split or re-fed, the same concentration of metal, calculated to potentially represent chronic, low-level exposure was re-added to the culture flask (Table IV).

4.2.3. Protein Extraction Process

4.2.3.1. Mammalian Cell Cultures

For extraction of the proteins from all sample types, a RIPA (radioimmunoprecipitation assay) protein extraction protocol was used. To begin, a 7X protease inhibitor was prepared by adding 1 protease inhibitor pellet (cOmplete™ Mini, EDTA-free Protease Inhibitor Cocktail tablets) to 1.5 mL of biological grade water (Fisher Scientific, HyPure™ Molecular Biology Grade Water, Nuclease-Free). A mixture of RIPA buffer (Boston BioProduct Inc. RIPA Buffer pH=7.4±0.15) and diluted 7X protease inhibitor (1X RIPA + protease inhibitor) was prepared.

Samples were collected from the cell cultures by removing growth media from the cell culture flasks and adding 5 mL of Trypsin to dissociate the adherent cells from the bottom of the flask. All 5 mL of Trypsin was then collected and added to a labeled 15 mL sterile falcon tube. The falcon tubes were then added to a centrifuge and spun at 1400 rpm for 5 minutes to pellet the cells. The cells were then washed in cold, filtered 1X PBS (Gibco, Dulbecco's Phosphate Buffered Saline, [-] Calcium Chloride [-] Magnesium Chloride) and re-pelleted in the same

manner as above. The supernatant was then aspirated off and the tubes were immediately placed onto ice. The pelleted cells were then re-suspended in 250 μ L of 1X RIPA + protease inhibitor and the tubes were vortexed for 10 seconds and placed back on ice to incubate for 10 minutes. This process was repeated 3 times for a total of 30 minutes. The mixtures were then transferred to a 1.5 mL microcentrifuge tube and the tubes were spun in a pre-chilled 4°C centrifuge for 15 minutes at top speed (18,000 rpm). The supernatant or unreduced lysate was then transferred to a new, labeled microcentrifuge tube and stored in the -80°C freezer for further use.

4.2.3.2. Meconium Samples

Approximately 0.01 g of each of the 13 meconium samples collected in a previous study, was added to a labeled microcentrifuge tube. To each tube, 150 μ L of 1X RIPA + protease inhibitor was added to each meconium sample in the tube. The tubes were immediately placed on ice and vortexed for 10 seconds and incubated on ice for 10 minutes for 3 rotations totaling 30 minutes. The tubes were then spun in a pre-chilled 4°C centrifuge for 15 minutes at top speed (18,000 rpm). The supernatant or unreduced lysate was then transferred to a new, labeled microcentrifuge tube and stored in the -80°C freezer for further use.

4.2.4. Determination of Sample Protein Concentration(s)

To determine the total protein concentration in each sample, a Bicinchoninic Acid Assay (BCA) was performed for all samples collected throughout the experiment. To do so, the protocol provided in the Pierce™ BCA Protein Assay Kit was followed and all reagents used were those provided by the kit (Fisher Scientific, Pierce™ BCA Protein Assay Kit).

A standard curve was generated ranging from 0 – 300 μ g/mL bovine serum albumin (BSA) using stock BSA provided (2 mg/mL in 0.9% saline and 0.05% sodium azide) (Appendix A, Table IX). Additionally, total protein levels were assumed to be significant so 1:50 and 1:100

dilutions were performed on each sample type to be analyzed to ensure protein concentrations fell within the range of the standard curve (Appendix A, Table X). All dilutions were performed in potassium phosphate buffer (100 mM pH=7.5) prepared in the laboratory.

Samples and standard dilutions were plated in 25 μ L triplicates in a 96-well plate and 200 μ L of a working reagent (WR) consisting of 50 parts BCA reagent A (sodium carbonate, sodium bicarbonate, bicinchoninic acid, and sodium tartrate in 0.1 M sodium hydroxide) and 1 part of BCA reagent B (4% cupric sulfate), both provided in the PierceTM BCA Protein Assay Kit, was added to each well. An ultraviolet-visible spectrophotometer (UV-Vis) was then used to obtain absorbance measurements at 450 nm and 620 nm.

To determine the total amount of protein present in each sample, multiple BCA assays were performed. Before generation of the standard curve, a calculation was performed to correct the absorbance of all samples (4). A standard curve was then generated and a linear regression equation was obtained (Figure 15). The linear regression equation and dilution factor were then used to determine the protein concentration in each sample (5). A calculation was then performed to determine what volume of each sample was required to load 40 μ g protein into the SDS-PAGE gels (6).

$$\text{Std. and unk. abs} - \text{Avg blank abs} = \text{corrected abs signal} \quad (4)$$

where std is standard, unk is unknown, abs is absorbance, and avg is average.

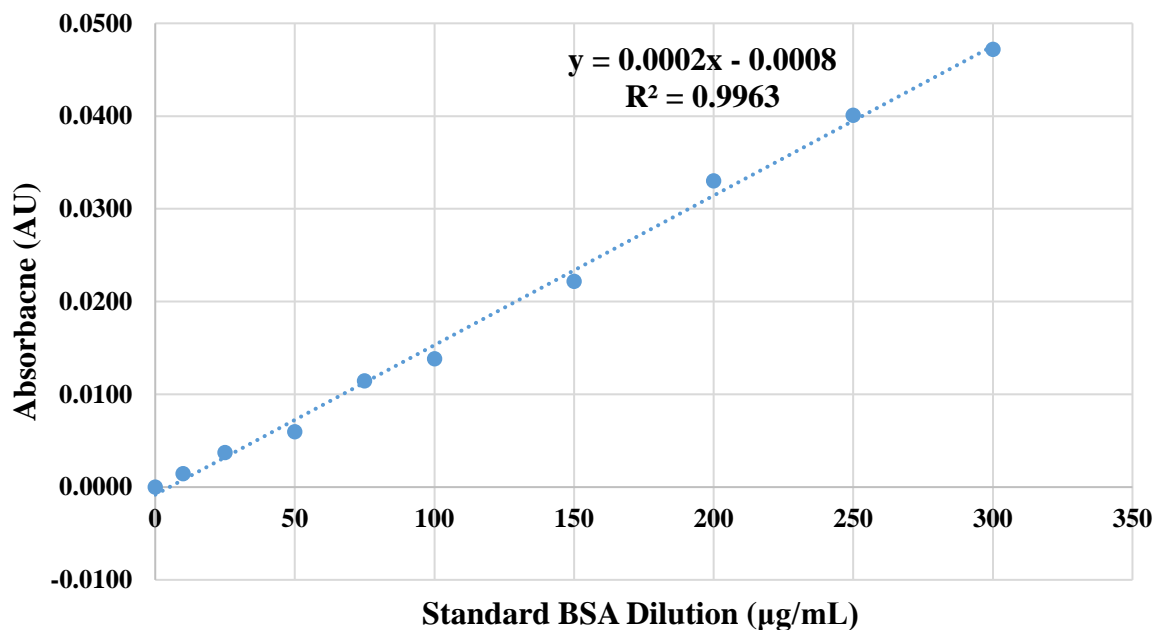


Figure 15: Meconium Sample BCA Analysis (450 nm)
Standard curve graph obtained from a UV-Vis spectrophotometer at a wavelength of 450 nm. Generated from a BCA assay of meconium samples.

$$Y = 0.0002x - 0.0008 \quad (5)$$

$$x = 0.0114$$

$$x = \frac{0.0114 + 0.0008}{0.0002} = \bar{6}1.0 \frac{\mu\text{g protein}}{\text{mL sample}} \times 100 = \bar{6}.1 \times 10^2 \frac{\mu\text{g protein}}{\text{mL sample}}$$

where the value for x was obtained from the average standardized values of meconium Sample 3 and the bar above the numbers denotes significant figures.

$$\begin{aligned} 40.0 \mu\text{g protein desired} \div \bar{6}.1 \times 10^2 \frac{\mu\text{g protein}}{\text{mL sample}} \\ = \bar{6}.56 \mu\text{L of sample required} \end{aligned} \quad (6)$$

where the bar above the numbers denote significant figures.

This method of protein content determination was used for all samples in this investigation to ensure that equal amounts of protein were loaded into each SDS-PAGE gel. A

table of the overall protein concentrations and calculated loading volumes in all the metal exposure cell samples and meconium samples can be found in Appendix B (Table XI).

4.2.5. Western Blot Analysis

Using the calculated total protein concentrations, it was determined what volume was required of each sample so that the sample wells in the sodium dodecyl sulfate-polyacrylamide (SDS-PAGE) gel were loaded with 40 μ g of overall protein (Appendix B, Table XI). The unreduced samples were then diluted 3:1 in sample buffer (Bio-Rad 4x Laemmli sample buffer) with β -mercaptoethanol (β ME) (Fluka, 2-Mercaptoethanol, 0.5 M in H₂O, 20°C). The now reduced samples were then added to a hot block at approximately 90°C for 10 minutes to denature the sample proteins. The samples were then quickly spun down in a mini centrifuge before being added to a 4-15% SDS-PAGE gel (Bio-Rad, Mini-PROTEAN® TGX™ precast gel 4-15%) in an electrophoresis cassette chamber filled with 1X SDS running buffer (Bio-Rad, 10X Tris/Glycine/SDS Buffer). To the gels containing samples, 8 μ L of protein standard (Bio-Rad, Precision Plus Protein™ Standards, Dual Color) was added to a sample well on each end of the gel. The gel was electrophoresed at 200 V for approximately 35 minutes.

To transfer the proteins from the SDS-PAGE gel to a nitrocellulose membrane, a sandwich was prepared in the following order in a dish containing transfer buffer: (25 mM Tris base, 190 mM glycine, 0.1% SDS, 20% methanol, pH=8.3), sponge, 2 sheets of filter paper (Bio-Rad, Mini Trans-Blot® Filter paper, 75.x10 cm) SDS-PAGE gel, nitrocellulose membrane (Bio-Rad, Nitrocellulose Membranes, 0.45 μ m, 7x8.5 cm), 2 additional sheets of filter paper, sponge. The sandwich was then placed inside the cassette, with the side of the cassette closer to the nitrocellulose membrane facing the positive (red) electrode. The chamber was filled with transfer

buffer and electrophoresis was performed on the apparatus for 1.5 hours at 150 mA constant current.

After electrophoresis was complete, the membrane was rinsed quickly with deionized water, dried in between two paper towels, and transferred to a labeled Ziploc bag. At this step, the western blots containing meconium samples were stained with Ponceau S stain (Research Products International, Ponceau S Staining Solution) to visualize protein loading, as it was determined that the western blot loading control protein, Vinculin, was not detected in the meconium samples. After a staining period of 30 minutes, an image was captured of the membranes and 1X TBST was used to rinse the stain from the membranes so they could be used for the rest of the western blotting procedure.

The membrane was then wet with 1X Tris-buffered saline (TBS) diluted from 10X TBS (24 g Tris-HCl, 5.6 g Tris base, 88 g NaCl, pH=7.6) and washed 2 times for 5 minutes each in 1X TBST (Tris-buffered saline, 0.1% Tween 20). The membrane was then added to a Ziploc bag containing 50 mL of blotto solution made of 7.5% non-fat dry milk (NFDM) (w/v) in 1X TBST and placed on a tilt table in the walk-in refrigerator set at 4°C to block overnight.

The blocking solution was discarded, and the membrane was washed in 1X TBST 3 times (twice fast, once for 10 minutes). The membrane was then cut to allow incubation of two primary antibodies, the Vinculin control and the metal-specific protein of interest. Each membrane section was then added to a labeled Ziploc bag containing 10 mL of primary antibody diluted 1:1000 in 1X TBST with 5% NFDM (w/v) and incubated at room temperature for 1.5 hours.

The primary antibody solutions were then removed from the bags and 3 room temperature 1X TBST washes were performed on the membranes (1 quick, 2 for 10 minutes each). The membranes were blocked one last time in 1X TBST containing 10% NFDM (w/v) for

20 minutes. The membranes were then added to a new Ziploc bag containing 10 mL of secondary antibody diluted 1:10000 in 1X TBST containing 5% NFDM (w/v) and incubated at room temperature for an hour. Three room temperature washes (1 quick, 2 for 10 minutes each) were then performed with 1X TBST. The membranes were then incubated in 1X enhanced chemiluminescence (ECL) substrate, prepared following the protocol provided with the ECL kit (Invitrogen, Novex® ECL, HRP Chemiluminescent Substrate Reagent Kit), for 2 minutes and then analyzed using a ChemiDoc XRS+ imager (Bio-Rad, Molecular Imager®, ChemiDoc™ XRS+ with Image Lab™ software). The software provided with the imager was then used to annotate and normalize densitometric values between control samples and exposure samples to obtain quantitative values for the western blots.

To analyze As exposure blots, a primary antibody specific for the human AS3MT protein was used (proteintech®, AS3MT Rabbit Polyclonal Antibody, 27270-1-AP). To analyze Cu exposure blots, a primary antibody specific for a high-affinity copper transport protein, CTR1, was used (abcam, Anti-SLC31A1/CTR1 antibody [EPR7936], ab129067). To analyze Mn exposure blots, a primary antibody specific for a multi-metal transport protein, ZNT10, was used (abcam, Anti-SLC30a10 antibody, ab229954). To analyze Zn exposure blots, a primary antibody specific for a Zn transport protein, ZNT1 (Invitrogen, SLC30a1 Polyclonal Antibody, Pa5-42481) was used. The same anti-rabbit secondary antibody was used for all the western blots (abcam, Goat Anti-Rabbit IgG (HRP), ab205718). To analyze the control protein, an antibody specific for the protein Vinculin (Sigma-Aldrich, Monoclonal Anti-Vinculin antibody produced in mouse, V4505) and a rabbit anti-mouse secondary antibody (Invitrogen, ZyMax™, Rabbit anti-Mouse IgG (H+L) HRP Conjugate) were used on the mammalian cell lines membranes.

4.2.6. Enzyme-Linked Immunoassay Analysis

In order to obtain data for cytokine expression of Human Tumor Necrosis Factor alpha (TNF- α) and Interleukin-6 (IL-6), enzyme-linked immunoassays (ELISA) were performed. The protocols provided with the TNF- α kit (Invitrogen, Human TNF alpha Uncoated ELISA, 88-7346) and IL-6 kit (Invitrogen, Human IL-6 Uncoated ELISA, 88-7066) were followed directly and all reagents used were those provided by the kits or additional materials required by the kit manufacturer. All sample dilutions, 1:10 for the meconium samples and 1:250 for the cell cultures, were performed in ELISA/ELISAPOT Diluent provided in the kit. For preparation of coating buffer and wash buffer, 1X PBS was used, and Tween 20 (Thermo Fisher, Tween® 20, Ultrapure) was also used for the wash buffer. Additionally, 2 N sulfuric acid (H₂SO₄) was used as the stop solution for the assays (Fisher Scientific, Sulfuric Acid, Trace Metal Grade).

Following the protocol, a standard curve was generated, and the linear regression equation and R-squared values obtained from the standard curve graph were used to calculate the concentration of each cytokine in the samples. The data obtained from the ELISA plates were then used to calculate cytokine expression from each metal exposure scenario compared to the control for both cell lines. Cytokine concentrations were determined for each meconium sample using the data, as no control meconium samples were able to be obtained, so comparisons were not able to be made.

5. Results

5.1. Preliminary Bioavailability Study

For the preliminary study, As, Cd, Cu, Mn, Pb, and Zn were selected to be quantified from the Greely neighborhood environmental samples collected. Each participant submitted a yard soil sample and a household dust sample. All samples were acid digested and analyzed for total metal concentrations via ICP-OES. The samples were then subjected to conditions found in the human stomach and intestinal digest phases and quantified by ICP-MS. The total amount of metal found in a sample was then compared to the amount of that metal found in the simulated stomach or intestinal fraction of the same sample and this allowed for determination of metal bioavailability (Figure 16, Figure 17, Figure 18, Figure 19, Figure 20, Figure 21). The raw data used to generate the boxplots can be found in Appendix C (Table XII, Table XIII, Table XIV, Table XVI, Table XV, and Table XVII)

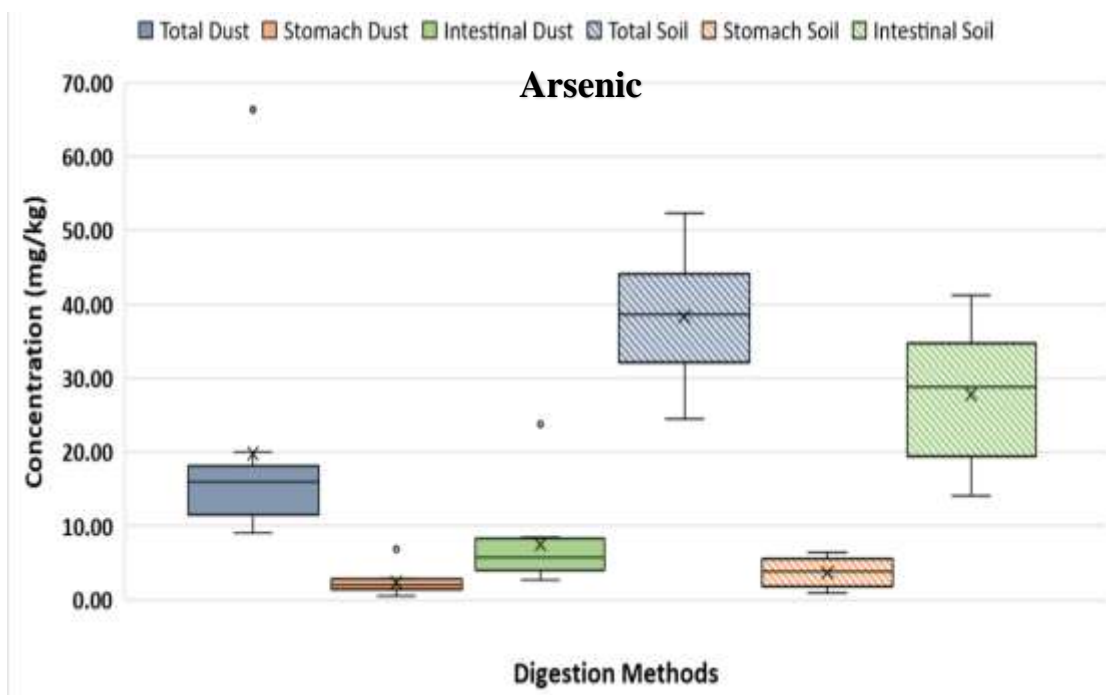


Figure 16: Arsenic Total Metal and Bioavailability Data
Arsenic soil and dust data from ICP-OES (total) and ICP-MS (stomach and intestinal) analysis of three different digestion methods utilized in this study N=10.

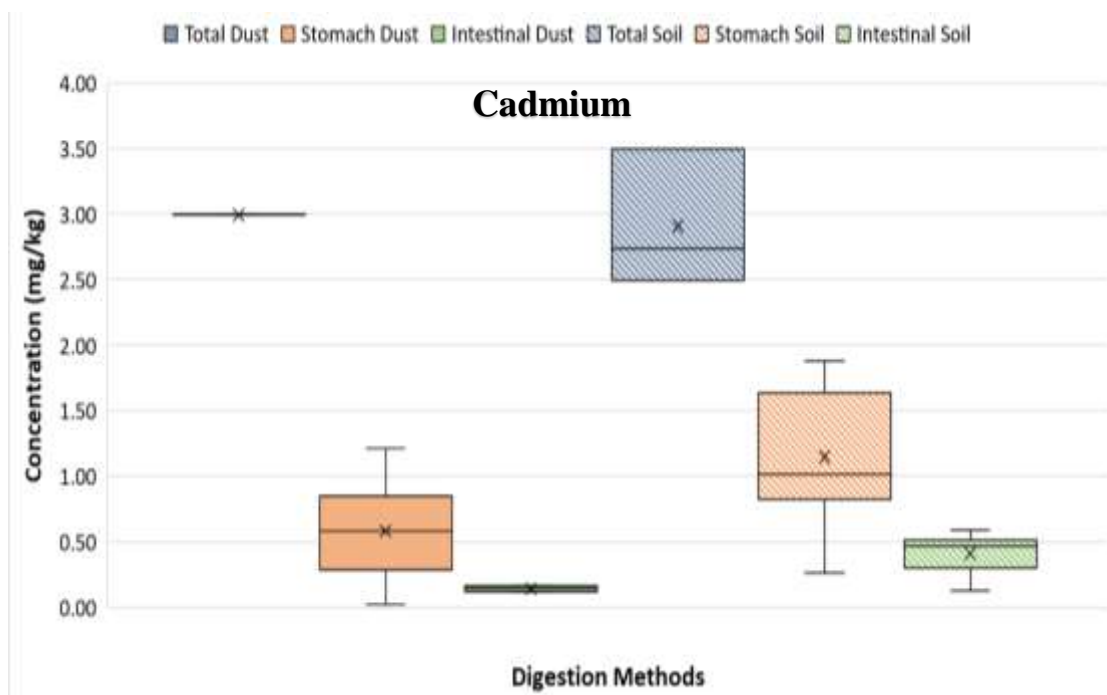


Figure 17: Cadmium Total Metal and Bioavailability Data
Cadmium soil and dust data from ICP-OES (total) and ICP-MS (stomach and intestinal) analysis of three different digestion methods utilized in this study N=10.

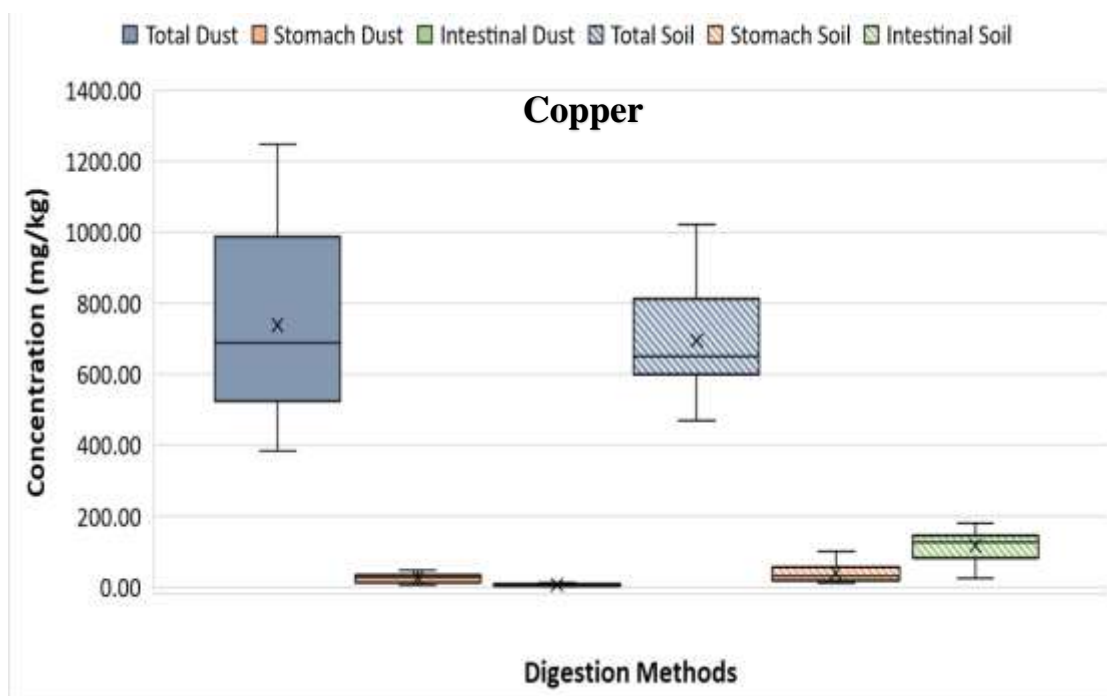


Figure 18: Copper Total Metal and Bioavailability Data
Copper soil and dust data from ICP-OES (total) and ICP-MS (stomach and intestinal) analysis of three different digestion methods utilized in this study N=10.

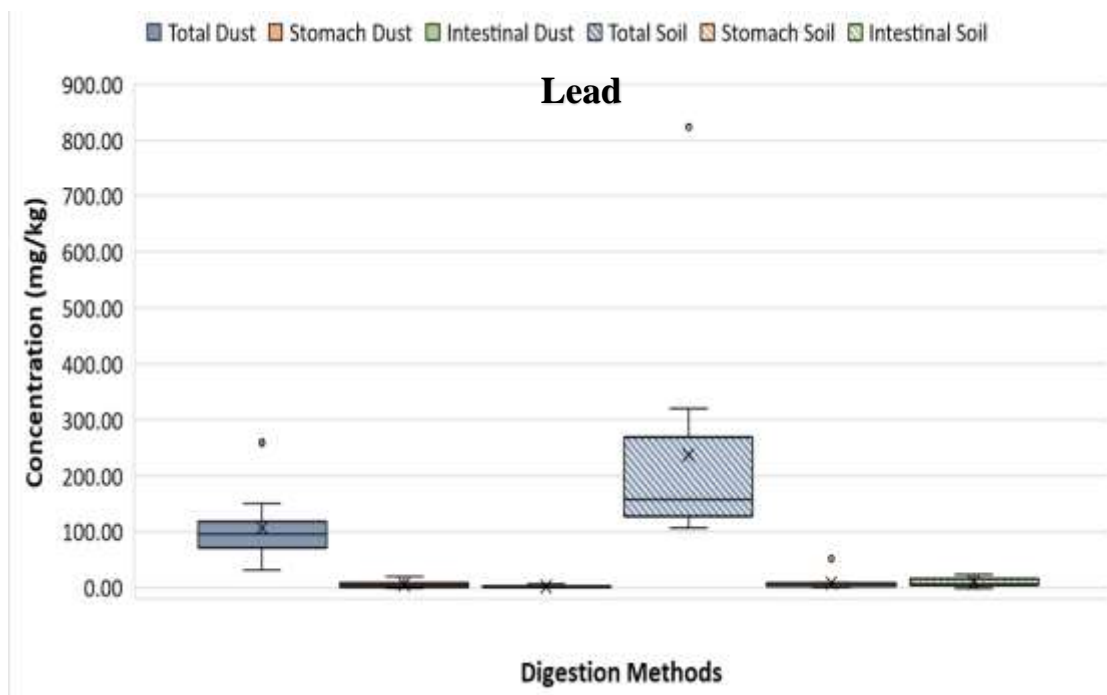


Figure 19: Lead Total Metal and Bioavailability Data
Lead soil and dust data from ICP-OES (total) and ICP-MS (stomach and intestinal) analysis of three different digestion methods utilized in this study N=10.

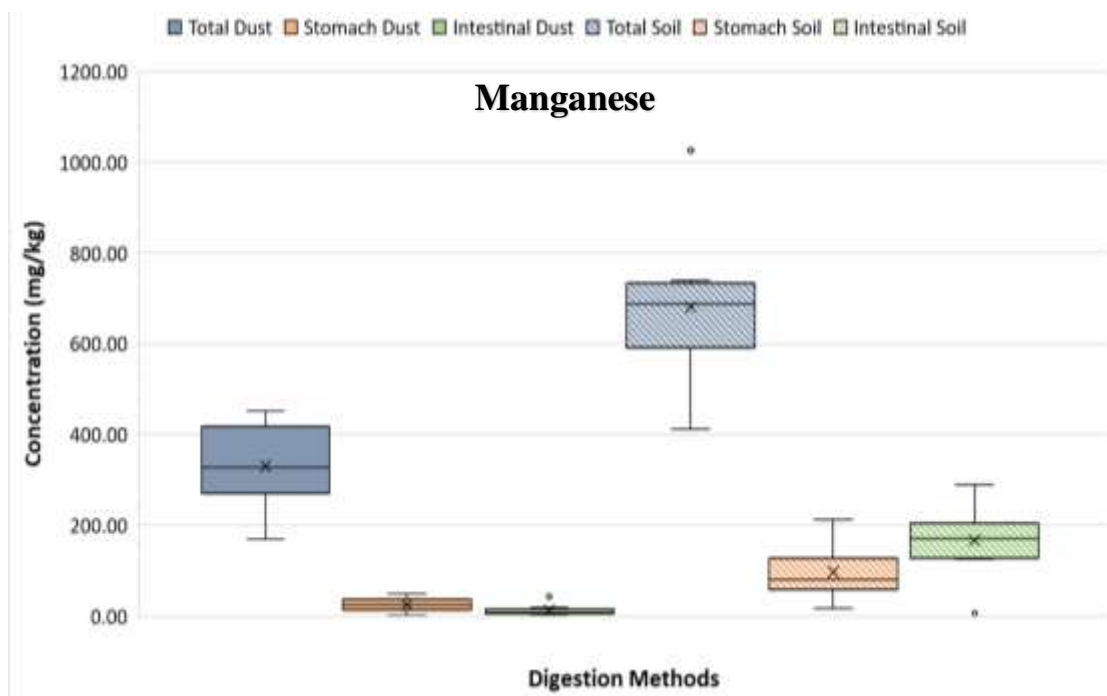


Figure 20: Manganese Total Metal and Bioavailability Data
Manganese soil and dust data from ICP-OES (total) and ICP-MS (stomach and intestinal) analysis of three different digestion methods utilized in this study N=10.



Figure 21: Zinc Total Metal and Bioavailability Data
Zinc soil and dust data from ICP-OES (total) and ICP-MS (stomach and intestinal) analysis of three different digestion methods utilized in this study N=10.

In the stomach phase, Zn from the dust samples had the highest median percent bioavailability at approximately 30%, while Cd from the soil samples had median percent bioavailability at approximately 46% (Table VI and Table VII). For the intestinal phase, As had the highest median percent bioavailability in both samples at approximately 42% from the dust samples and 74% from the soil samples (Table VI and Table VII). Refer to Appendix D for the average metal concentrations and bioavailability percentages in the stomach (Table XVIII) and intestinal digest samples (Table XIX). It was determined that total Cd levels were overall relatively low in the Butte environmental samples, and, while Pb was present in all samples, the bioavailability of the metal was low in both stomach and intestinal phases and numerous studies have focused solely on Pb in the community already. The bioavailability work determined that As, Cu, Mn, and Zn would be the four metals of interest for the in-vitro cell study to determine protein expression.

Table VI: Bioavailability Analysis of Dust Samples

Metal	Average Total Conc. (mg/kg) ±0.01	Median Total Conc. (mg/kg) ±0.01	Stomach Bioavailability Range	Median Stomach Bioavailability	Intestinal Bioavailability Range	Median Intestinal Bioavailability
Arsenic	19.81	15.98	4.18% - 17.94%	13.07%	20.72% - 48.64%	42.16%
Cadmium	2.99	2.99	19.85%	19.85%	BDL	BDL
Copper	737.10	688.81	1.25% - 7.65%	3.66%	0.17% - 1.60%	0.70%
Manganese	330.52	327.67	0.92% - 48.52%	25.61%	3.90% - 43.35%	7.69%
Lead	106.94	96.56	0.03% - 11.37%	6.58%	0.39% - 4.74%	2.11%
Zinc	733.25	687.31	2.19% - 49.77%	30.42%	0.93% - 5.31%	2.61%

ICP-MS analysis of dust samples for the stomach and intestinal phases compared to ICP-OES data for the total dust metal concentrations to determine percent bioavailability

Table VII: Bioavailability Analysis of Soil Samples

Metal	Average Total Conc. (mg/kg) ±0.01	Median Total Conc. (mg/kg) ±0.01	Stomach Bioavailability Range	Median Stomach Bioavailability	Intestinal Bioavailability Range	Median Intestinal Bioavailability
Arsenic	38.37	38.61	3.11% - 16.32%	11.11%	53.97% - 84.08%	73.68%
Cadmium	2.91	2.74	10.53% - 75.44%	46.02%	12.97% - 20.47%	16.55%
Copper	694.27	648.77	1.94% - 12.65%	4.85%	2.83% - 22.93%	19.13%
Manganese	680.05	688.06	2.96% - 29.11%	12.73%	1.31 - 43.75%	23.36%
Lead	237.39	157.27	0.46% - 6.28%	2.23%	2.89% - 19.25%	4.96%
Zinc	598.97	567.62	8.12% - 38.35%	22.95%	1.41% - 25.85%	7.41%

ICP-MS analysis of soil samples for the stomach and intestinal phases compared to ICP-OES data for the total dust metal concentrations to determine percent bioavailability

The overall metal concentrations were used to determine what metal concentrations would represent low-level metal exposure in the Butte environment (Table VIII). These values were approximated since the concentrations in the Greely neighborhood were not completely representative of the entire area of Butte. These calculated concentrations were then used to determine the overall exposure ratio for a mixture of the four metals of interest for this study (Table VIII). It is important to acknowledge this ratio, as the metals are not distributed equally in the Butte environment, which may impact competition between metals in certain proteins or other molecules in the human body.

Table VIII: Metal Exposure Ratios for Study Elements of Concern

Metal	Average Total Concentration (mol/L)	Exposure Ratio
Arsenic	8.01×10^{-7}	0.04
Cadmium	2.25×10^{-5}	1.00
Copper	1.84×10^{-5}	0.82
Manganese	2.04×10^{-5}	0.91
Overall Exposure Ratio		0.04As: 1.00Cu: 0.82Mn: 0.91Zn

5.2. Biological Experiments

5.2.1. Meconium Protein Determination

It was determined that the Vinculin control protein was not present or possibly expressed at such low levels in the meconium samples that it was not a viable control. Therefore, Ponceau S Stain was used to visualize protein loading for the meconium sample western blots (Figure 22).

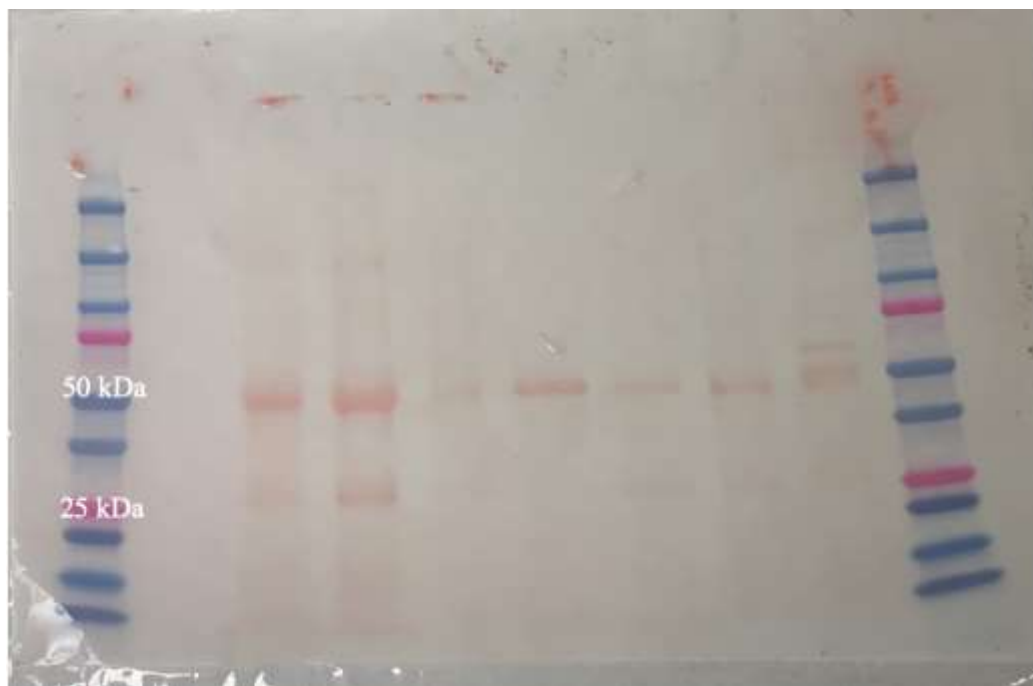


Figure 22: Ponceau S-Stained Nitrocellulose Membrane Containing Meconium Samples
Lane 1 (far right): Precision Standard, Lane 2: Blank, Lane 3: Sample 10, Lane 4: Sample 9, Lane 5: Sample 8, Lane 6: Sample 7, Lane 7: Sample 3, Lane 8: Sample 2, Lane 9: Sample 1, Lane 10: Precision Plus Protein™ Standard. White text on figure indicating relevant kDa values.

From the Ponceau S-stained western blots, researchers were able to ensure that protein transfer from the SDS-PAGE gel to the nitrocellulose membrane was successful. The stained membranes also provided a general idea of the size of proteins present in the meconium samples. In Figure 22, dark bands can be seen between 25-50 kilodaltons (kDa). All meconium western blots showed similar results for the Ponceau S-Stained membranes.

5.2.2. Arsenic Protein Expression Analysis

5.2.2.1. Meconium Western Blots

To determine whether any of the proteins present in the meconium samples were the arsenic biomethylation protein, AS3MT, western blots were performed on the 13 meconium samples previously collected (Figure 23 and Figure 24). Originally, 16 meconium samples were collected, but the complete content of samples 4-6 was used in the previous study.

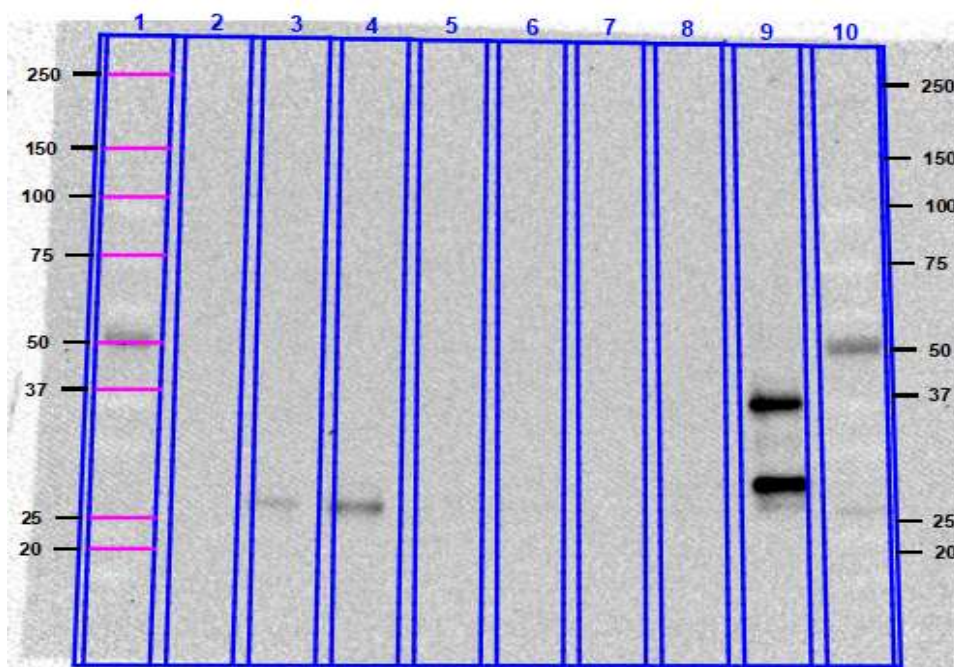


Figure 23: AS3MT Western Blot Analysis of Meconium Samples 1-3 and 7-10
Lane 1: Protein Standard, Lane 2: Blank, Lane 3: Sample 10, Lane 4: Sample 9, Lane 5: Sample 8, Lane 6: Sample 7, Lane 7: Sample 3, Lane 8: Sample 2, Lane 9: Sample 1, Lane 10: Protein Standard.

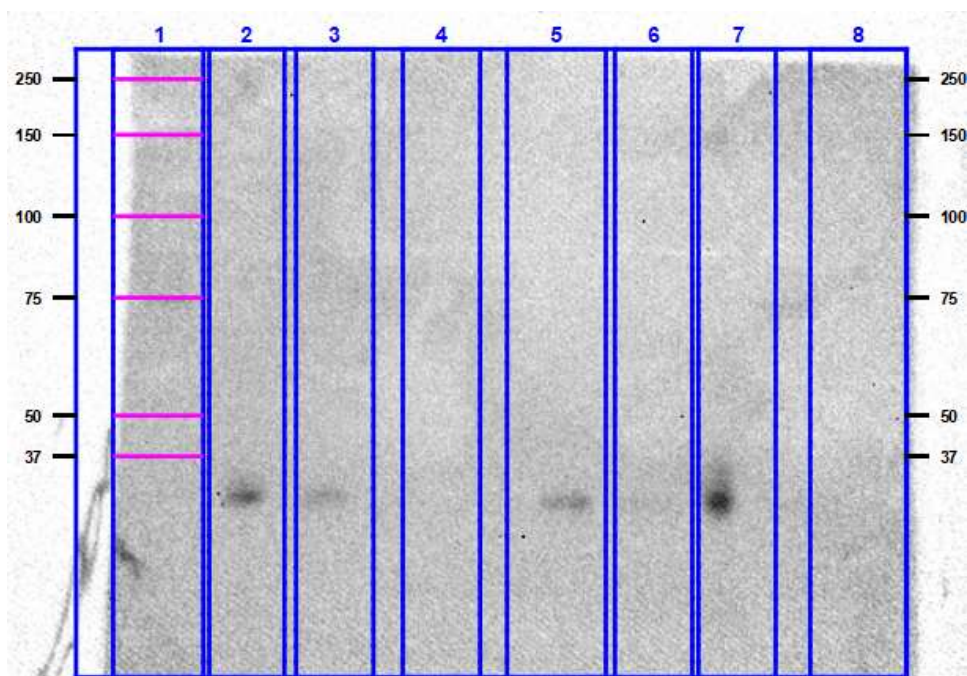


Figure 24: AS3MT Western Blot Analysis of Meconium samples 11-16
Lane 1: Protein Standard, Lane 2: Sample 16, Lane 3: Sample 15, Lane 4: Sample 14, Lane 5: Sample 13,
Lane 6: Sample 12, Lane 7: Sample 11, Lane 8: Protein Standard.

If AS3MT was present in any of the samples, bands should have appeared around 39-41 kDa on the western blots (AS3MT Rabbit Polyclonal Antibody, 27270-1-AP: Data Sheet). Bands did appear on the AS3MT analysis western blots, but not at the correct molecular weight, suggesting that AS3MT was not able to be detected in the samples. Since the control protein, Vinculin, was not detected in the western blot samples and a control meconium sample was not able to be obtained, densitometric and comparison analysis were not able to be performed on the meconium samples.

5.2.2.2. HEK293 Western Blot

The western blots performed on the HEK293 samples exposed to different As exposure scenarios (Table V) were used to determine if AS3MT was present in any of the samples from this cell line (Figure 25). Since it was determined that the Vinculin control protein, a cytoskeleton protein found in adherent cell lines, was present in both cell lines, it was not

necessary to stain the membranes to determine protein loading. Once the western blots were analyzed using the ChemiDoc XRS+, the Image Lab software was then used to obtain densitometric data that could be normalized against the control cell culture to assess the protein content of each sample.

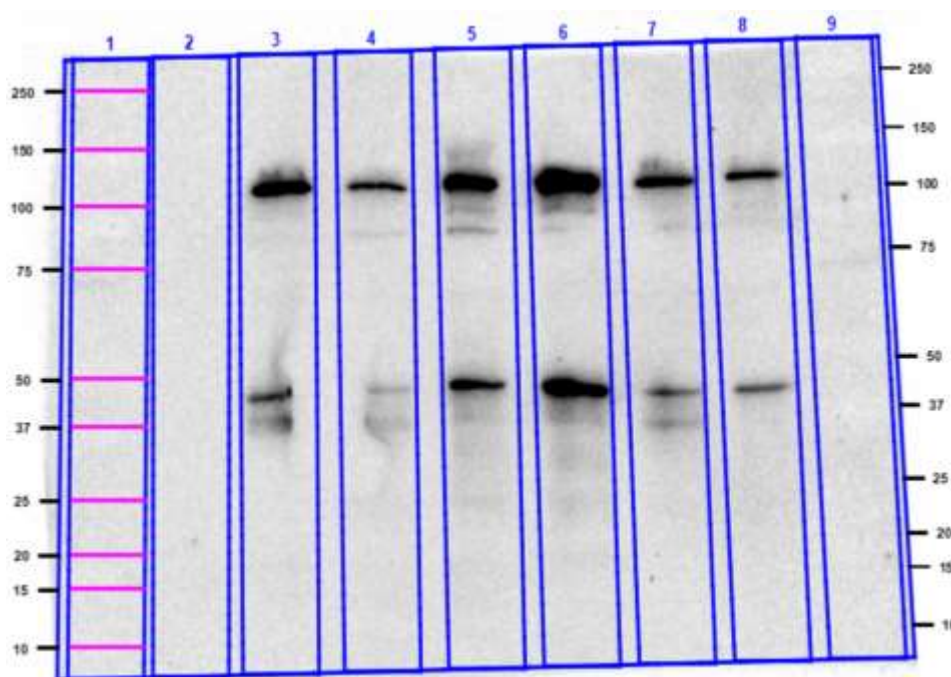


Figure 25: AS3MT Western Blot Analysis of Varying Metal Exposures in HEK293 Cells
Lane 1: Protein Standard, Lane 2: Blank, Lane 3: As:Cu:Mn:Zn Exposure, Lane 4: As:Zn Exposure, Lane 5: As:Mn Exposure, Lane 6: As:Cu Exposure, Lane 7: As Exposure, Lane 8: Control, Lane 9: Protein Standard.

If Vinculin was present, bands should have appeared around 130 kDa (Monoclonal Anti-Vinculin antibody, V4505: Data Sheet) and if AS3MT was present, bands should have appeared between 39-41 kDa (AS3MT Rabbit Polyclonal Antibody, 27270-1-AP: Data Sheet). In Figure 25, it can be seen that bands are present between 100-150 kDa and between 37 - 50 kDa. The bands appearing at the higher molecular weight represent Vinculin, and the bands at the lower molecular weight represent AS3MT. These results indicate that the AS3MT protein was present in all the As-exposed HEK293 samples.

To determine if there was a change in protein expression in any of the samples, densitometric values of the Vinculin bands were collected for the varying exposure samples and normalized against the densitometric value for the Vinculin in the control sample. This gave a normalization factor for each sample, which was then multiplied by the normalized densitometric volume collected for the bands representing the AS3MT proteins. These normalized AS3MT values were then compared to the control value, set at 100%, and the percent expression of AS3MT in each sample type was calculated (Figure 26).

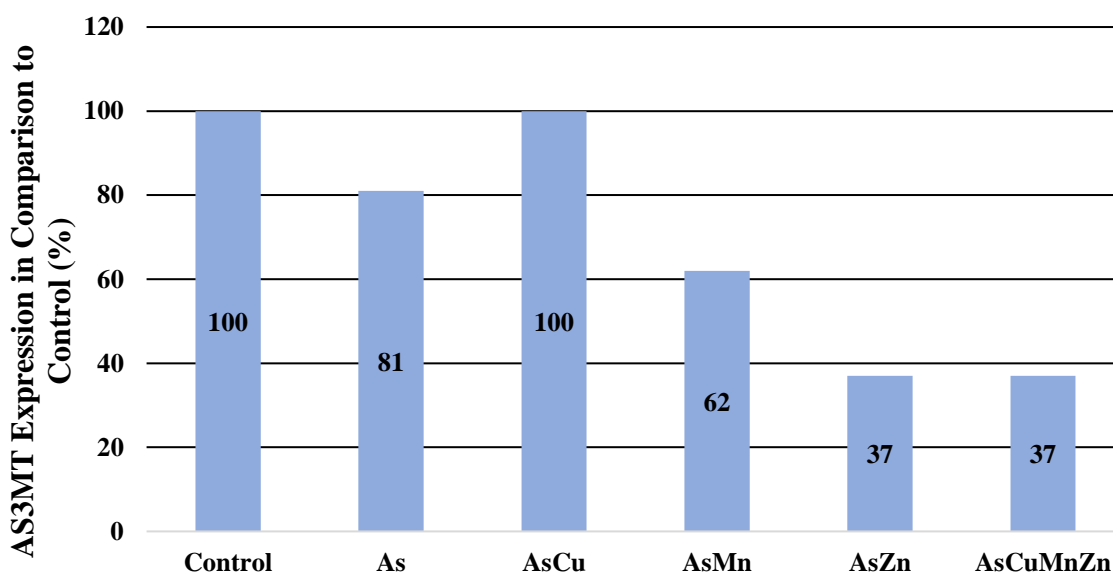


Figure 26: AS3MT Expression in Arsenic-Treated HEK293 Cells
Graph of AS3MT protein expression (%) in different As exposure scenarios in comparison to control in HEK293 cells.

Based off the normalized data collected, AS3MT expression was shown to decrease in all but one As exposure scenario. The samples that were calculated to have the highest decrease in percent expression were those exposed to the mixture of As and Zn and the mixture of all four metals. Expression of AS3MT in both samples was calculated have a 63% decrease in protein

expression when compared to the control. The raw normalization data for the As-exposed HEK293 cells can be seen in Appendix E (Table XX).

5.2.2.3. BEAS-2B Western Blot

The western blots performed on the BEAS-2B samples exposed to different As exposure scenarios (Table V) were used to determine if AS3MT was present in any of the samples in this cell line (Figure 27).

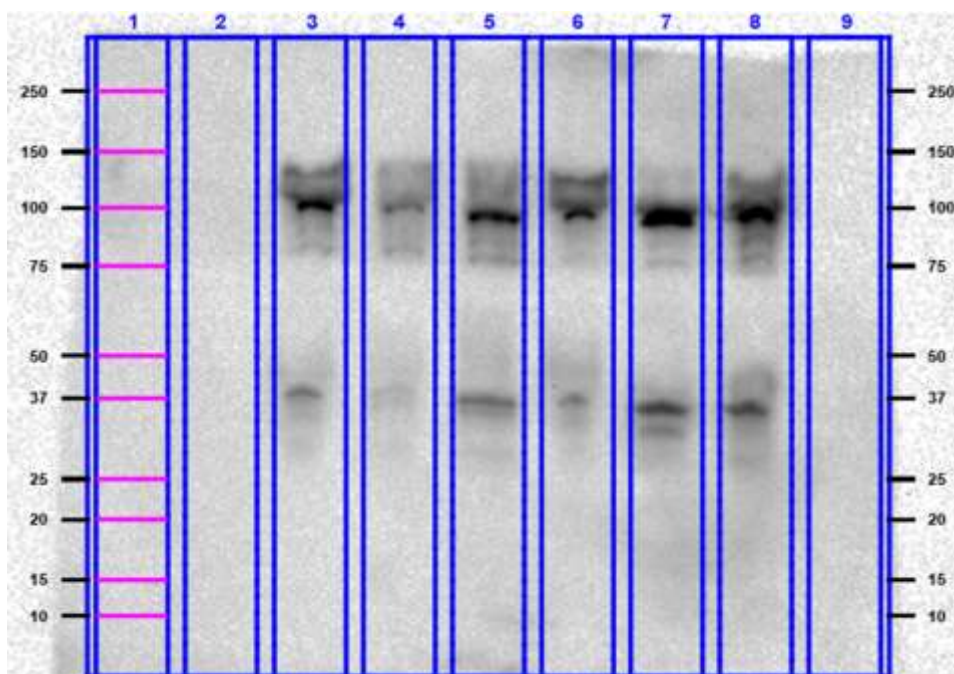


Figure 27: AS3MT Western Blot Analysis of Varying Metal Exposures in BEAS-2B Cells
Lane 1: Precision Plus Protein™ Standard, Lane 2: Blank, Lane 3: As:Cu:Mn:Zn Exposure, Lane 4: As:Zn Exposure, Lane 5: As:Mn Exposure, Lane 6: As:Cu Exposure, Lane 7: As Exposure, Lane 8: Control, Lane 9: Precision Plus Protein™ Standard.

Upon analysis of AS3MT western blots in BEAS-2B cell cultures, it can be seen that bands are present between 100-150 kDa and between 37 - 50 kDa. The bands appearing at the higher molecular weight verify that Vinculin is present in all the AS-exposed BEAS-2B samples analyzed. The bands that appeared between 37 and 50 kDa indicate that the AS3MT was also present in all the BEAS-2B samples analyzed. Densitometric and normalized values were

collected to assess AS3MT expression as a result of different metal exposure scenarios in the BEAS-2B cell line (Figure 28).

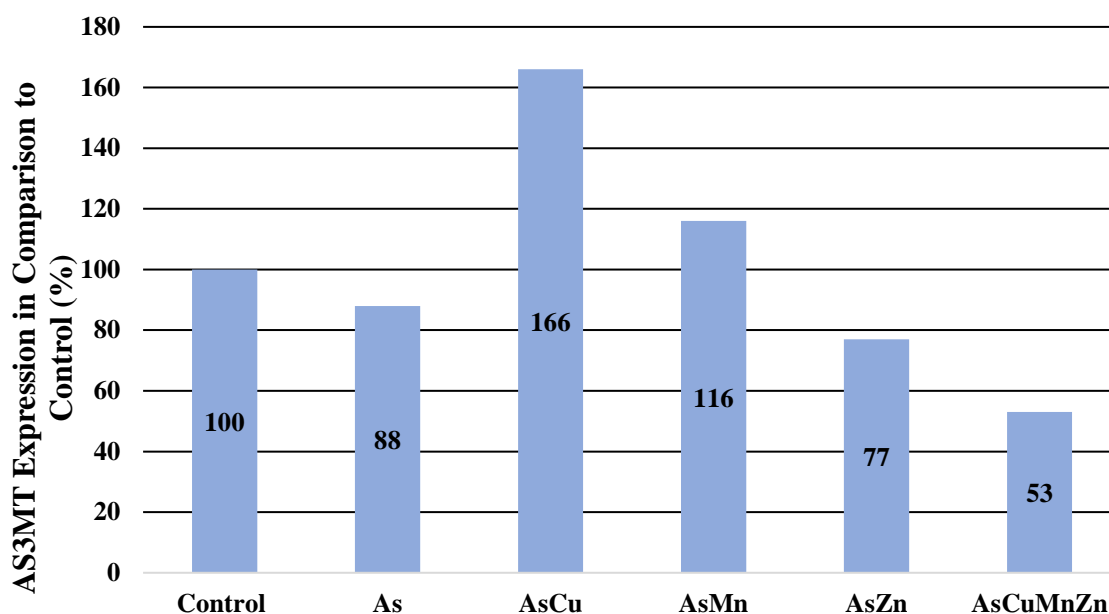


Figure 28: AS3MT Expression in Arsenic-Treated BEAS-2B Cells
Graph of AS3MT protein expression (%) in different As exposure scenarios in comparison to control in BEAS-2B cells.

Based on the normalized data collected, percent expression of AS3MT was calculated to be decreased in three exposure scenarios. All exposure scenarios calculated to have a decrease in expression from the As-exposed BEAS-2B cells were also calculated to have decreased expression in the As-exposed HEK-293 cells. The cell culture exposed to the mixture of As and Cu showed the highest increase of expression, at 66%, followed by the cell culture exposed to the mixture of As and Mn, which was calculated to be increased by 16%. The culture exposed to the mixture of all four metals was calculated to have a decrease in expression of 47% when compared to the control. This was the exposure scenario that resulted in the greatest decrease in percent expression. The raw normalization data for the As-exposed BEAS-2B cells can be seen in Appendix E (Table XXI).

5.2.3. Copper Protein Expression Analysis

5.2.3.1. Meconium Western Blots

To determine whether any of the proteins present in the meconium samples were the copper transport protein of interest, CTR1, a western blot was performed on the 13 meconium samples previously collected (Figure 29 and Figure 30). These western blots were also stained with Ponceau-S stain but showed identical results to the stained membrane shown previously (Figure 22).

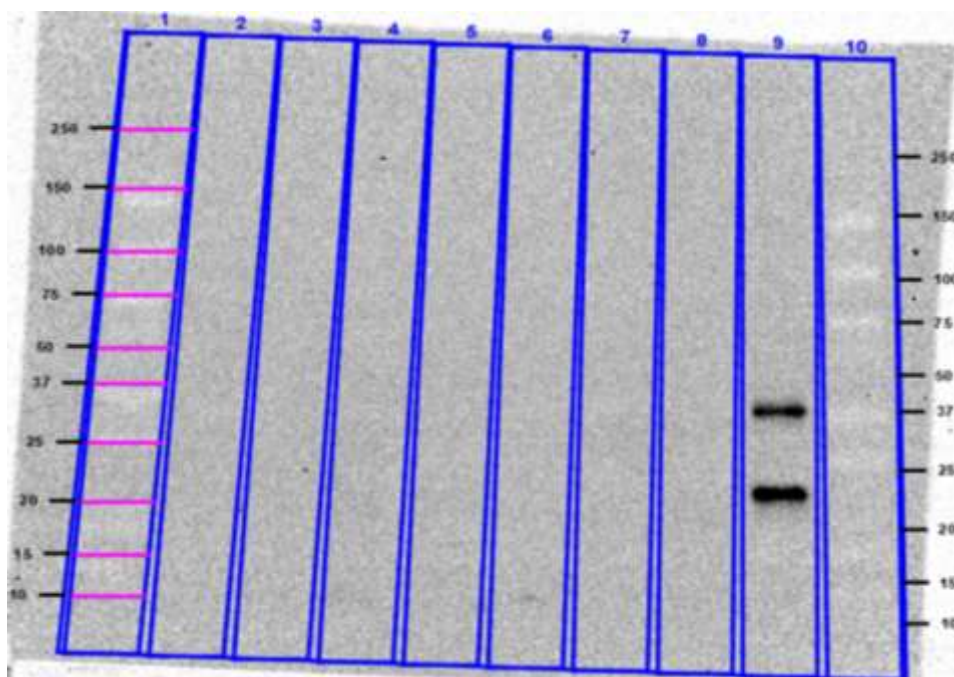


Figure 29: CTR1 Western Blot Analysis of Meconium Samples 1-3 and 7-10
Lane 1: Protein Standard, Lane 2: Blank, Lane 3: Sample 10, Lane 4: Sample 9, Lane 5: Sample 8, Lane 6: Sample 7, Lane 7: Sample 3, Lane 8: Sample 2, Lane 9: Sample 1, Lane 10: Protein Standard.

Analysis of the western blot for samples 1-3 and 7-10 shows that two bands that appeared in Lane 9 (Sample 1) and are of the same molecular weight as the two bands that were in Sample 1 for the AS3MT analysis of the meconium samples (Figure 23).

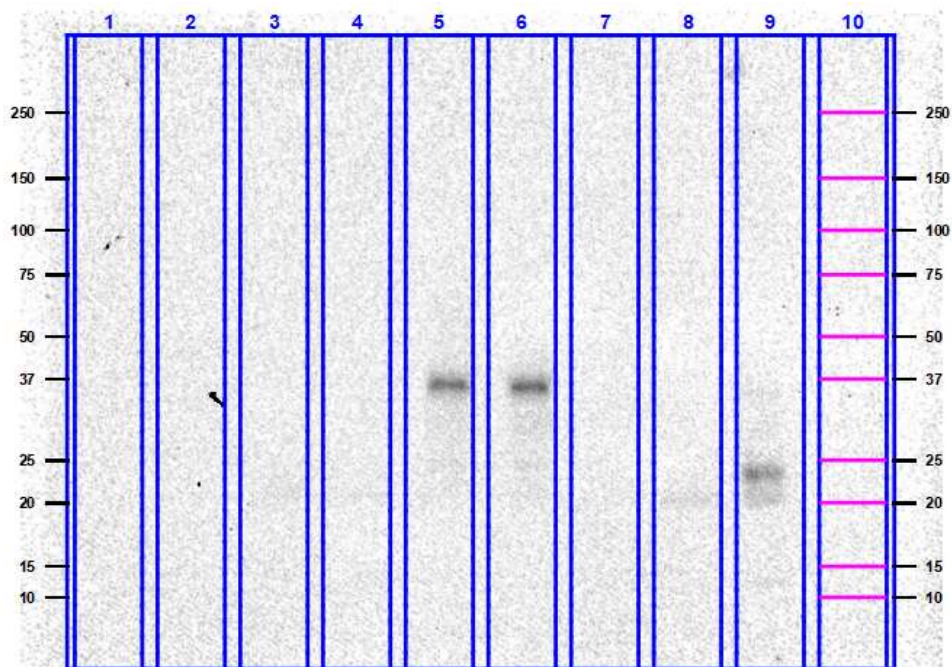


Figure 30: CTR1 Western Blot Analysis of Meconium samples 11-16
Lane 1: Protein Standard, Lane 2: Blank, Lane 3: Sample 16, Lane 4: Sample 15, Lane 5: Sample 14, Lane 6: Sample 14, Lane 7: Sample 13, Lane 8: Sample 12, Lane 9: Sample 11, Lane 10: Protein Standard.
Sample 14 was loaded twice due to a pipetting error.

The CTR1 antibody used in this study is known to bind to both a CTR1 precursor protein around 28 kDa and the mature protein around 35 kDa (Anti-SLC31A1/CTR1 antibody [EPR7936]: Data Sheet). The bands that appeared on this western blot are approximately the correct molecular weight, however they are the same molecular weight as the bands that appeared on the western blots analyzing the AS3MT protein. Because of this, it is more likely that these proteins are the same ones that appeared on the western blots analyzing AS3MT. The molecular weights of the bands seen in Lanes 5 and 6 are close enough to the 35 kDa mark, that they could be representative of the mature form of CTR1, but additional western blot analyses are warranted to confirm this result.

5.2.3.2. HEK 293 Western Blot

The western blots performed on the HEK293 samples exposed to different Cu exposure scenarios (Table V) were used to determine if CTR1 was present in any of the samples in this cell line (Figure 31).

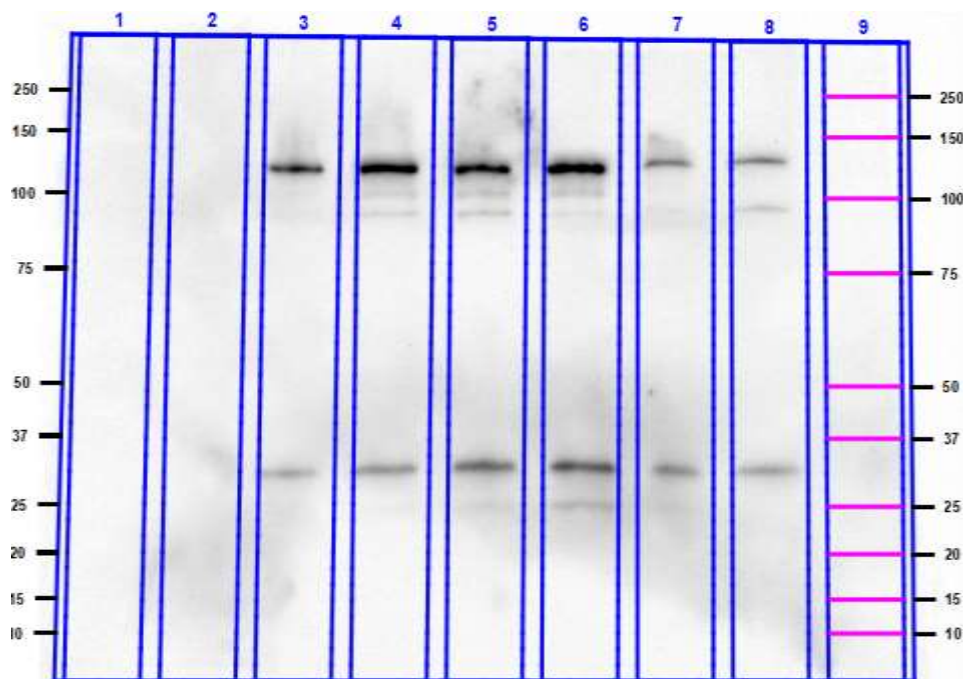


Figure 31: CTR1 Western Blot Analysis of Varying Metal Exposures in HEK293 Cells
 Lane 1: Protein Standard, Lane 2: Blank, Lane 3: As:Cu:Mn:Zn Exposure, Lane 4: Cu:Zn Exposure, Lane 5: Cu:Mn Exposure, Lane 6: As:Cu Exposure, Lane 7: Cu Exposure, Lane 8: Control, Lane 9: Protein Standard.

Analysis of the CTR1 western blot for HEK293 cells shows that bands are present between 100-150 kDa and between 25-37 kDa. The bands seen between 100-150 kDa indicate that Vinculin was present in all the Cu-exposed HEK293 samples analyzed. As previously mentioned, the CTR1 antibody used in this study is known to bind to both a CTR1 precursor protein around 28 kDa and the mature protein around 35 kDa. In Lanes 5 (CuMn exposure) and 6 (AsCu exposure), clear bands are present at both these molecular weights. In lanes 4 (CuZn exposure) and 7 (Cu exposure), a clear band is present at 35 kDa, as well as, what appears to be, a faint band around 28 kDa. This indicates that both the mature protein and the precursor protein

for CTR1 were present in these samples. Densitometric and normalized values were collected to assess CTR1 expression as a result of different metal exposure scenarios in the HEK293 cell line (Figure 32).

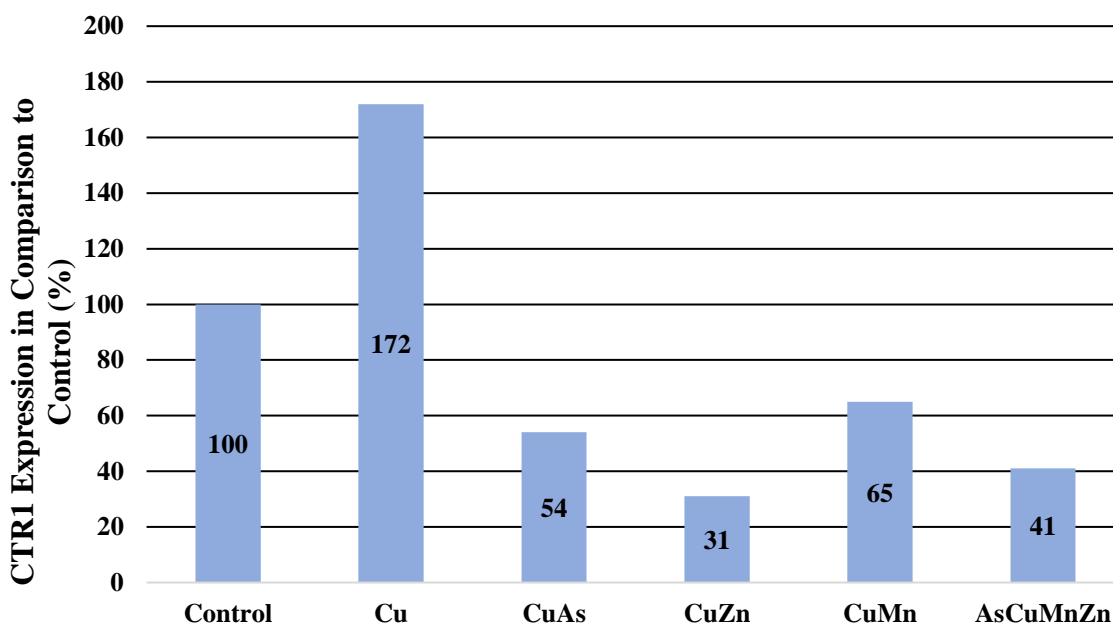


Figure 32: CTR1 Expression in Copper-Treated HEK293 Cells
Graph of CTR1 protein expression (%) in different Cu exposure scenarios in comparison to control in HEK293 cells

Based on the normalized densitometric data collected, the expression of CTR1 was calculated to be decreased in four exposure scenarios and increased in one exposure scenario. Expression of CTR1 in the culture exposed to Cu only was calculated to increase by 72%. Meanwhile, expression of CTR1 in the culture exposed to the mixture of Cu and Zn was calculated to be decreased by 69%, followed closely by the culture exposed to all four metals, which was decreased by 59% when compared to the control. The normalized data for the Cu-exposed HEK29 cells can be seen in Appendix E (Table XXII).

5.2.3.3. BEAS-2B Western Blot

The western blots performed on the BEAS-2B samples exposed to different Cu exposure scenarios (Table V) were used to determine if CTR1 was present in any of the samples in this cell line (Figure 33).

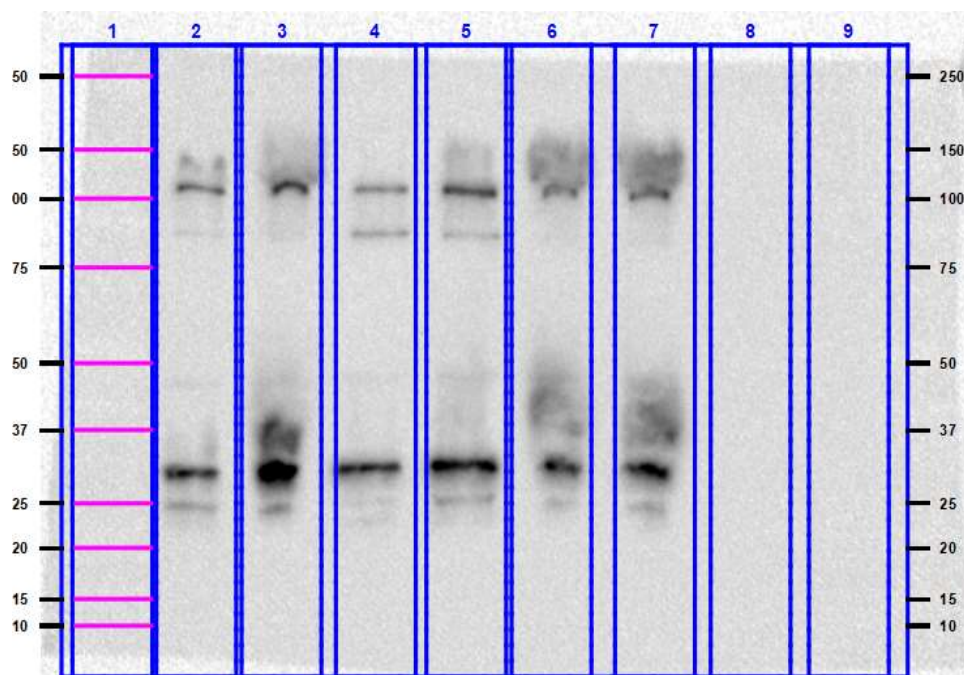


Figure 33: CTR1 Western Blot Analysis of Varying Metal Exposures in BEAS-2B Cells
Lane 1: Protein Standard, Lane 2: Control, Lane 3: Cu Exposure, Lane 4: As:Cu Exposure, Lane 5: Cu:Mn Exposure, Lane 6: Cu:Zn Exposure, Lane 7: As:Cu:Mn:Zn Exposure, Lane 8: Blank, Lane 9: Protein Standard.

Upon analysis, it can be seen that bands are present between 100-150 kDa and between 25-37 kDa. The bands seen between 100-150 kDa indicate that Vinculin is present in all the Cu-exposed BEAS-2B samples. All the sample lanes show a clear band at 35 kDa and some show a faint band at 28 kDa. This indicates that the mature CTR1 protein was present in all the samples and the precursor protein was present in some. Densitometric and normalized values were collected to assess CTR1 expression as a result of different metal exposure scenarios in the BEAS-2B cell line (Figure 34).

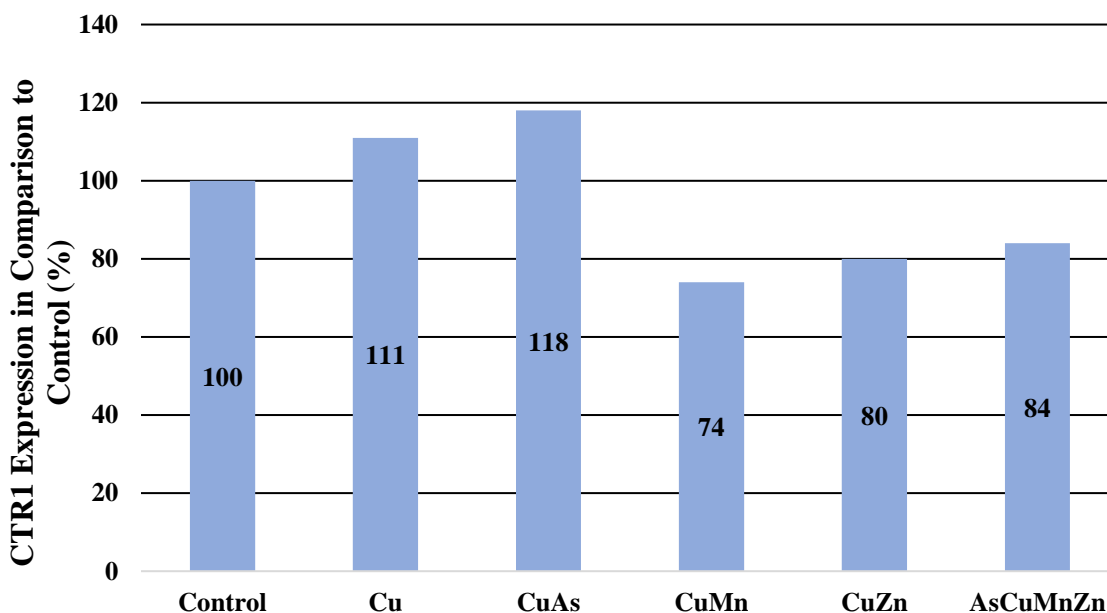


Figure 34: CTR1 Expression in Copper-Treated BEAS-2B Cells
 Graph of CTR1 protein expression (%) in different Cu exposure scenarios in comparison to control in BEAS-2B cell

Based on the normalized densitometric data collected, the expression of CTR1 was calculated to be decreased in three exposure scenarios and increased in two exposure scenarios. The cell culture exposed to Cu and As was calculated to have the greatest increase of expression, at 18%, followed by the cell culture exposed to Cu only, which was increased by 11% when compared to the control. Meanwhile, the cell culture exposed to Cu and Mn was calculated to have the greatest decrease in expression, at 31%, and the cell cultures exposed to the mixture of Cu and Zn and the mixture of all four metals were both downregulated by about 20%. The normalized data for the Cu-exposed BEAS-2B cells can be seen in Appendix E (Table XXIII)

5.2.4. Manganese Protein Expression Analysis

5.2.4.1. Meconium Western Blots

To determine whether any of the proteins present in the meconium samples were the manganese transport protein of interest, ZNT10, a western blot was performed on the 13

meconium samples previously collected (Figure 35 and Figure 36). The western blots for analysis of this protein were also stained with Ponceau-S stain but showed identical results to the stained membrane above (Figure 22).

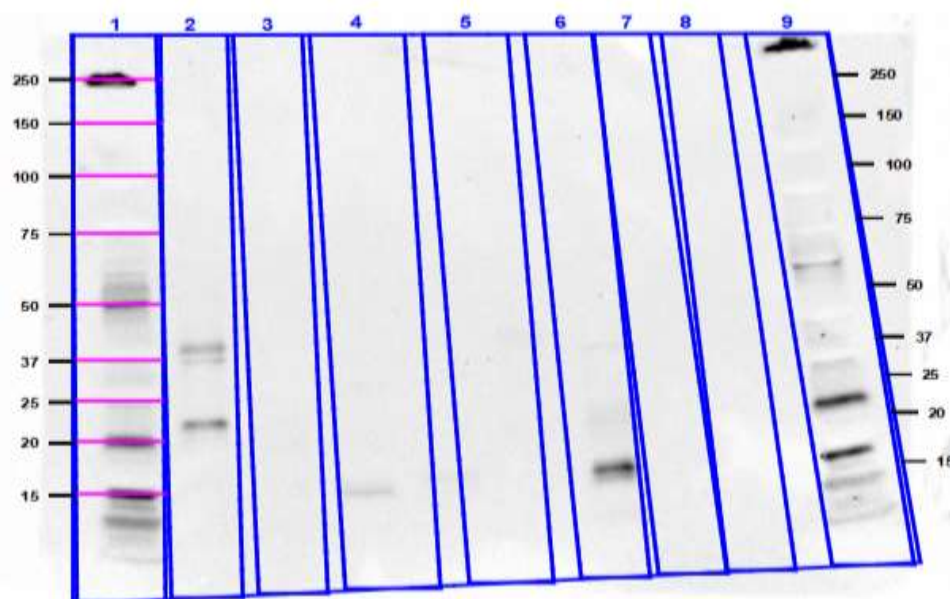


Figure 35: ZNT10 Western Blot Analysis of Meconium Samples 1-3 and 7-9

Lane 1: Protein Standard, Lane 2: Sample 1, Lane 3: Sample 2, Lane 4: Sample 3, Lane 5: Sample 7, Lane 6: Sample 8, Lane 7: Sample 9, Lane 8: Blank, Lane 9: Protein Standard.

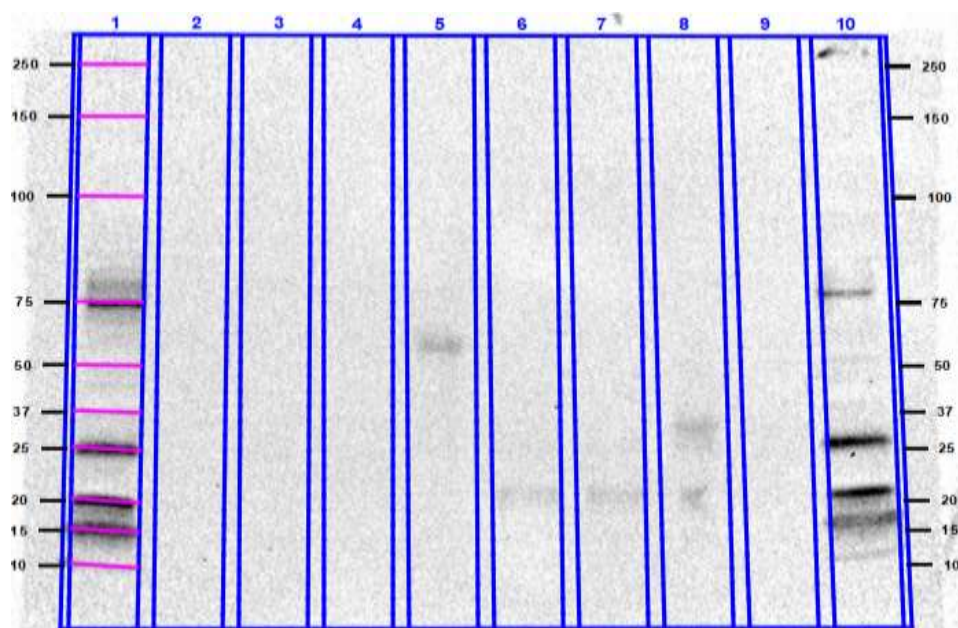


Figure 36: ZNT10 Western Blot Analysis of Meconium Samples 10-16

Lane 1: Protein Standard, Lane 2: Sample 10, Lane 3: Sample 11, Lane 4: Sample 12, Lane 5: Sample 13, Lane 6: Sample 14, Lane 7: Sample 15, Lane 8: Sample 16, Lane 9: Blank, Lane 10: Protein Standard.

If ZNT10 was present in any of the samples, bands should have appeared around 53 kDa on the western blots (Anti-SLC30a10 antibody, ab229954: Data Sheet). Bands at this molecular weight did not appear on either of the western blots, suggesting that ZNT10 was not able to be detected in the samples. The bands that did appear are approximately the same molecular weight as the ones that appeared on all other meconium western blots analyzed as well as the Ponceau S-stained membrane.

5.2.4.2. HEK293 and BEAS-2B Western Blots

The western blots performed on the HEK293 and BEAS-2B samples exposed to different Mn exposure scenarios (Table V: Mammalian Cell Line Metal Exposures) were used to determine if ZNT10 was present in any of the samples in both cell lines (Figure 37 and Figure 38).

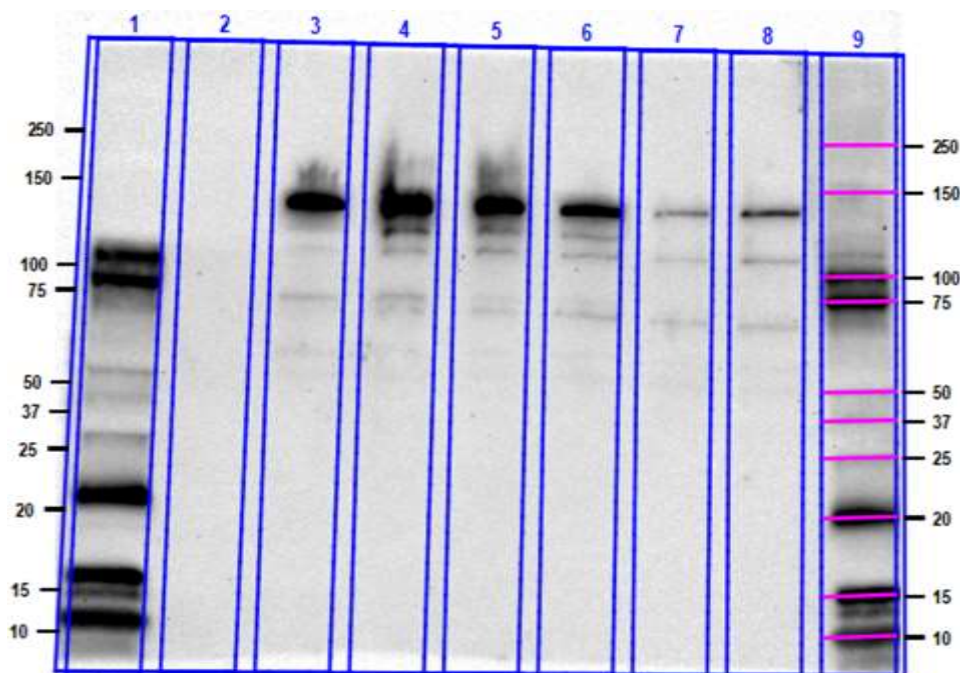


Figure 37: ZNT10 Western Blot Analysis of Varying Metal Exposures in HEK293 Cells
 Lane 1: Protein Standard, Lane 2: Blank, Lane 3: As:Cu:Mn:Zn Exposure, Lane 4: Mn:Zn Exposure,
 Lane 5: Cu:Mn Exposure, Lane 6: As:Mn Exposure, Lane 7: Mn Exposure, Lane 8: Control, Lane 9:
 Protein Standard.

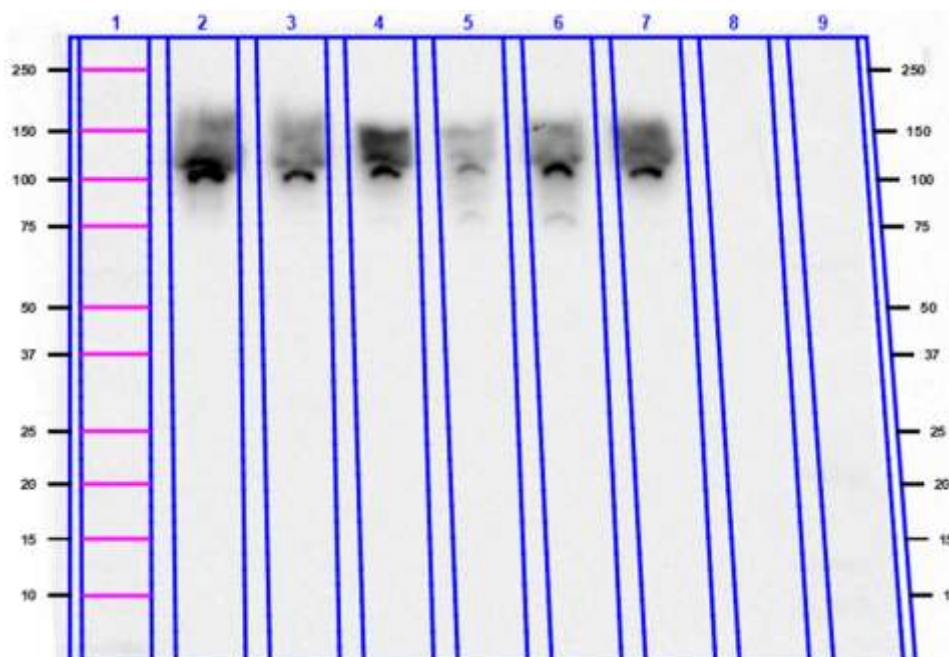


Figure 38: ZNT10 Western Blot Analysis of Varying Metal Exposures in BEAS-2B Cells
Lane 1: Protein Standard, Lane 2: Control, Lane 3: Mn Exposure, Lane 4: As:Mn Exposure, Lane 5: Cu:Mn Exposure, Lane 6: Mn:Zn Exposure , Lane 7: As:Cu:Mn:Zn Exposure, Lane 8; Blank, Lane 9: Protein Standard.

The only bands that appeared on the HEK293 (Figure 37) and BEAS-2B (Figure 38) western blots analyzing the presence of ZNT10 were those representatives of Vinculin, between 100-150 kDA. In Figure 37, multiple random lines can be seen towards the top of the membrane, but these bands are suggested to be from non-specific antibody binding of proteins that are not ZNT10. Since bands were not observed for the ZNT10 protein, densitometric analysis could not be performed to assess the expression of the protein in the different Mn exposure scenarios.

5.2.5. Zinc Protein Expression Analysis

5.2.5.1. Meconium Western Blots

To determine whether any of the proteins present in the meconium samples were the Zinc transport protein of interest, ZNT1, a western blot was performed on the 13 meconium samples previously collected (Figure 39 and Figure 40). The western blots for analysis of this protein

were also stained with Ponceau-S stain but showed identical results to the stained membrane above (Figure 22).

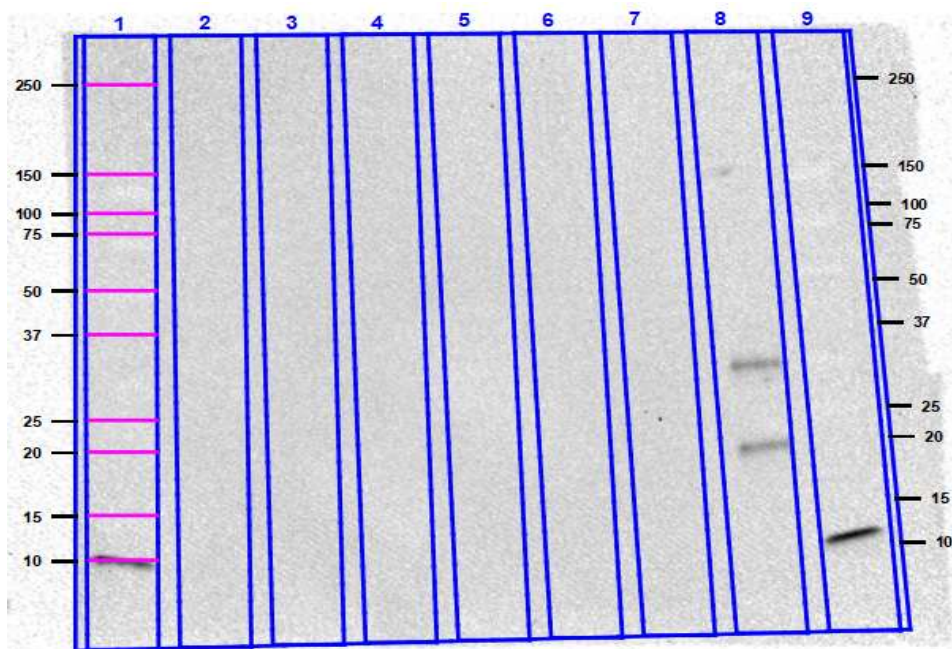


Figure 39: ZNT1 Western Blot Analysis of Meconium Samples 1-3 and 7-9
 Lane 1: Protein Standard, Lane 2: Blank, Lane 3: Sample 9, Lane 4: Sample 8, Lane 5: Sample 7, Lane 6: Sample 3, Lane 7: Sample 2, Lane 8: Sample 1, Lane 9: Protein Standard.

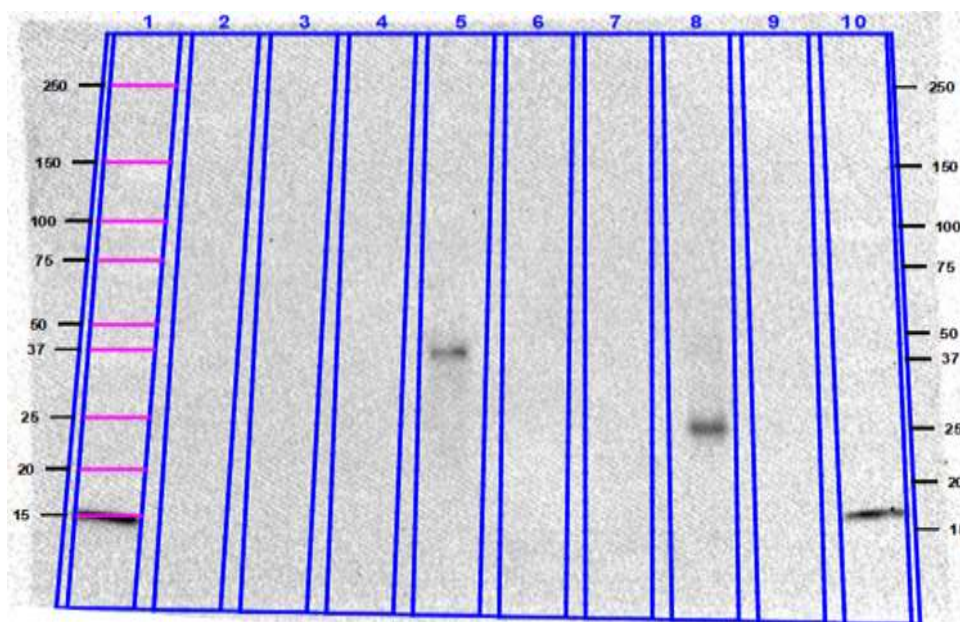


Figure 40: ZNT1 Western Blot Analysis of Meconium Samples 10-16
 Lane 1: Protein Standard, Lane 2: Blank, Lane 3: Sample 16, Lane 4: Sample 15, Lane 5: Sample 14, Lane 6: Sample 13, Lane 7: Sample 12, Lane 8: Sample 11, Lane 9: Sample 9, Lane 10: Protein Standard.

If ZNT1 was present in any of the samples, bands should have appeared around 70 kDA on the western blots (SLC30a1 Polyclonal Antibody, PA5-42481: Data Sheet). Bands at this molecular weight did not appear on either of the western blots (Figure 39 and Figure 40), suggesting that ZNT1 was not able to be detected in the samples. The bands that did appear are approximately the same molecular weight as the ones that appeared on all other meconium western blots analyzed as well as the Ponceau S-stained membrane.

5.2.5.2. HEK293 and BEAS-2B Western Blots

The western blots performed on the HEK293 and BEAS-2B samples exposed to different Zn exposure scenarios (Table V: Mammalian Cell Line Metal Exposures) were used to determine if ZNT1 was present in any of the analyzed samples in both cell lines (Figure 41 and Figure 42)

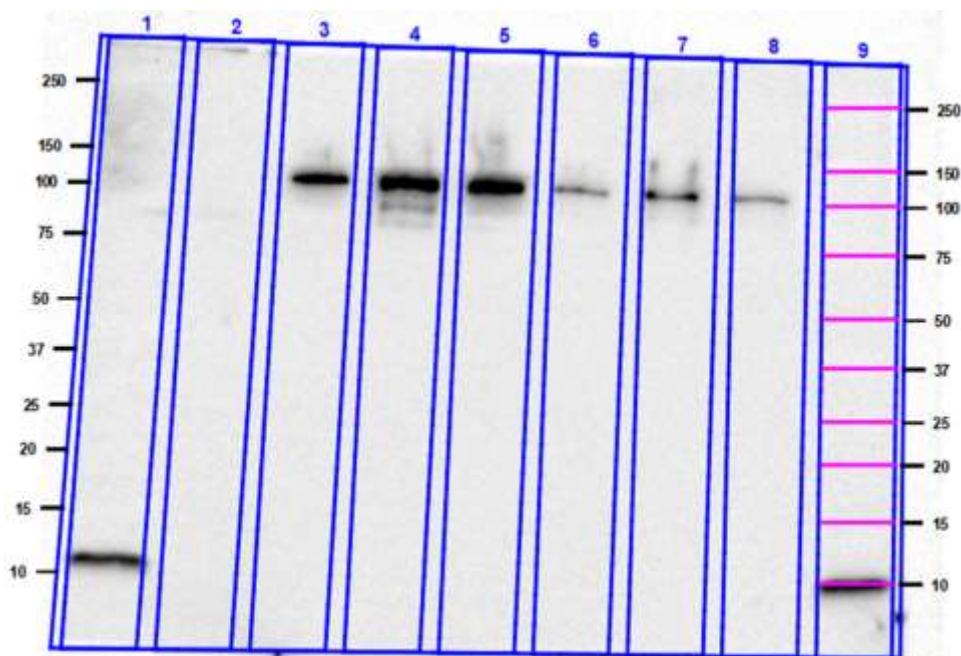


Figure 41: ZNT1 Western Blot Analysis of Varying Metal Exposures in HEK293 Cells
Lane 1: Protein Standard, Lane 2: Blank, Lane 3: As:Cu:Mn:Zn Exposure, Lane 4: Mn:Zn Exposure,
Lane 5: Cu:Zn Exposure, Lane 6: As:Zn Exposure, Lane 7: Zn Exposure, Lane 8: Control, Lane 9: Protein
Standard.

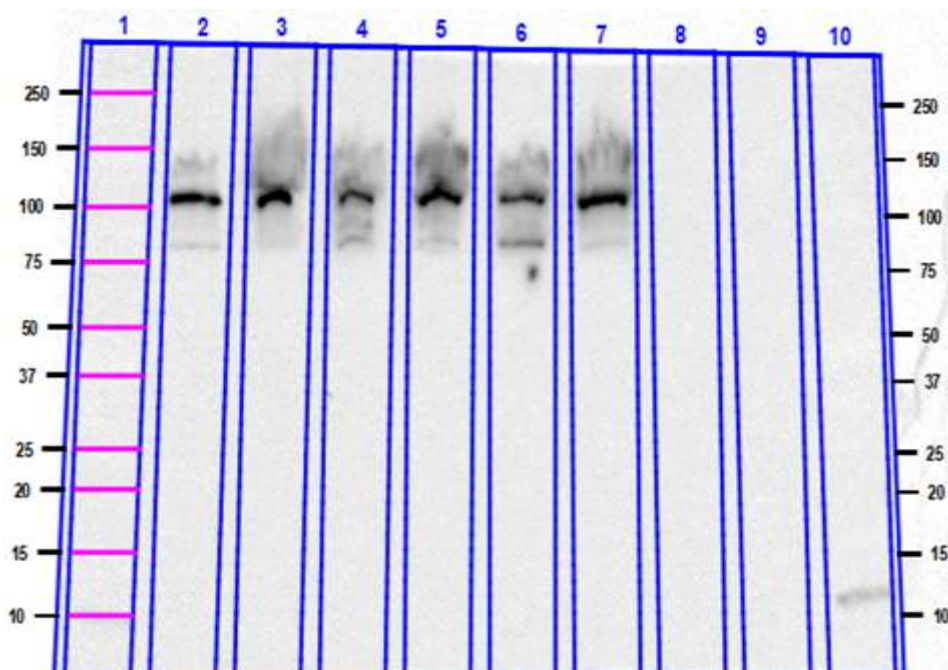


Figure 42: ZNT1 Western Blot Analysis of Varying Metal Exposures in BEAS-2B Cells
Lane 1: Protein Standard, Lane 2: Control, Lane 3: Zn Exposure, Lane 4: As:Zn Exposure, Lane 5: Cu:Zn Exposure, Lane 6: Mn:Zn Exposure, Lane 7: As:Cu:Mn:Zn Exposure, Lane 8: Blank, Lane 9: Blank, Lane 10: Protein Standard.

The only bands that appeared on the HEK293 (Figure 41) and BEAS-2B (Figure 42) western blots analyzing the presence of ZNT1 were those representatives of the Vinculin control protein between 100-150 kDA. Since bands were not observed for ZNT1, densitometric analysis could not be performed to assess the expression of the protein in the different Zn exposure scenarios.

5.2.6. Tumor Necrosis Factor alpha Analysis

5.2.6.1. HEK293 ELISA

To assess the expression of cytokine TNF- α as an indicator of oxidative stress, an Enzyme-Linked Immunoassay (ELISA) was performed on all the metal exposure scenarios in the HEK293 cells (Figure 43).

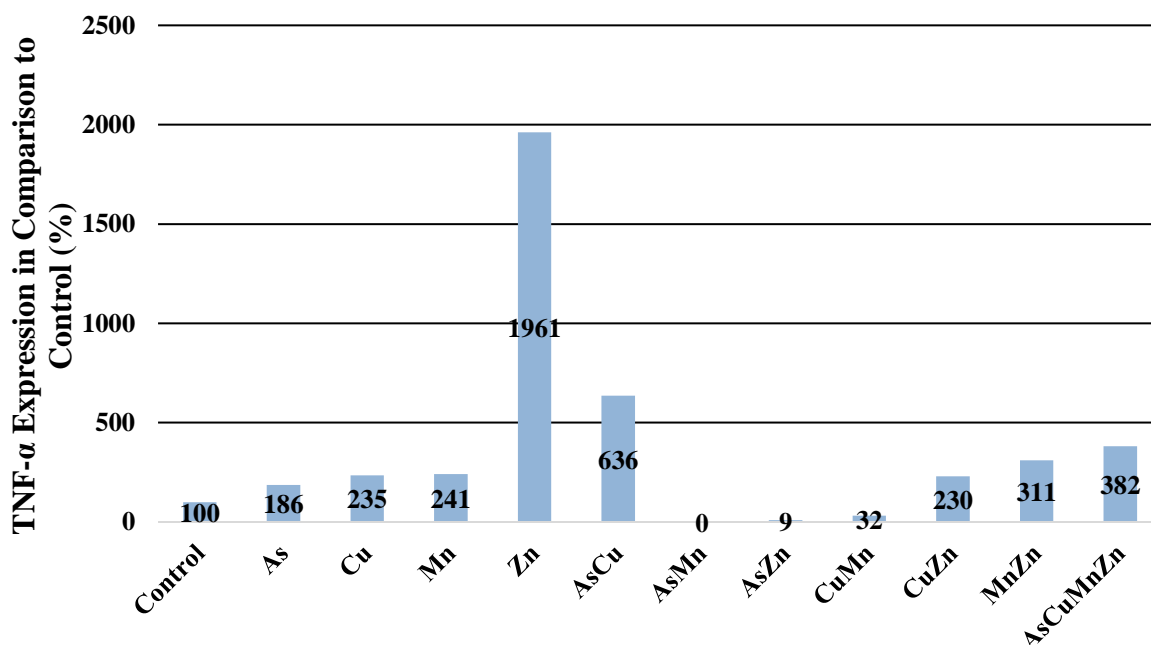


Figure 43: TNF- α ELISA Plate Results in HEK293 Cells
 Graph of TNF- α cytokine expression (%) in different metal exposure scenarios compared to the control in HEK293 cells.

Analyses of the ELISA plates was carried out using a UV-VIS spectrophotometer and the concentration of the cytokine in each HEK293 cell culture was calculated based on the equation generated from the standard curve. The same calculations that were performed to determine overall sample protein concentration through the BCA assays were used to calculate the cytokine content of the samples. The percent expression of TNF- α in each HEK293 exposure sample was calculated through comparison to the control sample. The raw and calculated data for the ELISA TNF- α analysis of the HEK293 cell cultures can be seen in Appendix F (Table XXIV).

Eight samples showed increased expression of TNF- α , while two showed decreased expression in comparison to the control. The expression of TNF- α in the cell culture exposed to Zn was calculated to be 1861% higher than the control, which seems disproportionately high. This was the cell culture calculated to have the highest greatest increase in percent expression of the cytokine, but others showed a considerable amount of upregulation as well. The culture

exposed to the mixture of As and Zn was calculated to have TNF- α expression 91% lower than the control. This was the sample calculated to have the greatest percent decrease of cytokine expression. Expression values were not able to be calculated for the culture that was exposed to the mixture of As and Mn.

5.2.6.2. BEAS-2B ELISA

To assess the expression of cytokine TNF- α as an indicator of oxidative stress, an ELISA was performed on all the metal exposure scenarios in the BEAS-2B cells (Figure 44).

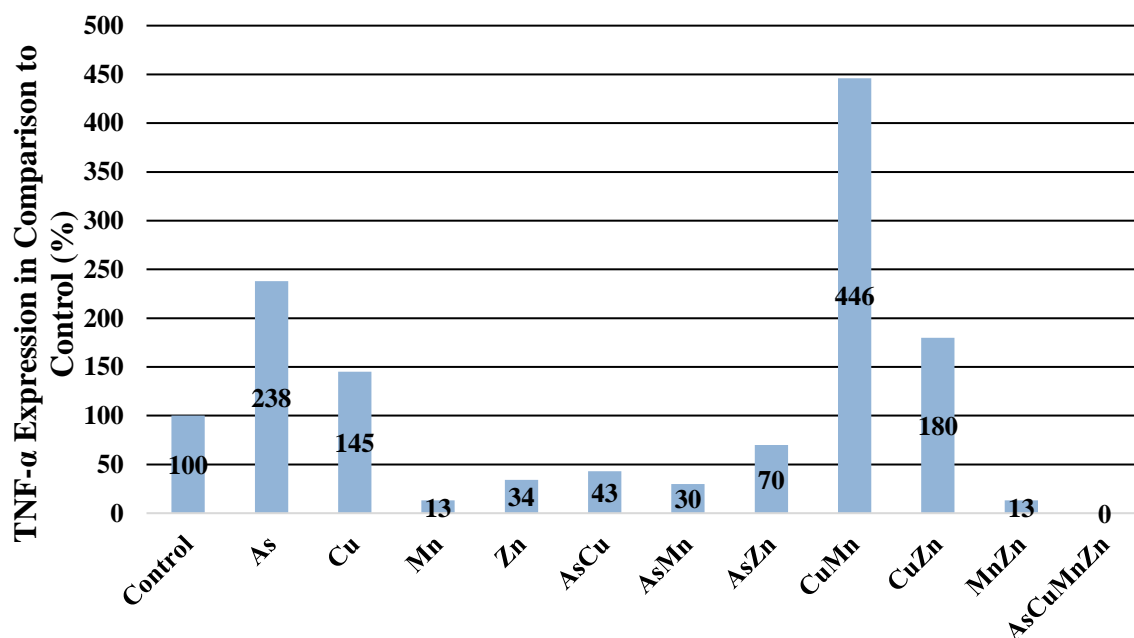


Figure 44: TNF- α ELISA Plate Results in BEAS-2B Cells
Graph of TNF alpha cytokine expression (%) in different metal exposure scenarios compared to the control in BEAS-2B cells.

Four BEAS-2B samples were calculated to have increased expression of TNF- α , while six showed decreased expression in comparison to the control. The expression of TNF- α in the cell culture exposed to the Cu and Mn mixture was calculated to be 346% greater than the control. This was the cell culture showing the greatest percent increases of TNF- α expression. The cell cultures exposed to Mn and the mixture of Mn and Zn were calculated to have an 87%

decrease in TNF- α expression when compared to the control. These two samples had the percent greatest decrease of TNF- α expression. Values were not able to be calculated for the cell culture exposed to the mixture of all four metals. The raw and calculated data for the ELISA TNF- α analysis of the BEAS-2B cell cultures can be seen in Appendix F (Table XXV).

5.2.6.3. Meconium ELISA

To assess the expression of cytokine TNF- α as an indicator of oxidative stress, an ELISA was performed on all the meconium samples (Figure 45).

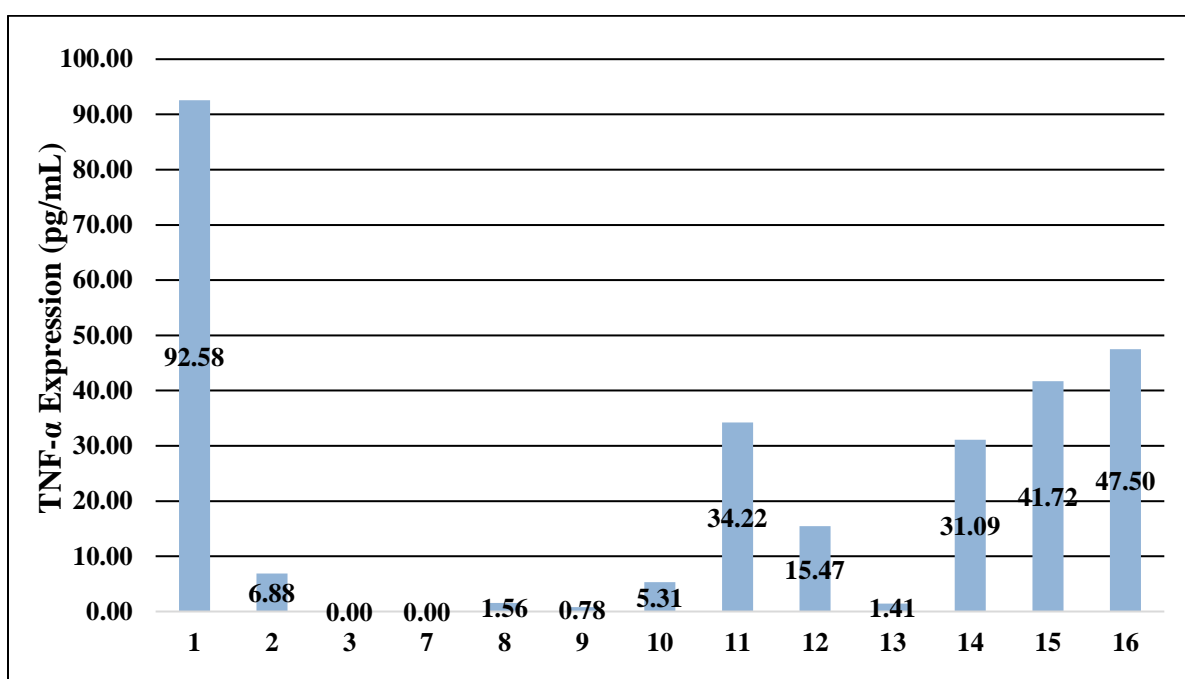


Figure 45: TNF- α ELISA Plate Results of the Meconium Samples
Graph of TNF- α cytokine concentration (pg/mL) in the 13 meconium samples investigated in this study.

A control sample was not able to be obtained for the meconium samples, so percent comparison of TNF- α expression was not able to be calculated for these samples. However, the concentration (pg/mL) of TNF- α in each sample was able to be calculated using the standard curve equation. Meconium Sample 1 was found to have the highest concentration of TNF- α at 92.58 pg/mL, while Sample 9 showed the lowest concentration of TNF- α at 0.78 pg/mL.

Including Sample 9, six samples were calculated to have a TNF- α concentration lower than 20.00 pg/mL, while Sample 1 was the only sample calculated to have a TNF- α concentration greater than 50.00 pg/mL. Cytokine concentrations were not able to be calculated for meconium Samples 3 and 7. The raw and calculated data for the TNF- α ELISA analysis of the meconium samples can be seen in Appendix F (Table XXVI).

5.2.7. Interleukin 6 Analysis

5.2.7.1. HEK293 ELISA

To assess the levels of the cytokine IL-6 as another indicator of oxidative stress, an ELISA was performed on all metal exposure scenarios in HEK293 cell cultures (Figure 46), BEAS-2B cell cultures (Figure 47), and meconium samples. Expression of IL-6 was not able to be detected in any of the meconium samples.

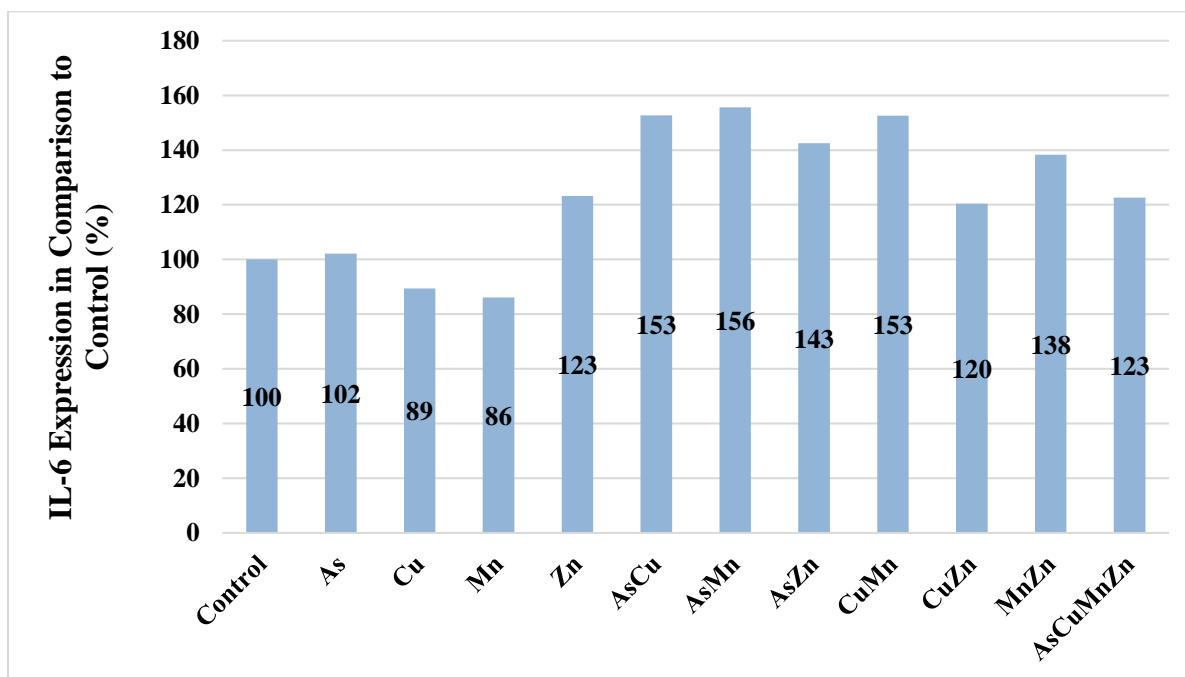


Figure 46: IL-6 ELISA Plate Results in HEK293 Cells
Graph of IL-6 cytokine expression (%) in different metal exposure scenarios compared to the control in HEK293 Cells.

Analysis of percent IL-6 expression in HEK293 cells indicated that nine cell cultures showed increased expression, while only two were calculated to have decreased expression when compared to the control. The percent expression of IL-6 in the cell culture exposed to the mixture of As and Mn was calculated to be 56% higher than the control, which was the cell culture showing the greatest percent increase of IL-6 expression. The samples exposed to As only and Cu only were calculated to have similar decreases in percentage expression when compared to the control, around 15%. The raw and calculated data for the IL-6 ELISA analysis of the HEK293 samples can be seen in Appendix G (Table XXVII).

5.2.7.2. BEAS-2B ELISA

To assess the levels of the cytokine IL-6 as another indicator of oxidative stress, an ELISA was performed on all metal exposure scenarios in the BEAS-2B cell cultures (Figure 47).

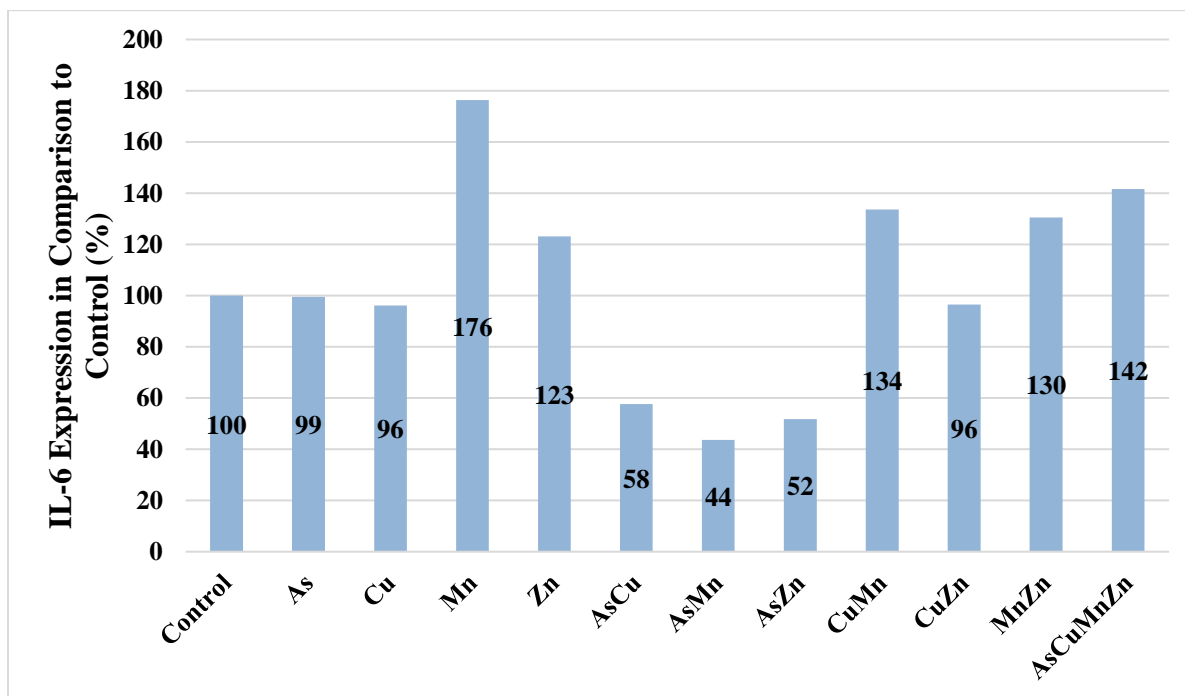


Figure 47: IL-6 ELISA Plate Results in BEAS-2B Cells
Graph of IL-6 cytokine expression (%) in different metal exposure scenarios compared to the control in BEAS-2B Cells.

Analysis of percent IL-6 expression in BEAS-2B cells indicates that five cell cultures showed increased expression, whereas six were calculated to have decreased expression when compared to the control. The expression of IL-6 in the cell culture exposed to Mn was calculated to be 76% higher than the control. This was the cell culture showing the greatest percent increase in IL-6 expression. The sample exposed to the mixture of As and Mn was calculated to have the greatest percent decrease of IL-6 expression at 66% lower than the control. The cell cultures exposed to the mixture of As only, Cu only, and the mixture of Cu and Zn showed comparable expressions to the control sample. The raw and calculated data for the IL-6 ELISA analysis of the meconium samples can be seen in Appendix G (Table XXVIII).

6. Discussion

6.1. Preliminary Bioavailability Study

Bioavailability is a measure of the amount of a substance that reaches the bloodstream after escaping first elimination, making it possible for the metal to have an active effect in the human body (Klassen, 2019). Many aspects could impact metal bioavailability, such as soil organic matter content, presence of organic microbes, pH, speciation, redox state, particle size, and clay content (Brandham *et al.*, 2004). These factors are not only relevant for metal bioavailability from soil samples, but also for dust samples, as approximately 60-80% of household dust is tracked in soil (Brandham *et al.*, 2004). It has been determined that the bioaccessibility/bioavailability of metals can majorly be accounted for by metals that are of the finest particle size (Madrid *et al.*, 2008). Additionally, soluble metal species tend to be more mobile and bioavailable, leading to these species being the most toxic metal fraction (de Paiva Magalhães *et al.*, 2015).

Of the many different physiochemical characteristics that can affect metal bioavailability, pH is thought to be one of the more influential characteristics (Olaniran *et al.*, 2013a). At an acidic pH, when more protons are available, metal-binding sites become saturated. Therefore, metals are less likely to form insoluble precipitates, since the compounds with which the metals would form precipitates are majorly protonated, so they exist mainly as free ionic species and are more bioavailable (Hughes and Poole, 1991). On the other hand, under basic conditions, where the proton concentration is low, metal ions can replace protons to form insoluble compounds, making them less bioavailable (Olaniran *et al.*, 2013a). It should be noted that a small change in pH can reduce the solubility and bioavailability of metals by several orders of magnitude (Olaniran *et al.*, 2013a).

The differences observed in the bioavailability of samples in this study are thought to be largely due to the pH of the environment from which the samples were collected as well as the pH adjustments performed throughout the physiological-based extraction test. Additionally, it was observed that a type of biofilm formed on the surface, and in some cases, throughout the digest tubes containing the stomach and intestinal digest fractions for analysis. Since the presence of organic microbes is known to have an effect on the bioavailability of metals, these biofilms could have affected the overall bioavailability of the metals as well.

6.2. Meconium Protein Expression

It was determined that none of the metal proteins of interest were able to be detected in the meconium samples analyzed in this study. The proteins of interest may be present during phases of fetal development, but since meconium is a product of maternal and fecal excretion, the proteins could have been easily degraded through metabolic processes. Proteins were found to be present in the meconium samples analyzed, but the identities of these proteins are unknown.

There were some bands detected at approximately the correct weight for the protein(s) of interest, but these bands also appeared on the western blots for completely unrelated proteins. Additionally, the molecular weights of the bands that appeared on all the membranes correlate closely with the molecular weights of the major bands that appeared on the stained membrane (Figure 22). Because of this, it is likely that the same proteins were detected in all the samples and were the same proteins that appeared on the stained membranes. These proteins were suggested to be present in high concentrations, which lead to the non-specific binding that was observed. Non-specific antibody binding is mostly controlled for by multiple blocking steps

throughout the western blotting process. However, many factors can result in non-specific binding of antibodies.

Tumor Necrosis Factor alpha was detected in all but two of the meconium samples. However, comparative expression values were not able to be calculated, as a meconium control sample was not able to be obtained for the study. Interleukin-6 was not found to be present in any of the meconium samples analyzed but could have been present in fetal meconium at some point during development. Expression of TNF- α in the meconium samples cannot be linked directly to metal exposure, as there are a variety of factors that could have induced the expression of the cytokine throughout fetal development. However, oxidative stress induced by metal exposures during gestation may have contributed to the levels of the cytokine detected in the samples.

It is suggested that the concentration of certain metals that play a role in inflammatory responses in the body could affect cytokine concentration. For example, Sample 1 was calculated to have the highest concentration of TNF- α , but the lowest concentration of Zn from the raw data of the previous meconium study (McDermott *et al.*, 2020). Since Zn is known to play a major role in inflammation repression, this indicates that there may be a possible link between the expression of the cytokine and the presence of Zn as well as other metals in the samples. No other obvious trends were observed between metal and TNF- α concentrations in the meconium samples. However, repeating a meconium study with more samples and a control versus mining exposed populations could help to determine the possible relationship between metal concentration ratios and TNF- α concentrations in these samples.

6.3.Arsenic Exposure Protein Expression

It was hypothesized that the expression of the human arsenic biomethylation protein, AS3MT, would be increased in the presence of excess As to deal with the additional As load that the to which the cell cultures were exposed. Also, that mixtures of As and other metals would affect protein expression differently than the single metal exposure due to varying metal interactions within the cells. Exposure to As by itself did not result in increased expression of AS3MT in either cell line. This is likely because the concentration of As to which the cell cultures were exposed was not a high enough to lead to accumulation of excess As levels in the cells. The exposure concentrations were not chosen to be toxic to the cells, but to potentially represent chronic, low-level exposure in Butte, MT. Exposures to metal mixtures were shown to affect the expression of AS3MT differently than exposure to As only, supporting the data that metal mixtures affect mammalian systems differently than single metal exposures. Both an increase and decrease were seen in AS3MT protein expression in cultures exposed to the metal mixtures, suggesting that different metal mixtures impact the activity of AS3MT differently.

Although the calculated expression values for each metal and metal mixture were different between the two cell lines utilized. The exposure scenarios followed the same trend between the cell lines. It was observed that exposure to As by itself decreased the expression of AS3MT comparatively in the lung and kidney cells. Exposure to the mixture of all four metals showed the greatest decrease in protein expression in both cell lines, which is suggested to be due to metal interactions disrupting the function of the protein. The HEK293 cells did show a greater decrease in AS3MT expression when compared to the BEAS-2B cells and no increase in AS3MT expression. This could be due to differences in membrane permeability between the cell types, which could lead to alterations in metal uptake between the cells and subsequent variations in protein expression.

There are many ways in which AS3MT function can be impacted by metal mixtures, including depletion of the major AS3MT cofactor, SAM, due to the cofactor being utilized in other proteins working to detoxify the metal mixtures. The presence of other metals also has potential to change As speciation, which could have affect the protein, as AS3MT methylates trivalent As species preferentially. Lastly, it is possible that the presence of other metals that induce the expression of metallothioneins or glutathione, such as Cu and Zn, may increase the presence of these antioxidant molecules, which sequester the As present, reducing the need for AS3MT protein. The possible routes as to how metal mixtures can affect the expression of proteins are nearly endless, and additional mechanistic studies would be necessary which are beyond the scope of this project.

6.4. Copper Exposure Protein Expression

It was hypothesized that the expression of the Copper Transport protein, CTR1, would be decreased in the presence of high Cu levels to avoid transport of excess Cu into the cells. This possible decrease in protein expression is suggested to be caused by the degradation of CTR1 in the presence of excess Cu levels, making it inactive and unable to transport Cu into the cells. Additionally, CTR1 is suggested to be required for Cu bioavailability, so in Cu high environments, it is suggested that expression of this protein will be decreased so that excess Cu does not become bioavailable to the cells. The primary antibody selected for the study can bind to an inactive precursor protein of CTR1, so it was expected that this precursor would be present in samples exposed to excess Cu levels or in samples where Cu transport into the cells was decreased. Mixtures of Cu and other metals were predicted to impact protein expression differently than the single metal Cu exposure due to varying metal interactions within the cells.

Unlike analysis of AS3MT, the comparative expression values obtained for CTR1 showed few trends between the HEK293 and BEAS-2B cell lines. However, exposure to Cu only did result in increased expression of CTR1 in both cell lines. This is not what was expected to happen but likely occurred because the concentration of Cu to which the cell cultures were exposed was not high enough to trigger a decrease in CTR1 expression. In both cell lines, there was expression of both the CTR1 precursor protein and mature protein in some samples. This precursor protein is inactive, indicating that there was a certain level of CTR1 inactivity in some of the exposure scenarios. Comparative values were not able to be obtained for the precursor protein, as the protein was not expressed in all samples and background noise was too high in some lanes for the image lab software to report a reading.

As noted above, changes in protein expression in the two cell lines could be due to different cell membrane permeabilities which could lead to alterations in metal uptake between the cells and subsequent variations in protein expression. Another common trend seen in both cell lines was that metal mixtures containing Cu, Zn, and Mn were shown to decrease the expression of CTR1. These three metals are all trace micronutrients and may compete for transport proteins, as they are all transported by solute carrier proteins. Not only could interactions between these metals result in a change in CTR1 expression, but there may have been competition between these solute carrier proteins that resulted in changes to the activity of the CTR1 protein. Additionally, Cu and Zn are next to each other in the Irving-Williams series describing affinities of metals in protein binding sites, indicating that there may be increased competition between these two metals. Again, the possible routes as to how metal mixtures can affect protein expression are nearly endless, however, the mechanisms discussed above have been proposed for this study.

6.5. Manganese Exposure Protein Expression

It was hypothesized that the expression Zinc Transporter 10 protein, ZNT10, which has highest the affinity for Mn, would be increased in the presence of Mn to export excess Mn out of cells. Also, that cultures exposed to metal mixtures were hypothesized to have expressions different than the single metal exposure due to metal mixture interactions occurring within the cells. This protein did not appear in any of the samples, so expression comparisons could not be performed. This does not mean that that protein was not present in the samples, as many factors could have caused the lack of results obtained for analysis of this protein. However, since the Vinculin samples appeared on the western blots, it is suggested that the primary antibody selected for the investigation did not work. Some non-specific antibody binding was suspected in the western blot analyses for these proteins, which could be because the ZNT10 protein is part of the SLC30 family of proteins. This is a large protein family, so it is possible that the non-specific binding was of different proteins in this family. Other proteins should be investigated for Mn transport in future studies.

6.6. Zinc Exposure Protein Expression

It was hypothesized that the expression Zinc Transporter 1 protein, ZNT1, would be increased in the presence of Zn to avoid Zn toxicity within the cells and that metal mixtures would affect expression different than the single metal exposure. This protein did not appear in any of the samples, so expression comparisons could not be performed. This does not mean that the protein was not present in the samples, as many factors could have caused the lack of results obtained for analysis of this protein. However, since the Vinculin samples appeared on the western blots, it is suggested that the primary antibody selected for the investigation did not work. Other proteins should be investigated for Zn transport in future studies.

6.7. Cytokine Expression

Analysis of cytokine expression in the cell cultures was performed to assess oxidative stress induced by the varying metal exposure scenarios. It was expected that expression changes would be consistent between the two cell lines and that there would be increased expression of both cytokines in all exposure scenarios. A decrease in TNF- α expression was seen in only two exposure scenarios in the HEK293 cell lines, while the rest of the exposures resulted in a considerable increase in the expression of the cytokine. Analysis of TNF- α expression in BEAS-2B cells indicated that only four exposure scenarios resulted in an increase in cytokine expression and the rest a decrease. In HEK293 cells, an increase in IL-6 expression was seen in all but two of the exposure scenarios. Expression of IL-6 in BEAS-2B cells was highly variable, as some samples showed comparable expression levels to the control sample, while others showed a considerable increase or decrease in expression of the cytokine. Overall, many factors can be attributed to the varying changes in cytokine expression, but exposure to the metals and metal mixtures is suggested to be the major factor.

The lack of agreement between cytokine expression values in the two cell lines could have been caused by varying metal uptake due to membrane permeability differences and the subsequent stress caused by that metal uptake. Additionally, the two cell lines could have different mechanisms to deal with oxidative stress or other factors that can lead to the expression of these cytokines.

7. Conclusions

It has been suggested that exposure to single metals and metals mixture found in Butte Montana's mining contaminated environment can have negative health consequences for those living in the Butte area. A preliminary study was performed to determine the average concentrations of As, Cd, Cu, Pb, Mn, and Zn from residential soil and household dust samples from houses near current and historic mining operations. The bioavailability of each metal was then assessed to determine what percent of the metals found to be present may be able to have an active effect in the human body. Results of this preliminary study showed that As, Mn, and Pb levels were highest in the soil samples, whereas levels of the Cd, Cu, and Zn were highest in the dust samples. The bioavailability of the metals was determined to be highest in the stomach phase for the dust samples and highest in the intestinal phase for the soil samples.

To determine the possible health effects of the metal concentrations found to be present within the Butte community, the expression of four proteins and two inflammatory markers was analyzed in meconium samples of babies born in Butte and HEK293 and BEAS-2B cultures. These cell cultures were exposed to single metal and metal mixtures calculated to be representative of low-level exposure scenarios in Butte. Expression of the proteins of interest was investigated through western blot analyses, while enzyme-linked immunoassays were used to analyze the expression of the select cytokines.

The protein AS3MT was selected to examine the effects of As and As metal mixture exposures in meconium and cell culture samples. This protein was found to be present in all exposure scenarios in both cell lines, but not in the meconium samples. The expression of the protein was found to be impacted differently between exposure to As only and exposure to the metal mixtures.

The protein CTR1 was selected to investigate the effects of Cu and Cu metal mixture exposures in all sample types. This protein was also found to be present in all cell cultures analyzed and was not able to be detected in the meconium samples. Like that of AS3MT, the expression of CTR1 was found to be affected differently by exposure to Cu only and to Cu metal mixtures.

The proteins selected to investigate the effects of Mn and Zn, ZNT10 and ZNT1 respectively, were not detected in any of the cell culture or meconium samples, so comparison analyses were not performed for these proteins. Other transport proteins should be investigated for these two metals in future studies.

The cytokines TNF- α and IL-6 were selected to investigate oxidative stress caused by exposure to metal and metal mixtures. The proinflammatory cytokine TNF- α was detected in a majority of the cell culture and meconium samples. There was no obvious trend observed in the expression of this cytokine in different exposure scenarios between the two cell lines, but increased expression was seen in some of the exposure scenarios possibly suggesting that the exposures caused an increase in oxidative stress. A varying range of concentrations was seen for TNF- α in the meconium samples, but was not strongly correlated with any one given metal concentration.

Expression of IL-6 in the cell cultures was similar to that of TNF- α , as there was a high amount of variability between the samples and cell types. Some samples showed comparable expression levels to the control sample, while others showed a considerable increase and decrease in expression of the cytokine. Analysis of IL-6 in the meconium samples was not performed, as detectable levels of the cytokine were not found to be present in this sample matrix or possibly had degraded. These samples were collected some time ago and stored at -80°C. It is

possible that some or many proteins are not stable under these storage conditions. Results should be re-confirmed with fresh samples in the future.

8. Recommendations and Future Directions

If the bioavailability study were to be repeated, obtaining information on the characteristics of the soil and dust samples before analysis could provide insight into the predicted bioavailability of each sample. Working to limit the biofilm formation in the digest tubes could help to limit biological interactions within the samples, which may have affected the bioavailability data collected. Also, a larger number of samples and samples collected from various neighborhoods within Butte would provide more information about metal distribution and bioavailability within the entire Butte community.

The results of the meconium sample analyses warrant further investigation to gain a deeper understanding of how meconium can provide insight into the intrauterine gestational environment. If this study were to be repeated, obtaining a control sample would allow for a comparative analysis of proteins found to be present. This would provide information as to how the environment in which the fetus was gestated affects the expression of proteins of interest, if detected. The RIPA extraction protocol used was a pretty simple and robust extraction procedure and meconium samples are fairly dirty, so using a more in-depth extraction protocol could provide cleaner samples for western blot analysis and possibly clearer results. Analyzing the protein content of the meconium samples sooner after collection may also provide different results, as few proteins are stable when stored long-term.

Additionally, the investigations of protein and cytokine expression should be repeated in an attempt to gain more consistent results between the cell lines. Consistency of results will allow researchers to gain a better understanding of how metal mixtures interact within biological systems. Being able to investigate protein expression through the use of more than one primary antibody specific for that protein would also provide better insight into the behavior of the

proteins under the different exposure conditions. Investigating multiple proteins related to each metal in an increased number of cell lines would also provide a more holistic prediction of the effects of metals and metal mixtures in a mammalian system, as living systems are emergent and involve complex interactions of multiple subsystems.

9. References Cited

- Ajees, A. A.; Marapakala, K.; Packianathan, C.; Sankaran, B.; Rosen, B. P. Structure of an as(III) s -Adenosylmethionine Methyltransferase: Insights into the Mechanism of Arsenic Biotransformation. *Biochemistry* **2012**, *51* (27), 5476–5485. <https://doi.org/10.1021/bi3004632>.
- Ali, H.; Khan, E. Trophic Transfer, Bioaccumulation, and Biomagnification of Non-Essential Hazardous Heavy Metals and Metalloids in Food Chains/Webs—Concepts and Implications for Wildlife and Human Health. *Human and Ecological Risk Assessment: An International Journal* **2019**, *25* (6), 1353–1376. <https://doi.org/10.1080/10807039.2018.1469398>.
- Ali, H.; Khan, E.; Ilahi, I. Environmental Chemistry and Ecotoxicology of Hazardous Heavy Metals: Environmental Persistence, Toxicity, and Bioaccumulation. *Journal of Chemistry* **2019**, *2019*, 1–14. <https://doi.org/10.1155/2019/6730305>.
- Al-Saleh, I.; Shinwari, N.; Mashhour, A.; Rabah, A. Birth Outcome Measures and Maternal Exposure to Heavy Metals (Lead, Cadmium and Mercury) in Saudi Arabian Population. *International Journal of Hygiene and Environmental Health* **2014**, *217* (2–3), 205–218. <https://doi.org/10.1016/j.ijheh.2013.04.009>.
- Anaconda County Smelter Health Consultation. Agency for Toxic Substances and Disease Registry (ATSDR) **October 17, 2019**. https://www.atsdr.cdc.gov/HAC/pha/AnacondaCoSmelter/Anaconda_Co_Smelter_HC-508.pdf
- Andrade, V. M.; Aschner, M.; Marreilha dos Santos, A. P. Neurotoxicity of Metal Mixtures. In *Neurotoxicity of Metals*; Aschner, M., Costa, L. G., Eds.; Springer International Publishing: Cham, 2017; Vol. 18, pp 227–265. https://doi.org/10.1007/978-3-319-60189-2_12.
- Andrews, G. K.; Wang, H.; Dey, S. K.; Palmiter, R. D. Mousezinc Transporter 1 Gene Provides an Essential Function during Early Embryonic Development. *genesis* **2004**, *40* (2), 74–81. <https://doi.org/10.1002/gene.20067>.
- Araya, M.; Pizarro, F.; Olivares, M.; Arredondo, M.; González, M.; Méndez, M. Understanding Copper Homeostasis in Humans and Copper Effects on Health. *Biological Research* **2006**, *39* (1), 183–187. <https://doi.org/10.4067/S0716-97602006000100020>.
- Aschner M, Costa LG. Neurotoxicity of metals. In: *Advances in Neurobiology*. Editor-in-Chief: Schousboe A: Springer, **2011–2018**, *18*, 3–49.
- Aschner, M. The Functional Significance of Brain Metallothioneins. *FASEB j.* **1996**, *10* (10), 1129–1136. <https://doi.org/10.1096/fasebj.10.10.8751715>.
- Aschner, M.; Guilarte, T. R.; Schneider, J. S.; Zheng, W. Manganese: Recent Advances in Understanding Its Transport and Neurotoxicity. *Toxicology and Applied Pharmacology* **2007**, *221* (2), 131–147. <https://doi.org/10.1016/j.taap.2007.03.001>.

Au, C.; Benedetto, A.; Aschner, M. Manganese Transport in Eukaryotes: The Role of DMT1. *NeuroToxicology* **2008**, 29 (4), 569–576. <https://doi.org/10.1016/j.neuro.2008.04.022>.

Ballatori, N. Transport of Toxic Metals by Molecular Mimicry. *Environmental Health Perspectives* **2002**, 110 (suppl 5), 689–694. <https://doi.org/10.1289/ehp.02110s5689>.

Bao, B.; Prasad, A. S.; Beck, F. W. J.; Godmere, M. Zinc Modulates MRNA Levels of Cytokines. *American Journal of Physiology-Endocrinology and Metabolism* **2003**, 285 (5), E1095–E1102. <https://doi.org/10.1152/ajpendo.00545.2002>.

Barakat, M. A. New Trends in Removing Heavy Metals from Industrial Wastewater. *Arabian Journal of Chemistry* **2011**, 4 (4), 361–377. <https://doi.org/10.1016/j.arabjc.2010.07.019>.

Barceloux, D. G.; Barceloux, D. Zinc. *Journal of Toxicology: Clinical Toxicology* **1999**, 37 (2), 279–292. <https://doi.org/10.1081/CLT-100102426>.

Bartolome, B.; Cordoba, S.; Nieto, S.; Fernandez-Herrera, J.; Garcia-Diez, A. Acute Arsenic Poisoning: Clinical and Histopathological Features. *Br J Dermatol* **1999**, 141 (6), 1106–1109. <https://doi.org/10.1046/j.1365-2133.1999.03213.x>.

Benveniste, E. N. Cytokine Actions in the Central Nervous System. *Cytokine & Growth Factor Reviews* **1998**, 9 (3–4), 259–275. [https://doi.org/10.1016/S1359-6101\(98\)00015-X](https://doi.org/10.1016/S1359-6101(98)00015-X).

Bergquist, E. R.; Fischer, R. J.; Sugden, K. D.; Martin, B. D. Inhibition by Methylated Organoarsenicals of the Respiratory 2-Oxo-Acid Dehydrogenases. *Journal of Organometallic Chemistry* **2009**, 694 (6), 973–980. <https://doi.org/10.1016/j.jorganchem.2008.12.028>.

Beyersmann, D. Homeostasis and Cellular Functions of Zinc. *Mat.-wiss. u. Werkstofftech.* **2002**, 33 (12), 764–769. <https://doi.org/10.1002/mawe.200290008>.

Beyersmann, D.; Hartwig, A. Carcinogenic Metal Compounds: Recent Insight into Molecular and Cellular Mechanisms. *Arch Toxicol* **2008**, 82 (8), 493. <https://doi.org/10.1007/s00204-008-0313-y>.

Bird, A. J. Cellular Sensing and Transport of Metal Ions: Implications in Micronutrient Homeostasis. *J Nutr Biochem* **2015**, 26 (11), 1103–1115. <https://doi.org/10.1016/j.jnutbio.2015.08.002>.

Bost, M.; Houdart, S.; Oberli, M.; Kalonji, E.; Huneau, J.-F.; Margaritis, I. Dietary Copper and Human Health: Current Evidence and Unresolved Issues. *Journal of Trace Elements in Medicine and Biology* **2016**, 35, 107–115. <https://doi.org/10.1016/j.jtemb.2016.02.006>.

Bradley, J. TNF-Mediated Inflammatory Disease. *J. Pathol.* **2008**, 214 (2), 149–160. <https://doi.org/10.1002/path.2287>.

Brewer, G. J. The Risks of Free Copper in the Body and the Development of Useful Anticopper Drugs: *Current Opinion in Clinical Nutrition and Metabolic Care* **2008**, *11* (6), 727–732. <https://doi.org/10.1097/MCO.0b013e328314b678>.

Bridges, C. C.; Zalups, R. K. Molecular and Ionic Mimicry and the Transport of Toxic Metals. *Toxicology and Applied Pharmacology* **2005**, *204* (3), 274–308. <https://doi.org/10.1016/j.taap.2004.09.007>.

Bulcke, F.; Dringen, R.; Scheiber, I. F. Neurotoxicity of Copper. In *Neurotoxicity of Metals*; Aschner, M., Costa, L. G., Eds.; Springer International Publishing: Cham, 2017; Vol. 18, pp 313–343. https://doi.org/10.1007/978-3-319-60189-2_16.

Calatayud, M.; Barrios, J. A.; Vélez, D.; Devesa, V. In Vitro Study of Transporters Involved in Intestinal Absorption of Inorganic Arsenic. *Chem. Res. Toxicol.* **2012**, *25* (2), 446–453. <https://doi.org/10.1021/tx200491f>.

Calderón, J.; Navarro, M. E.; Jimenez-Capdeville, M. E.; Santos-Diaz, M. A.; Golden, A.; Rodriguez-Leyva, I.; Borja-Aburto, V.; Díaz-Barriga, F. Exposure to Arsenic and Lead and Neuropsychological Development in Mexican Children. *Environmental Research* **2001**, *85* (2), 69–76. <https://doi.org/10.1006/enrs.2000.4106>.

Casarett and Doull's Toxicology: The Basic Science of Poisons, Ninth edition.; Klaassen, C. D., Ed.; McGraw-Hill Education: New York, 2019

Chakraborti, D.; Mukherjee, S. C.; Saha, K. C.; Chowdhury, U. K.; Rahman, M. M.; Sengupta, M. K. Arsenic Toxicity from Homeopathic Treatment. *Journal of Toxicology: Clinical Toxicology* **2003**, *41* (7), 963–967. <https://doi.org/10.1081/CLT-120026518>.

Chasapis, C. T.; Loutsidou, A. C.; Spiliopoulou, C. A.; Stefanidou, M. E. Zinc and Human Health: An Update. *Arch Toxicol* **2012**, *86* (4), 521–534. <https://doi.org/10.1007/s00204-011-0775-1>.

Chen, S.-J.; Yan, X.-J.; Chen, Z. Arsenic in Tissues, Organs, and Cells. In *Encyclopedia of Metalloproteins*; Kretsinger, R. H., Uversky, V. N., Permyakov, E. A., Eds.; Springer: New York, NY, 2013; pp 135–138. https://doi.org/10.1007/978-1-4614-1533-6_491.

Choi, B.-S.; Zheng, W. Copper Transport to the Brain by the Blood-Brain Barrier and Blood-CSF Barrier. *Brain Research* **2009**, *1248*, 14–21. <https://doi.org/10.1016/j.brainres.2008.10.056>.

Choi, S.; Hong, D. K.; Choi, B. Y.; Suh, S. W. Zinc in the Brain: Friend or Foe? *IJMS* **2020**, *21* (23), 8941. <https://doi.org/10.3390/ijms21238941>.

Cholanians, A. B.; Phan, A. V.; Ditzel, E. J.; Camenisch, T. D.; Lau, S. S.; Monks, T. J. From the Cover: Arsenic Induces Accumulation of α -Synuclein: Implications for Synucleinopathies and Neurodegeneration. *Toxicol. Sci.* **2016**, *153* (2), 271–281. <https://doi.org/10.1093/toxsci/kfw117>.

Choo, X. Y.; Alukaidey, L.; White, A. R.; Grubman, A. Neuroinflammation and Copper in Alzheimer's Disease. *International Journal of Alzheimer's Disease* **2013**, 2013, 1–12. <https://doi.org/10.1155/2013/145345>.

Chowanadisai, W.; Kelleher, S. L.; Lönnerdal, B. Zinc Deficiency Is Associated with Increased Brain Zinc Import and LIV-1 Expression and Decreased ZnT-1 Expression in Neonatal Rats. *J Nutr* **2005**, 135 (5), 1002–1007. <https://doi.org/10.1093/jn/135.5.1002>.

Chua, A. C. G.; Morgan, E. H. Manganese Metabolism Is Impaired in the Belgrade Laboratory Rat. *Journal of Comparative Physiology B: Biochemical, Systemic, and Environmental Physiology* **1997**, 167 (5), 361–369. <https://doi.org/10.1007/s003600050085>.

Ciesielski, T.; Weuve, J.; Bellinger, D. C.; Schwartz, J.; Lanphear, B.; Wright, R. O. Cadmium Exposure and Neurodevelopmental Outcomes in U.S. Children. *Environ Health Perspect* **2012**, 120 (5), 758–763. <https://doi.org/10.1289/ehp.1104152>.

Clark, I. A.; Allewa, L. M.; Vissel, B. The Roles of TNF in Brain Dysfunction and Disease. *Pharmacology & Therapeutics* **2010**, 128 (3), 519–548. <https://doi.org/10.1016/j.pharmthera.2010.08.007>.

Cobbina, S. J.; Chen, Y.; Zhou, Z.; Wu, X.; Feng, W.; Wang, W.; Li, Q.; Zhao, T.; Mao, G.; Wu, X.; Yang, L. Interaction of Four Low Dose Toxic Metals with Essential Metals in Brain, Liver and Kidneys of Mice on Sub-Chronic Exposure. *Environmental Toxicology and Pharmacology* **2015a**, 39 (1), 280–291. <https://doi.org/10.1016/j.etap.2014.11.030>.

Cobbina, S. J.; Chen, Y.; Zhou, Z.; Wu, X.; Zhao, T.; Zhang, Z.; Feng, W.; Wang, W.; Li, Q.; Wu, X.; Yang, L. Toxicity Assessment Due to Sub-Chronic Exposure to Individual and Mixtures of Four Toxic Heavy Metals. *Journal of Hazardous Materials* **2015b**, 294, 109–120. <https://doi.org/10.1016/j.jhazmat.2015.03.057>.

Cohen, S. M.; Arnold, L. L.; Eldan, M.; Lewis, A. S.; Beck, B. D. Methylated Arsenicals: The Implications of Metabolism and Carcinogenicity Studies in Rodents to Human Risk Assessment. *Critical Reviews in Toxicology* **2006**, 36 (2), 99–133. <https://doi.org/10.1080/10408440500534230>.

Coppin, J.-F.; Qu, W.; Waalkes, M. P. Interplay between Cellular Methyl Metabolism and Adaptive Efflux during Oncogenic Transformation from Chronic Arsenic Exposure in Human Cells*. *Journal of Biological Chemistry* **2008**, 283 (28), 19342–19350. <https://doi.org/10.1074/jbc.M802942200>.

Crossgrove, J.; Zheng, W. Manganese Toxicity upon Overexposure. *NMR Biomed.* **2004**, 17 (8), 544–553. <https://doi.org/10.1002/nbm.931>.

Cullen, W. R.; Reimer, K. J. Arsenic Speciation in the Environment. *Chem. Rev.* **1989**, 89 (4), 713–764. <https://doi.org/10.1021/cr00094a002>.

Davies, K. M.; Hare, D. J.; Cottam, V.; Chen, N.; Hilgers, L.; Halliday, G.; Mercer, J. F. B.; Double, K. L. Localization of Copper and Copper Transporters in the Human Brain. *Metallomics* **2013**, *5* (1), 43–51. <https://doi.org/10.1039/C2MT20151H>.

Davies, K. M.; Hare, D. J.; Cottam, V.; Chen, N.; Hilgers, L.; Halliday, G.; Mercer, J. F. B.; Double, K. L. Localization of Copper and Copper Transporters in the Human Brain. *Metallomics* **2013**, *5* (1), 43–51. <https://doi.org/10.1039/C2MT20151H>.

de Paiva Magalhães, D.; da Costa Marques, M. R.; Baptista, D. F.; Buss, D. F. Metal Bioavailability and Toxicity in Freshwaters. *Environ Chem Lett* **2015**, *13* (1), 69–87. <https://doi.org/10.1007/s10311-015-0491-9>.

de Romaña, D. L.; Olivares, M.; Uauy, R.; Araya, M. Risks and Benefits of Copper in Light of New Insights of Copper Homeostasis. *Journal of Trace Elements in Medicine and Biology* **2011**, *25* (1), 3–13. <https://doi.org/10.1016/j.jtemb.2010.11.004>.

Decourt, B.; Lahiri, D. K.; Sabbagh, M. N. Targeting Tumor Necrosis Factor Alpha for Alzheimer's Disease. *Curr Alzheimer Res* **2017**, *14* (4), 412–425. <https://doi.org/10.2174/1567205013666160930110551>.

Desai, V.; Kaler, S. G. Role of Copper in Human Neurological Disorders. *The American Journal of Clinical Nutrition* **2008**, *88* (3), 855S–858S. <https://doi.org/10.1093/ajcn/88.3.855S>.

DeWitt, M. R.; Chen, P.; Aschner, M. Manganese Efflux in Parkinsonism: Insights from Newly Characterized SLC30A10 Mutations. *Biochemical and Biophysical Research Communications* **2013**, *432* (1), 1–4. <https://doi.org/10.1016/j.bbrc.2013.01.058>.

Dodani, S. C.; Firl, A.; Chan, J.; Nam, C. I.; Aron, A. T.; Onak, C. S.; Ramos-Torres, K. M.; Paek, J.; Webster, C. M.; Feller, M. B.; Chang, C. J. Copper Is an Endogenous Modulator of Neural Circuit Spontaneous Activity. *PNAS* **2014**, *111* (46), 16280–16285. <https://doi.org/10.1073/pnas.1409796111>.

Dong, J.; Atwood, C. S.; Anderson, V. E.; Siedlak, S. L.; Smith, M. A.; Perry, G.; Carey, P. R. Metal Binding and Oxidation of Amyloid- β within Isolated Senile Plaque Cores: Raman Microscopic Evidence. *Biochemistry* **2003**, *42* (10), 2768–2773. <https://doi.org/10.1021/bi0272151>.

Donsante, A.; Johnson, P.; Jansen, L. A.; Kaler, S. G. Somatic Mosaicism in Menkes Disease Suggests Choroid Plexus-Mediated Copper Transport to the Developing Brain. *Am. J. Med. Genet.* **2010**, *152A* (10), 2529–2534. <https://doi.org/10.1002/ajmg.a.33632>.

Duffus, J. H. “Heavy Metals” a Meaningless Term? (IUPAC Technical Report). *Pure and Applied Chemistry* **2002**, *74* (5), 793–807. <https://doi.org/10.1351/pac200274050793>.

Eide, D. J. Zinc Transporters and the Cellular Trafficking of Zinc. *Biochimica et Biophysica Acta (BBA) - Molecular Cell Research* **2006**, 1763 (7), 711–722.
<https://doi.org/10.1016/j.bbamcr.2006.03.005>.

Engwa, G. A.; Ferdinand, P. U.; Nwalo, F. N.; Unachukwu, M. N. Mechanism and Health Effects of Heavy Metal Toxicity in Humans. *Poisoning in the Modern World - New Tricks for an Old Dog?* **2019**. <https://doi.org/10.5772/intechopen.82511>.

Erikson, K. M.; Thompson, K.; Aschner, J.; Aschner, M. Manganese Neurotoxicity: A Focus on the Neonate. *Pharmacology & Therapeutics* **2007**, 113 (2), 369–377.
<https://doi.org/10.1016/j.pharmthera.2006.09.002>.

Erta, M.; Quintana, A.; Hidalgo, J. Interleukin-6, a Major Cytokine in the Central Nervous System. *Int. J. Biol. Sci.* **2012**, 8 (9), 1254–1266. <https://doi.org/10.7150/ijbs.4679>.

Escudero-Lourdes, C.; Uresti-Rivera, E. E.; Oliva-González, C.; Torres-Ramos, M. A.; Aguirre-Bañuelos, P.; Gandolfi, A. J. Cortical Astrocytes Acutely Exposed to the Monomethylarsonous Acid (MMAIII) Show Increased Pro-Inflammatory Cytokines Gene Expression That Is Consistent with APP and BACE-1: Over-Expression. *Neurochem Res* **2016**, 41 (10), 2559–2572.
<https://doi.org/10.1007/s11064-016-1968-z>.

Essential Elements for Life https://saylordotorg.github.io/text_general-chemistry-principles-patterns-and-applications-v1.0/s05-08-essential-elements-for-life.html

Faller, P. Copper and Zinc Binding to Amyloid- β^2 : Coordination, Dynamics, Aggregation, Reactivity and Metal-Ion Transfer. *ChemBioChem* **2009**, 10 (18), 2837–2845.
<https://doi.org/10.1002/cbic.200900321>.

Ferguson-Miller, S.; Babcock, G. T. Heme/Copper Terminal Oxidases. *Chem. Rev.* **1996**, 96 (7), 2889–2908. <https://doi.org/10.1021/cr950051s>.

Firdaus, F.; Zafeer, Mohd. F.; Waseem, M.; Ullah, R.; Ahmad, M.; Afzal, M. Thymoquinone Alleviates Arsenic Induced Hippocampal Toxicity and Mitochondrial Dysfunction by Modulating MPTP in Wistar Rats. *Biomedicine & Pharmacotherapy* **2018**, 102, 1152–1160.
<https://doi.org/10.1016/j.biopha.2018.03.159>.

Foy, H. M.; Tarmapai, S.; Eamchan, P.; Metdilogkul, O. Chronic Arsenic Poisoning from Well Water in a Mining Area in Thailand. *Asia Pac J Public Health* **1992**, 6 (3), 150–152.
<https://doi.org/10.1177/101053959200600306>.

Frazzini, V.; Rockabrand, E.; Mocchegiani, E.; Sensi, S. L. Oxidative Stress and Brain Aging: Is Zinc the Link? *Biogerontology* **2006**, 7 (5), 307–314. <https://doi.org/10.1007/s10522-006-9045-7>.

Friedlich, A. L.; Lee, J.-Y.; Groen, T. van; Cherny, R. A.; Volitakis, I.; Cole, T. B.; Palmiter, R. D.; Koh, J.-Y.; Bush, A. I. Neuronal Zinc Exchange with the Blood Vessel Wall Promotes

- Cerebral Amyloid Angiopathy in an Animal Model of Alzheimer's Disease. *J. Neurosci.* **2004**, 24 (13), 3453–3459. <https://doi.org/10.1523/JNEUROSCI.0297-04.2004>.
- Fu, X.; Zhang, Y.; Jiang, W.; Monnot, A. D.; Bates, C. A.; Zheng, W. Regulation of Copper Transport Crossing Brain Barrier Systems by Cu-ATPases: Effect of Manganese Exposure. *Toxicological Sciences* **2014**, 139 (2), 432–451. <https://doi.org/10.1093/toxsci/kfu048>.
- García, J. A. O.; Gallardo, D. C.; Tortajada, J. F. i; García, M. M. P.; Grimalt, J. O. Meconium and Neurotoxicants: Searching for a Prenatal Exposure Timing. *Archives of Disease in Childhood* **2006**, 91 (8), 642–646. <https://doi.org/10.1136/adc.2005.084129>.
- Garza-Lombó, C.; Pappa, A.; Panayiotidis, M. I.; Gonsébat, M. E.; Franco, R. Arsenic-Induced Neurotoxicity: A Mechanistic Appraisal. *J Biol Inorg Chem* **2019**, 24 (8), 1305–1316. <https://doi.org/10.1007/s00775-019-01740-8>.
- Gibbons, R. A.; Dixon, S. N.; Hallis, K.; Russell, A. M.; Sansom, B. F.; Symonds, H. W. Manganese Metabolism in Cows and Goats. *Biochimica et Biophysica Acta (BBA) - General Subjects* **1976**, 444 (1), 1–10. [https://doi.org/10.1016/0304-4165\(76\)90218-X](https://doi.org/10.1016/0304-4165(76)90218-X).
- Golmohammadi, J.; Jahanian-Najafabadi, A.; Aliomrani, M. Chronic Oral Arsenic Exposure and Its Correlation with Serum S100B Concentration. *Biol Trace Elem Res* **2019**, 189 (1), 172–179. <https://doi.org/10.1007/s12011-018-1463-2>.
- Granzotto, A.; Sensi, S. L. Intracellular Zinc Is a Critical Intermediate in the Excitotoxic Cascade. *Neurobiology of Disease* **2015**, 81, 25–37. <https://doi.org/10.1016/j.nbd.2015.04.010>.
- Gregus, Z.; Klaassen, C. D. Disposition of Metals in Rats: A Comparative Study of Fecal, Urinary, and Biliary Excretion and Tissue Distribution of Eighteen Metals. *Toxicol Appl Pharmacol* **1986**, 85 (1), 24–38. [https://doi.org/10.1016/0041-008x\(86\)90384-4](https://doi.org/10.1016/0041-008x(86)90384-4).
- Grünecker, B.; Kaltwasser, S. F.; Zappe, A. C.; Bedenk, B. T.; Bicker, Y.; Spoormaker, V. I.; Wotjak, C. T.; Czisch, M. Regional Specificity of Manganese Accumulation and Clearance in the Mouse Brain: Implications for Manganese-Enhanced MRI. *NMR in Biomedicine* **2013**, 26 (5), 542–556. <https://doi.org/https://doi.org/10.1002/nbm.2891>.
- Guilarte, T. R. Manganese and Parkinson's Disease: A Critical Review and New Findings. *Environ Health Perspect* **2010**, 118 (8), 1071–1080. <https://doi.org/10.1289/ehp.0901748>.
- Guo, Y.; Smith, K.; Lee, J.; Thiele, D. J.; Petris, M. J. Identification of Methionine-Rich Clusters That Regulate Copper-Stimulated Endocytosis of the Human Ctr1 Copper Transporter. *Journal of Biological Chemistry* **2004**, 279 (17), 17428–17433. <https://doi.org/10.1074/jbc.M401493200>.
- Gupta, A.; Lutsenko, S. Human Copper Transporters: Mechanism, Role in Human Diseases and Therapeutic Potential. *Future Medicinal Chemistry* **2009**, 1 (6), 1125–1142. <https://doi.org/10.4155/fmc.09.84>.

Gybina, A. A.; Tkac, I.; Prohaska, J. R. Copper Deficiency Alters the Neurochemical Profile of Developing Rat Brain. *Nutritional Neuroscience* **2009**, *12* (3), 114–122. <https://doi.org/10.1179/147683009X423265>.

Haase, H.; Rink, L. The Immune System and the Impact of Zinc during Aging. *Immunity & Ageing* **2009**, *6* (1), 9. <https://doi.org/10.1186/1742-4933-6-9>.

Hailer, M. K.; Peck, C. P.; Calhoun, M. W.; West, R. F.; James, K. J.; Siciliano, S. D. Assessing Human Metal Accumulations in an Urban Superfund Site. *Environmental Toxicology and Pharmacology* **2017**, *54*, 112–119. <https://doi.org/10.1016/j.etap.2017.06.001>.

Harischandra, D. S.; Ghaisas, S.; Zenitsky, G.; Jin, H.; Kanthasamy, A.; Anantharam, V.; Kanthasamy, A. G. Manganese-Induced Neurotoxicity: New Insights Into the Triad of Protein Misfolding, Mitochondrial Impairment, and Neuroinflammation. *Front. Neurosci.* **2019**, *13*, 654. <https://doi.org/10.3389/fnins.2019.00654>.

Harris, E. D. Copper Homeostasis: The Role of Cellular Transporters. *Nutrition Reviews* **2009**, *59* (9), 281–285. <https://doi.org/10.1111/j.1753-4887.2001.tb07017.x>.

Harris, W. R.; Chen, Y. Electron Paramagnetic Resonance and Difference Ultraviolet Studies of Mn²⁺ Binding to Serum Transferrin. *Journal of Inorganic Biochemistry* **1994**, *54* (1), 1–19. [https://doi.org/10.1016/0162-0134\(94\)85119-0](https://doi.org/10.1016/0162-0134(94)85119-0).

Helston, R. M.; Phillips, S. R.; McKay, J. A.; Jackson, K. A.; Mathers, J. C.; Ford, D. Zinc Transporters in the Mouse Placenta Show a Coordinated Regulatory Response to Changes in Dietary Zinc Intake. *Placenta* **2007**, *28* (5–6), 437–444. <https://doi.org/10.1016/j.placenta.2006.07.002>.

Henn, B. C.; Schnaas, L.; Ettinger, A. S.; Schwartz, J.; Lamadrid-Figueroa, H.; Hernández-Avila, M.; Amarasiriwardena, C.; Hu, H.; Bellinger, D. C.; Wright, R. O.; Téllez-Rojo, M. M. Associations of Early Childhood Manganese and Lead Coexposure with Neurodevelopment. *Environmental Health Perspectives* **2012**, *120* (1), 126–131. <https://doi.org/10.1289/ehp.1003300>

History & Culture | City and County of Butte-Silver Bow, MT
<https://co.silverbow.mt.us/481/History-Culture>.

Hong, J.; Wang, Y.; McDermott, S.; Cai, B.; Aelion, C. M.; Lead, J. The Use of a Physiologically-Based Extraction Test to Assess Relationships between Bioaccessible Metals in Urban Soil and Neurodevelopmental Conditions in Children. *Environmental Pollution* **2016**, *212*, 9–17. <https://doi.org/10.1016/j.envpol.2016.01.001>.

Huang, L.; Tepasamorndech, S. The SLC30 Family of Zinc Transporters – A Review of Current Understanding of Their Biological and Pathophysiological Roles. *Molecular Aspects of Medicine* **2013**, *34* (2–3), 548–560. <https://doi.org/10.1016/j.mam.2012.05.008>.

Hughes, M. F. Arsenic Toxicity and Potential Mechanisms of Action. *Toxicology Letters* **2002**, *133* (1), 1–16. [https://doi.org/10.1016/S0378-4274\(02\)00084-X](https://doi.org/10.1016/S0378-4274(02)00084-X).

Hughes, M. N.; Poole, R. K. Y. 1991. Metal Speciation and Microbial Growth—the Hard (and Soft) Facts. *Microbiology*, *137* (4), 725–734. <https://doi.org/10.1099/00221287-137-4-725>.

Human biomonitoring: facts and figures <https://www.euro.who.int/en/media-centre/events/events/2015/04/ehp-mid-term-review/publications/human-biomonitoring-facts-and-figures>.

Hung, Y. H.; Bush, A. I.; Cherny, R. A. Copper in the Brain and Alzheimer's Disease. *J Biol Inorg Chem* **2010**, *15* (1), 61–76. <https://doi.org/10.1007/s00775-009-0600-y>.

Hung, Y. H.; Bush, A. I.; La Fontaine, S. Links between Copper and Cholesterol in Alzheimer's Disease. *Front. Physiol.* **2013**, *4*. <https://doi.org/10.3389/fphys.2013.00111>.

Hunter, C. A.; Jones, S. A. IL-6 as a Keystone Cytokine in Health and Disease. *Nat Immunol* **2015**, *16* (5), 448–457. <https://doi.org/10.1038/ni.3153>.

Imperato, M.; Adamo, P.; Naimo, D.; Arienzo, M.; Stanzione, D.; Violante, P. Spatial Distribution of Heavy Metals in Urban Soils of Naples City (Italy). *Environmental Pollution* **2003**, *124* (2), 247–256. [https://doi.org/10.1016/S0269-7491\(02\)00478-5](https://doi.org/10.1016/S0269-7491(02)00478-5).

Incorvaia, C.; Frati, F.; Verna, N.; D'Alò, S.; Motolese, A.; Pucci, S. Allergy and the Skin: Allergy and the Skin. *Clinical & Experimental Immunology* **2008**, *153*, 27–29. <https://doi.org/10.1111/j.1365-2249.2008.03718.x>.

Inoue, K.; O'Bryant, Z.; Xiong, Z.-G. Zinc-Permeable Ion Channels: Effects on Intracellular Zinc Dynamics and Potential Physiological/Pathophysiological Significance. *Curr Med Chem* **2015**, *22* (10), 1248–1257.

Iwata, A.; Iwatsubo, T.; Ihara, R.; Suzuki, K.; Matsuyama, Y.; Tomita, N.; Arai, H.; Ishii, K.; Senda, M.; Ito, K.; Ikeuchi, T.; Kuwano, R.; Matsuda, H.; Alzheimer's Disease Neuroimaging Initiative; Japanese Alzheimer's Disease Neuroimaging Initiative. Effects of Sex, Educational Background, and Chronic Kidney Disease Grading on Longitudinal Cognitive and Functional Decline in Patients in the Japanese Alzheimer's Disease Neuroimaging Initiative Study. *Alzheimer's & Dementia: Translational Research & Clinical Interventions* **2018**, *4* (1), 765–774. <https://doi.org/10.1016/j.trci.2018.06.008>.

Jadhav, S. H.; Sarkar, S. N.; Ram, G. C.; Tripathi, H. C. Immunosuppressive Effect of Subchronic Exposure to a Mixture of Eight Heavy Metals, Found as Groundwater Contaminants in Different Areas of India, Through Drinking Water in Male Rats. *Arch Environ Contam Toxicol* **2007**, *53* (3), 450–458. <https://doi.org/10.1007/s00244-006-0177-1>.

Jaishankar, M.; Tseten, T.; Anbalagan, N.; Mathew, B. B.; Beeregowda, K. N. Toxicity, Mechanism and Health Effects of Some Heavy Metals. *Interdisciplinary Toxicology* **2014**, 7 (2), 60–72. <https://doi.org/10.2478/intox-2014-0009>.

John, E.; Laskow, T. C.; Buchser, W. J.; Pitt, B. R.; Basse, P. H.; Butterfield, L. H.; Kalinski, P.; Lotze, M. T. Zinc in Innate and Adaptive Tumor Immunity. *J Transl Med* **2010**, 8 (1), 118. <https://doi.org/10.1186/1479-5876-8-118>.

Jomova, K.; Jenisova, Z.; Feszterova, M.; Baros, S.; Liska, J.; Hudecova, D.; Rhodes, C. J.; Valko, M. Arsenic: Toxicity, Oxidative Stress and Human Disease: Toxicity of Arsenic. *J. Appl. Toxicol.* **2011**, n/a-n/a. <https://doi.org/10.1002/jat.1649>.

Kalay, M.; Canli, M. Elimination of essential (Cu, Zn) and non-essential (Cd, Pb) metals from tissues of a freshwater fish *Tilapia zilli*. *Turk J Zool* **2000**, 24(4):429–36

Karri, V.; Schuhmacher, M.; Kumar, V. Heavy Metals (Pb, Cd, As and MeHg) as Risk Factors for Cognitive Dysfunction: A General Review of Metal Mixture Mechanism in Brain. *Environmental Toxicology and Pharmacology* **2016**, 48, 203–213. <https://doi.org/10.1016/j.etap.2016.09.016>.

Kennedy, T.; Ghio, A. J.; Reed, W.; Samet, J.; Zagorski, J.; Quay, J.; Carter, J.; Dailey, L.; Hoidal, J. R.; Devlin, R. B. Copper-Dependent Inflammation and Nuclear Factor- κ B Activation by Particulate Air Pollution. *Am J Respir Cell Mol Biol* **1998**, 19 (3), 366–378. <https://doi.org/10.1165/ajrcmb.19.3.3042>.

Khairul, I.; Wang, Q. Q.; Jiang, Y. H.; Wang, C.; Naranmandura, H. Metabolism, Toxicity and Anticancer Activities of Arsenic Compounds. *Oncotarget* **2017**, 8 (14), 23905–23926. <https://doi.org/10.18632/oncotarget.14733>.

Kishimoto, T.; Akira, S.; Narazaki, M.; Taga, T. Interleukin-6 Family of Cytokines and Gp130. *Blood* **1995**, 86 (4), 1243–1254. <https://doi.org/10.1182/blood.V86.4.1243.bloodjournal8641243>.

Koenigsknecht-Talboo, J. Microglial Phagocytosis Induced by Fibrillar -Amyloid and IgGs Are Differentially Regulated by Proinflammatory Cytokines. *Journal of Neuroscience* **2005**, 25 (36), 8240–8249. <https://doi.org/10.1523/JNEUROSCI.1808-05.2005>.

Krebs, N.; Langkammer, C.; Goessler, W.; Ropele, S.; Fazekas, F.; Yen, K.; Scheurer, E. Assessment of Trace Elements in Human Brain Using Inductively Coupled Plasma Mass Spectrometry. *Journal of Trace Elements in Medicine and Biology* **2014**, 28 (1), 1–7. <https://doi.org/10.1016/j.jtemb.2013.09.006>.

Kuo, Y.-M.; Gybina, A. A.; Pyatskowit, J. W.; Gitschier, J.; Prohaska, J. R. Copper Transport Protein (Ctr1) Levels in Mice Are Tissue Specific and Dependent on Copper Status. *The Journal of Nutrition* **2006**, 136 (1), 21–26. <https://doi.org/10.1093/jn/136.1.21>.

- Kuo, Y.-M.; Zhou, B.; Cosco, D.; Gitschier, J. The Copper Transporter CTR1 Provides an Essential Function in Mammalian Embryonic Development. *Proceedings of the National Academy of Sciences* **2001**, 98 (12), 6836–6841. <https://doi.org/10.1073/pnas.111057298>.
- Kuriwaki, J.; Nishijo, M.; Honda, R.; Tawara, K.; Nakagawa, H.; Hori, E.; Nishijo, H. Effects of Cadmium Exposure during Pregnancy on Trace Elements in Fetal Rat Liver and Kidney. *Toxicology Letters* **2005**, 156 (3), 369–376. <https://doi.org/10.1016/j.toxlet.2004.12.009>.
- Lagerkvist, B. J.; Zetterlund, B. Assessment of Exposure to Arsenic among Smelter Workers: A Five-Year Follow-Up. *Am. J. Ind. Med.* **1994**, 25 (4), 477–488. <https://doi.org/10.1002/ajim.4700250403>.
- Lech, T.; Sadlik, J. K. Copper Concentration in Body Tissues and Fluids in Normal Subjects of Southern Poland. *Biol Trace Elem Res* **2007**, 118 (1), 10–15. <https://doi.org/10.1007/s12011-007-0014-z>.
- Lenartowicz, M.; Krzeptowski, W.; Lipiński, P.; Grzmil, P.; Starzyński, R.; Pierzchała, O.; Møller, L. B. Mottled Mice and Non-Mammalian Models of Menkes Disease. *Front. Mol. Neurosci.* **2015**, 8. <https://doi.org/10.3389/fnmol.2015.00072>.
- Li, Y.; Jiao, Q.; Xu, H.; Du, X.; Shi, L.; Jia, F.; Jiang, H. Biometal Dyshomeostasis and Toxic Metal Accumulations in the Development of Alzheimer's Disease. *Front. Mol. Neurosci.* **2017**, 10, 339. <https://doi.org/10.3389/fnmol.2017.00339>.
- Li, Y.; Xu, X.-J.; Liu, J.-X.; Zheng, L.-K.; Chen, G.-J.; Chen, S.-J.; Huo, X. [Determination of meconium lead level of newborn by graphite furnace atomic absorption spectrometry]. *Guang Pu Xue Yu Guang Pu Fen Xi* **2008**, 28 (2), 447–449.
- Lichten, L. A.; Cousins, R. J. Mammalian Zinc Transporters: Nutritional and Physiologic Regulation. *Annu. Rev. Nutr.* **2009**, 29 (1), 153–176. <https://doi.org/10.1146/annurev-nutr-033009-083312>.
- Lisowska-Myjak, B.; Skarżyńska, E.; Bakun, M. Meconium Proteins as a Source of Biomarkers for the Assessment of the Intrauterine Environment of the Fetus. *Journal of Developmental Origins of Health and Disease* **2018**, 9 (3), 329–337. <https://doi.org/10.1017/S2040174418000028>.
- Liu, Y.; Byrne, P.; Wang, H.; Koltick, D.; Zheng, W.; Nie, L. H. A Compact DD Neutron Generator-Based NAA System to Quantify Manganese (Mn) in Bone *in Vivo*. *Physiol. Meas.* **2014**, 35 (9), 1899–1911. <https://doi.org/10.1088/0967-3334/35/9/1899>.
- Liu, Y.; McDermott, S.; Lawson, A.; Aelion, C. M. The Relationship between Mental Retardation and Developmental Delays in Children and the Levels of Arsenic, Mercury and Lead in Soil Samples Taken near Their Mother's Residence during Pregnancy. *Int J Hyg Environ Health* **2010**, 213 (2), 116–123. <https://doi.org/10.1016/j.ijheh.2009.12.004>.

Liu, Z.; Shen, J.; Carbrey, J. M.; Mukhopadhyay, R.; Agre, P.; Rosen, B. P. Arsenite Transport by Mammalian Aquaglyceroporins AQP7 and AQP9. *Proceedings of the National Academy of Sciences* **2002**, 99 (9), 6053–6058. <https://doi.org/10.1073/pnas.092131899>.

Locksley, R. M.; Killeen, N.; Lenardo, M. J. The TNF and TNF Receptor Superfamilies. *Cell* **2001**, 104 (4), 487–501. [https://doi.org/10.1016/S0092-8674\(01\)00237-9](https://doi.org/10.1016/S0092-8674(01)00237-9).

Long, L.-L.; Li, X.-R.; Huang, Z.-K.; Jiang, Y.-M.; Fu, S. X.; Zheng, W. Relationship Between Changes in Brain MRI and ¹H-MRS, Severity of Chronic Liver Damage, and Recovery After Liver Transplantation. *Exp Biol Med (Maywood)* **2009**, 234 (9), 1075–1085. <https://doi.org/10.3181/0903-RM-118>.

Lucchini, R. G.; Dorman, D. C.; Elder, A.; Veronesi, B. Neurological Impacts from Inhalation of Pollutants and the Nose–Brain Connection. *NeuroToxicology* **2012**, 33 (4), 838–841. <https://doi.org/10.1016/j.neuro.2011.12.001>.

Lucchini, R.; Placidi, D.; Cagna, G.; Fedrigli, C.; Oppini, M.; Peli, M.; Zoni, S. Manganese and Developmental Neurotoxicity. *Neurotoxicity of Metals* **2017**, 13–34. https://doi.org/10.1007/978-3-319-60189-2_2.

Lutsenko, S. Copper Trafficking to the Secretory Pathway. *Metallomics* **2016**, 8 (9), 840–852. <https://doi.org/10.1039/C6MT00176A>.

MacDonald, R. S. The Role of Zinc in Growth and Cell Proliferation. *The Journal of Nutrition* **2000**, 130 (5), 1500S–1508S. <https://doi.org/10.1093/jn/130.5.1500S>.

Madrid, F.; Biasioli, M.; Ajmone-Marsan, F. Availability and Bioaccessibility of Metals in Fine Particles of Some Urban Soils. *Arch Environ Contam Toxicol* **2008**, 55 (1), 21–32. <https://doi.org/10.1007/s00244-007-9086-1>.

Manganese | Toxicological Profile | ATSDR
<https://wwwn.cdc.gov/TSP/ToxProfiles/ToxProfiles.aspx?id=102&tid=23>

Manthari, R. K.; Tikka, C.; Ommati, M. M.; Niu, R.; Sun, Z.; Wang, J.; Zhang, J.; Wang, J. Arsenic Induces Autophagy in Developmental Mouse Cerebral Cortex and Hippocampus by Inhibiting PI3K/Akt/MTOR Signaling Pathway: Involvement of Blood–Brain Barrier's Tight Junction Proteins. *Arch Toxicol* **2018**, 92 (11), 3255–3275. <https://doi.org/10.1007/s00204-018-2304-y>.

Mao, J.; Yang, J.; Zhang, Y.; Li, T.; Wang, C.; Xu, L.; Hu, Q.; Wang, X.; Jiang, S.; Nie, X.; Chen, G. Arsenic Trioxide Mediates HAPI Microglia Inflammatory Response and Subsequent Neuron Apoptosis through P38/JNK MAPK/STAT3 Pathway. *Toxicology and Applied Pharmacology* **2016**, 303, 79–89. <https://doi.org/10.1016/j.taap.2016.05.003>.

Marapakala, K.; Qin, J.; Rosen, B. P. Identification of Catalytic Residues in the as(Iii) s - Adenosylmethionine Methyltransferase. *Biochemistry* **2012**, *51* (5), 944–951.

<https://doi.org/10.1021/bi201500c>.

Maret, W. Cellular Zinc and Redox States Converge in the Metallothionein/Thionein Pair. *The Journal of Nutrition* 2003, *133* (5), 1460S-1462S. <https://doi.org/10.1093/jn/133.5.1460S>.

Marreiro, D. do N.; Cruz, K. J. C.; Morais, J. B. S.; Beserra, J. B.; Severo, J. S.; de Oliveira, A. R. S. Zinc and Oxidative Stress: Current Mechanisms. *Antioxidants (Basel)* **2017**, *6* (2).

<https://doi.org/10.3390/antiox6020024>.

Mathys, Z. K.; White, A. R. Copper and Alzheimer's Disease. In *Neurotoxicity of Metals*; Aschner, M., Costa, L. G., Eds.; Springer International Publishing: Cham, 2017; Vol. 18, pp 199–216. https://doi.org/10.1007/978-3-319-60189-2_10.

McCord, J. M.; Fridovich, I. Superoxide Dismutase. An Enzymic Function for Erythrocyte (Hemocytin). *J Biol Chem* **1969**, *244* (22), 6049–6055.

McDermott, S.; Bao, W.; Cai, B.; Lawson, A.; Aelion, C. M. Are Different Soil Metals during Pregnancy Associated with Mild and Severe Intellectual Disability in Children? *ISEE Conference Abstracts* **2013**, *2013* (1), 3624. <https://doi.org/10.1289/isee.2013.P-1-10-02>.

McDermott, S.; Hailer, M. K.; Lead, J. R. Meconium Identifies High Levels of Metals in Newborns from a Mining Community in the U.S. *Science of The Total Environment* **2020**, *707*, 135528. <https://doi.org/10.1016/j.scitotenv.2019.135528>.

McDermott, S.; Wu, J.; Cai, B.; Lawson, A.; Marjorie Aelion, C. Probability of Intellectual Disability Is Associated with Soil Concentrations of Arsenic and Lead. *Chemosphere* **2011**, *84* (1), 31–38. <https://doi.org/10.1016/j.chemosphere.2011.02.088>.

Michalke, B.; Fernsebner, K. New Insights into Manganese Toxicity and Speciation. *Journal of Trace Elements in Medicine and Biology* **2014**, *28* (2), 106–116. <https://doi.org/10.1016/j.jtemb.2013.08.005>.

Michelsen-Correa, S.; Martin, C. F.; Kirk, A. B. Evaluation of Fetal Exposures to Metals and Metalloids through Meconium Analyses: A Review. *IJERPH* 2021, *18* (4), 1975. <https://doi.org/10.3390/ijerph18041975>.

Mikheev, A. M.; Nabekura, T.; Kaddoumi, A.; Bammler, T. K.; Govindarajan, R.; Hebert, M. F.; Unadkat, J. D. Profiling Gene Expression in Human Placentae of Different Gestational Ages: An OPRU* Network and UW SCOR Study. *Reprod Sci* **2008**, *15* (9), 866–877.

<https://doi.org/10.1177/1933719108322425>.

Miller, W. H.; Schipper, H. M.; Lee, J. S.; Singer, J.; Waxman, S. Mechanisms of Action of Arsenic Trioxide. *Cancer Res* **2002**, *62* (14), 3893–3903.

Minghetti, L. Role of Inflammation in Neurodegenerative Diseases. *Current Opinion in Neurology* **2005**, 18 (3), 315–321. <https://doi.org/10.1097/01.wco.0000169752.54191.97>.

Mocchegiani, E.; Muzzioli, M.; Giacconi, R. Zinc, Metallothioneins, Immune Responses, Survival Andageing. *Biogerontology* **2000**, 1 (2), 133–143. <https://doi.org/10.1023/A:1010095930854>.

Molloy, S. A.; Kaplan, J. H. Copper-Dependent Recycling of HCTR1, the Human High Affinity Copper Transporter. *Journal of Biological Chemistry* **2009**, 284 (43), 29704–29713. <https://doi.org/10.1074/jbc.M109.000166>.

Monnot, A. D.; Zheng, G.; Zheng, W. Mechanism of Copper Transport at the Blood–Cerebrospinal Fluid Barrier: Influence of Iron Deficiency in an *in Vitro* Model. *Exp Biol Med (Maywood)* **2012**, 237 (3), 327–333. <https://doi.org/10.1258/ebm.2011.011170>.

Montana Department of Environmental Quality, Project Report: Background Concentrations of Inorganic Constituents in Montana Surface Soils. Hydrometric Inc. 2013.

Montana Department of Public Health and Human Services. Montana Central Tumor Registry Annual Report, Cancer in Montana 2012-2016. https://mtcancercoalition.org/wp-content/uploads/2019/04/MCTR-Annual-Report_2012-2016.pdf

Morello, M.; Canini, A.; Mattioli, P.; Sorge, R. P.; Alimonti, A.; Bocca, B.; Forte, G.; Martorana, A.; Bernardi, G.; Sancesario, G. Sub-Cellular Localization of Manganese in the Basal Ganglia of Normal and Manganese-Treated Rats. *NeuroToxicology* 2008, 29 (1), 60–72. <https://doi.org/10.1016/j.neuro.2007.09.001>.

Morris, D. R.; Levenson, C. W. Neurotoxicity of Zinc. In *Neurotoxicity of Metals*; Aschner, M., Costa, L. G., Eds.; Springer International Publishing: Cham, 2017; Vol. 18, pp 303–312. https://doi.org/10.1007/978-3-319-60189-2_15.

Mukke, V. K.; Chinte, D. N. Impact of Heavy Metal Induced Alterations in Lipase Activity of Fresh Water Crab, *Barytelphusa Guerini*. *Journal of Chemical and Pharmaceutical Research* **2012**, 4 (5).

Nadaska G, Lesny J, Michalik I. Environmental aspect of manganese chemistry. **2012**, 1–16. http://heja.szif.hu/ENV/ENV_100702-A/env100702a.pdf

Niño, S. A.; Martel-Gallegos, G.; Castro-Zavala, A.; Ortega-Berlanga, B.; Delgado, J. M.; Hernández-Mendoza, H.; Romero-Guzmán, E.; Ríos-Lugo, J.; Rosales-Mendoza, S.; Jiménez-Capdeville, M. E.; Zarazúa, S. Chronic Arsenic Exposure Increases A β (1–42) Production and Receptor for Advanced Glycation End Products Expression in Rat Brain. *Chem. Res. Toxicol.* **2018**, 31 (1), 13–21. <https://doi.org/10.1021/acs.chemrestox.7b00215>.

Nose, Y.; Kim, B.-E.; Thiele, D. J. Ctr1 Drives Intestinal Copper Absorption and Is Essential for Growth, Iron Metabolism, and Neonatal Cardiac Function. *Cell Metabolism* **2006**, *4* (3), 235–244. <https://doi.org/10.1016/j.cmet.2006.08.009>.

O’Neal, S. L.; Hong, L.; Fu, S.; Jiang, W.; Jones, A.; Nie, L. H.; Zheng, W. Manganese Accumulation in Bone Following Chronic Exposure in Rats: Steady-State Concentration and Half-Life in Bone. *Toxicology Letters* **2014**, *229* (1), 93–100. <https://doi.org/10.1016/j.toxlet.2014.06.019>.

O’Neal, S. L.; Zheng, W. Manganese Toxicity Upon Overexposure: A Decade in Review. *Curr Envir Health Rpt* **2015**, *2* (3), 315–328. <https://doi.org/10.1007/s40572-015-0056-x>.

Olaniran, A.; Balgobind, A.; Pillay, B. Bioavailability of Heavy Metals in Soil: Impact on Microbial Biodegradation of Organic Compounds and Possible Improvement Strategies. *IJMS* **2013**, *14* (5), 10197–10228. <https://doi.org/10.3390/ijms140510197>.

Ostrea, E. M.; Bielawski, D. M.; Posecion, N. C.; Corrion, M.; Villanueva-Uy, E.; Jin, Y.; Janisse, J. J.; Ager, J. W. A Comparison of Infant Hair, Cord Blood and Meconium Analysis to Detect Fetal Exposure to Environmental Pesticides. *Environmental Research* **2008**, *106* (2), 277–283. <https://doi.org/10.1016/j.envres.2007.08.014>.

Oulhote, Y.; Mergler, D.; Bouchard, M. F. Sex- and Age-Differences in Blood Manganese Levels in the U.S. General Population: National Health and Nutrition Examination Survey 2011–2012. *Environ Health* **2014**, *13* (1), 87. <https://doi.org/10.1186/1476-069X-13-87>.

Palumaa, P. Copper Chaperones. The Concept of Conformational Control in the Metabolism of Copper. *FEBS Letters* **2013**, *587* (13), 1902–1910. <https://doi.org/10.1016/j.febslet.2013.05.019>.

Penkowa, M. (2006). Metallothionein I + II expression and roles during neuropathology in the CNS. *Danish Medical Bulletin*, *53*(2), 105–121.

Perry, J. J. P.; Shin, D. S.; Getzoff, E. D.; Tainer, J. A. The Structural Biochemistry of the Superoxide Dismutases. *Biochimica et Biophysica Acta (BBA) - Proteins and Proteomics* **2010**, *1804* (2), 245–262. <https://doi.org/10.1016/j.bbapap.2009.11.004>.

Petrack, J. S.; Jagadish, B.; Mash, E. A.; Aposhian, H. V. Monomethylarsonous Acid (MMA^{III}) and Arsenite: LD₅₀ in Hamsters and In Vitro Inhibition of Pyruvate Dehydrogenase. *Chem. Res. Toxicol.* **2001**, *14* (6), 651–656. <https://doi.org/10.1021/tx000264z>.

Petris, M. J.; Smith, K.; Lee, J.; Thiele, D. J. Copper-Stimulated Endocytosis and Degradation of the Human Copper Transporter, HCTR1. *Journal of Biological Chemistry* **2003**, *278* (11), 9639–9646. <https://doi.org/10.1074/jbc.M209455200>.

Phatak, V. M.; Muller, P. A. J. Metal Toxicity and the P53 Protein: An Intimate Relationship. *Toxicol. Res.* **2015**, *4* (3), 576–591. <https://doi.org/10.1039/C4TX00117F>.

Post, J. E. Manganese Oxide Minerals: Crystal Structures and Economic and Environmental Significance. *Proceedings of the National Academy of Sciences* **1999**, 96 (7), 3447–3454. <https://doi.org/10.1073/pnas.96.7.3447>.

Prohaska, J. R. Role of Copper Transporters in Copper Homeostasis. *The American Journal of Clinical Nutrition* **2008**, 88 (3), 826S-829S. <https://doi.org/10.1093/ajcn/88.3.826S>.

Quadri, M.; Federico, A.; Zhao, T.; Breedveld, G. J.; Battisti, C.; Delnooz, C.; Severijnen, L.-A.; Di Toro Mammarella, L.; Mignarri, A.; Monti, L.; Sanna, A.; Lu, P.; Punzo, F.; Cossu, G.; Willemsen, R.; Rasi, F.; Oostra, B. A.; van de Warrenburg, B. P.; Bonifati, V. Mutations in SLC30A10 Cause Parkinsonism and Dystonia with Hypermanganesemia, Polycythemia, and Chronic Liver Disease. *The American Journal of Human Genetics* **2012**, 90 (3), 467–477. <https://doi.org/10.1016/j.ajhg.2012.01.017>.

Que, E. L.; Bleher, R.; Duncan, F. E.; Kong, B. Y.; Gleber, S. C.; Vogt, S.; Chen, S.; Garwin, S. A.; Bayer, A. R.; Dravid, V. P.; Woodruff, T. K.; O'Halloran, T. V. Quantitative Mapping of Zinc Fluxes in the Mammalian Egg Reveals the Origin of Fertilization-Induced Zinc Sparks. *Nature Chemistry* **2015**, 7 (2), 130–139. <https://doi.org/10.1038/nchem.2133>.

Rae, T. D. Undetectable Intracellular Free Copper: The Requirement of a Copper Chaperone for Superoxide Dismutase. *Science* **1999**, 284 (5415), 805–808. <https://doi.org/10.1126/science.284.5415.805>.

Rahil-Khazen, R.; Bolann, B. J.; Myking, A.; Ulvik, R. J. Multi-Element Analysis of Trace Element Levels in Human Autopsy Tissues by Using Inductively Coupled Atomic Emission Spectrometry Technique (ICP-AES). *Journal of Trace Elements in Medicine and Biology* **2002**, 16 (1), 15–25. [https://doi.org/10.1016/S0946-672X\(02\)80004-9](https://doi.org/10.1016/S0946-672X(02)80004-9).

Ramos, P.; Santos, A.; Pinto, N. R.; Mendes, R.; Magalhães, T.; Almeida, A. Anatomical Region Differences and Age-Related Changes in Copper, Zinc, and Manganese Levels in the Human Brain. *Biol Trace Elem Res* **2014**, 161 (2), 190–201. <https://doi.org/10.1007/s12011-014-0093-6>.

Reaney, S. H.; Kwik-Urbe, C. L.; Smith, D. R. Manganese Oxidation State and Its Implications for Toxicity. *Chem. Res. Toxicol.* **2002**, 15 (9), 1119–1126. <https://doi.org/10.1021/tx025525e>.

Rehman, K.; Fatima, F.; Waheed, I.; Akash, M. S. H. Prevalence of Exposure of Heavy Metals and Their Impact on Health Consequences. *Journal of Cellular Biochemistry* **2018**, 119 (1), 157–184. <https://doi.org/https://doi.org/10.1002/jcb.26234>.

Reichard, J. F.; Schnekenburger, M.; Puga, A. Long Term Low-Dose Arsenic Exposure Induces Loss of DNA Methylation. *Biochemical and Biophysical Research Communications* **2007**, 352 (1), 188–192. <https://doi.org/10.1016/j.bbrc.2006.11.001>.

Rink, L. Zinc and the Immune System. *Proceedings of the Nutrition Society* **2000**, 59 (4), 541–552. <https://doi.org/10.1017/S0029665100000781>.

Robinson, N. J.; Winge, D. R. Copper Metallochaperones. *Annu. Rev. Biochem.* **2010**, 79 (1), 537–562. <https://doi.org/10.1146/annurev-biochem-030409-143539>.

Robison, G.; Zakharova, T.; Fu, S.; Jiang, W.; Fulper, R.; Barrea, R.; Zheng, W.; Pushkar, Y. X-Ray Fluorescence Imaging of the Hippocampal Formation after Manganese Exposure. *Metallomics* **2013**, 5 (11), 1554. <https://doi.org/10.1039/c3mt00133d>.

Rodrigues, E. G.; Bellinger, D. C.; Valeri, L.; Hasan, M. O. S. I.; Quamruzzaman, Q.; Golam, M.; Kile, M. L.; Christiani, D. C.; Wright, R. O.; Mazumdar, M. Neurodevelopmental Outcomes among 2- to 3-Year-Old Children in Bangladesh with Elevated Blood Lead and Exposure to Arsenic and Manganese in Drinking Water. *Environ Health* **2016**, 15 (1), 44. <https://doi.org/10.1186/s12940-016-0127-y>.

Rose-John, S. The Soluble Interleukin-6 Receptor and Related Proteins. *Best Pract Res Clin Endocrinol Metab* **2015**, 29 (5), 787–797. <https://doi.org/10.1016/j.beem.2015.07.001>.

Rothaug, M.; Becker-Pauly, C.; Rose-John, S. The Role of Interleukin-6 Signaling in Nervous Tissue. *Biochimica et Biophysica Acta (BBA) - Molecular Cell Research* **2016**, 1863 (6), 1218–1227. <https://doi.org/10.1016/j.bbamcr.2016.03.018>.

Safty, A.; Rashd, H. M.; Bayoumi, F. S. Susceptibility To Infection Among Nickel Electroplaters. <https://www.semanticscholar.org/paper/Susceptibility-To-Infection-Among-Nickel-Safty-Rashd/f48029a4019f335083ddd21dc02e7b414555249d>

Sallmann, S., Jüttler, E., Prinz, S., Petersen, N., Knopf, U., Weiser, T., & Schwaninger, M. (2000). Induction of interleukin-6 by depolarization of neurons. *The Journal of Neuroscience: The Official Journal of the Society for Neuroscience*, 20(23), 8637–8642.

Sánchez-Peña, L. C.; Petrosyan, P.; Morales, M.; González, N. B.; Gutiérrez-Ospina, G.; Del Razo, L. M.; Gonsebatt, M. E. Arsenic Species, AS3MT Amount, and AS3MT Gen Expression in Different Brain Regions of Mouse Exposed to Arsenite. *Environmental Research* **2010**, 110 (5), 428–434. <https://doi.org/10.1016/j.envres.2010.01.007>.

Sandström, B. Micronutrient Interactions: Effects on Absorption and Bioavailability. *British Journal of Nutrition* 2001, 85 (S2), S181–S185. <https://doi.org/10.1049/BJN2000312>.

Santello, M., & Volterra, A. (2012). TNF α in synaptic function: Switching gears. *Trends in Neurosciences*, 35(10), 638–647. <https://doi.org/10.1016/j.tins.2012.06.001>

Scheiber, I. F.; Dringen, R. Astrocyte Functions in the Copper Homeostasis of the Brain. *Neurochemistry International* **2013**, 62 (5), 556–565. <https://doi.org/10.1016/j.neuint.2012.08.017>.

Scheiber, I. F.; Mercer, J. F. B.; Dringen, R. Metabolism and Functions of Copper in Brain. *Progress in Neurobiology* 2014, 116, 33–57. <https://doi.org/10.1016/j.pneurobio.2014.01.002>.

Schlieff, M. L.; Craig, A. M.; Gitlin, J. D. NMDA Receptor Activation Mediates Copper Homeostasis in Hippocampal Neurons. *J. Neurosci.* **2005**, *25* (1), 239–246.

<https://doi.org/10.1523/JNEUROSCI.3699-04.2005>.

Schmalz, G.; Schuster, U.; Schweikl, H. Influence of Metals on IL-6 Release in Vitro. *Biomaterials* **1998**, *19* (18), 1689–1694. [https://doi.org/10.1016/S0142-9612\(98\)00075-1](https://doi.org/10.1016/S0142-9612(98)00075-1).

Shavali, S.; Sens, D. A. Synergistic Neurotoxic Effects of Arsenic and Dopamine in Human Dopaminergic Neuroblastoma SH-SY5Y Cells. *Toxicological Sciences* **2008**, *102* (2), 254–261. <https://doi.org/10.1093/toxsci/kfm302>.

Shen, S.; Li, X.-F.; Cullen, W. R.; Weinfeld, M.; Le, X. C. Arsenic Binding to Proteins. *Chem. Rev.* **2013**, *113* (10), 7769–7792. <https://doi.org/10.1021/cr300015c>.

Sheng, Y.; Butler Gralla, E.; Schumacher, M.; Cascio, D.; Cabelli, D. E.; Selverstone Valentine, J. Six-Coordinate Manganese(3+) in Catalysis by Yeast Manganese Superoxide Dismutase. *Proceedings of the National Academy of Sciences* **2012**, *109* (36), 14314–14319. <https://doi.org/10.1073/pnas.1212367109>.

Shi, H.; Shi, X.; Liu, K. J. Oxidative Mechanism of Arsenic Toxicity and Carcinogenesis. *Mol Cell Biochem* **2004**, *255* (1/2), 67–78. <https://doi.org/10.1023/B:MCBI.0000007262.26044.e8>.

Sialelli, J.; Urquhart, G. J.; Davidson, C. M.; Hursthouse, A. S. Use of a Physiologically Based Extraction Test to Estimate the Human Bioaccessibility of Potentially Toxic Elements in Urban Soils from the City of Glasgow, UK. *Environ Geochem Health* **2010**, *32* (6), 517–527. <https://doi.org/10.1007/s10653-010-9314-x>.

SILVER BOW CREEK/BUTTE AREA Site Profile

<https://cumulis.epa.gov/supercpad/SiteProfiles/index.cfm?fuseaction=second.cleanup&id=0800416>.

Singh, N.; Kumar, D.; Sahu, A. P. Arsenic in the Environment: Effects on Human Health and Possible Prevention. *J Environ Biol* **2007**, *28* (2 Suppl), 359–365.

Soares, F. A.; Fagundez, D. A.; Avila, D. S. Neurodegeneration Induced by Metals in *Caenorhabditis Elegans*. In *Neurotoxicity of Metals*; Aschner, M., Costa, L. G., Eds.; Springer International Publishing: Cham, 2017; Vol. 18, pp 355–383. https://doi.org/10.1007/978-3-319-60189-2_18.

Squitti, R.; Gorgone, G.; Panetta, V.; Lucchini, R.; Bucossi, S.; Albini, E.; Alessio, L.; Alberici, A.; Melgari, J. M.; Benussi, L.; Binetti, G.; Rossini, P. M.; Draicchio, F. Implications of Metal Exposure and Liver Function in Parkinsonian Patients Resident in the Vicinities of Ferroalloy Plants. *J Neural Transm* **2009**, *116* (10), 1281–1287. <https://doi.org/10.1007/s00702-009-0283-0>.

Stoltenberg, M.; Bruhn, M.; Søndergaard, C.; Doering, P.; West, M. J.; Larsen, A.; Troncoso, J. C.; Danscher, G. Immersion Autometallographic Tracing of Zinc Ions in Alzheimer Beta-

Amyloid Plaques. *Histochem Cell Biol* **2005**, 123 (6), 605–611. <https://doi.org/10.1007/s00418-005-0787-0>.

Stýblo, M.; Drobná, Z.; Jaspers, I.; Lin, S.; Thomas, D. J. The Role of Biomethylation in Toxicity and Carcinogenicity of Arsenic: A Research Update. *Environmental Health Perspectives* **2002**, 110 (suppl 5), 767–771. <https://doi.org/10.1289/ehp.110-1241242>.

Subramanian, K. S.; Meranger, J. Charles. Graphite Furnace Atomic Absorption Spectrometry with Nitric Acid Deproteinization for Determination of Manganese in Human Plasma. *Anal. Chem.* **1985**, 57 (13), 2478–2481. <https://doi.org/10.1021/ac00290a012>.

Szerdahelyi, P.; Kása, P. Histochemical Demonstration of Copper in Normal Rat Brain and Spinal Cord: Evidence of Localization in Glial Cells. *Histochemistry* **1986**, 85 (4), 341–347. <https://doi.org/10.1007/BF00493487>.

Takser, L.; Mergler, D.; de Grosbois, S.; Smargiassi, A.; Lafond, J. Blood Manganese Content at Birth and Cord Serum Prolactin Levels. *Neurotoxicology and Teratology* **2004**, 26 (6), 811–815. <https://doi.org/10.1016/j.ntt.2004.07.001>.

Tapiero, H.; Tew, K. D. Trace Elements in Human Physiology and Pathology: Zinc and Metallothioneins. *Biomedicine & Pharmacotherapy* **2003**, 57 (9), 399–411. [https://doi.org/10.1016/S0753-3322\(03\)00081-7](https://doi.org/10.1016/S0753-3322(03)00081-7).

Taylor, K. M. A Distinct Role in Breast Cancer for Two LIV-1 Family Zinc Transporters. *Biochemical Society Transactions* **2008**, 36 (6), 1247–1251. <https://doi.org/10.1042/BST0361247>.

Torres-Avila, M.; Leal-Galicia, P.; Sánchez-Peña, L. C.; Del Razo, L. M.; Gonsébat, M. E. Arsenite Induces Aquaglyceroporin 9 Expression in Murine Livers. *Environmental Research* **2010**, 110 (5), 443–447. <https://doi.org/10.1016/j.envres.2009.08.009>.

Toxicological Profile for Arsenic; U.S. Department of Health and Human Services, 2007. <https://doi.org/10.15620/cdc:11481>.

Turker, G.; Özsoy, G.; Özdemir, S.; Barutçu, B.; Gökalp, A. S. Effect of Heavy Metals in the Meconium on Preterm Mortality: Preliminary Study: Mortality and Heavy Metals. *Pediatr Int* **2013**, 55 (1), 30–34. <https://doi.org/10.1111/j.1442-200X.2012.03744.x>.

Tuschl, K.; Meyer, E.; Valdivia, L. E.; Zhao, N.; Dadswell, C.; Abdul-Sada, A.; Hung, C. Y.; Simpson, M. A.; Chong, W. K.; Jacques, T. S.; Woltjer, R. L.; Eaton, S.; Gregory, A.; Sanford, L.; Kara, E.; Houlden, H.; Cuno, S. M.; Prokisch, H.; Valletta, L.; Tiranti, V.; Younis, R.; Maher, E. R.; Spencer, J.; Straatman-Iwanowska, A.; Gissen, P.; Selim, L. A. M.; Pintos-Morell, G.; Coroleu-Lletget, W.; Mohammad, S. S.; Yoganathan, S.; Dale, R. C.; Thomas, M.; Rihel, J.; Bodamer, O. A.; Enns, C. A.; Hayflick, S. J.; Clayton, P. T.; Mills, P. B.; Kurian, M. A.; Wilson, S. W. Mutations in SLC39A14 Disrupt Manganese Homeostasis and Cause Childhood-Onset Parkinsonism–Dystonia. *Nat Commun* **2016**, 7 (1), 11601. <https://doi.org/10.1038/ncomms11601>.

Uede, K.; Furukawa, F. Skin Manifestations in Acute Arsenic Poisoning from the Wakayama Curry-Poisoning Incident. *Br J Dermatol* **2003**, 149 (4), 757–762. <https://doi.org/10.1046/j.1365-2133.2003.05511.x>.

US EPA, O. Population surrounding 1,857 superfund sites
<https://www.epa.gov/superfund/population-surrounding-1857-superfund-sites>.

Valko, M.; Morris, H.; Cronin, M. T. D. Metals, Toxicity and Oxidative Stress. *Current Medicinal Chemistry* **2005**, 12 (10), 1161–1208. <https://doi.org/10.2174/0929867053764635>.

van den Berghe, P. V.; Klomp, L. W. New Developments in the Regulation of Intestinal Copper Absorption. *Nutrition Reviews* **2009**, 67 (11), 658–672. <https://doi.org/10.1111/j.1753-4887.2009.00250.x>.

VasÅik, M. Metallothioneins: New Functional and Structural Insights. *Current Opinion in Chemical Biology* **2000**, 4 (2), 177–183. [https://doi.org/10.1016/S1367-5931\(00\)00082-X](https://doi.org/10.1016/S1367-5931(00)00082-X).

Wang, C.-Y.; Wang, T.; Zheng, W.; Zhao, B.-L.; Danscher, G.; Chen, Y.-H.; Wang, Z.-Y. Zinc Overload Enhances APP Cleavage and A β Deposition in the Alzheimer Mouse Brain. *PLoS ONE* **2010**, 5 (12), e15349. <https://doi.org/10.1371/journal.pone.0015349>.

Wang, D. B.; Kinoshita, C.; Kinoshita, Y.; Morrison, R. S. P53 and Mitochondrial Function in Neurons. *Biochimica et Biophysica Acta (BBA) - Molecular Basis of Disease* **2014**, 1842 (8), 1186–1197. <https://doi.org/10.1016/j.bbadis.2013.12.015>.

Wang, G.; Fowler, B. A. Roles of Biomarkers in Evaluating Interactions among Mixtures of Lead, Cadmium and Arsenic. *Toxicology and Applied Pharmacology* **2008**, 233 (1), 92–99. <https://doi.org/10.1016/j.taap.2008.01.017>.

Wang, G.; Yu, X.; Wang, D.; Xu, X.; Chen, G.; Jiang, X. Altered Levels of Zinc and N-Methyl-D-Aspartic Acid Receptor Underlying Multiple Organ Dysfunctions After Severe Trauma. *Med Sci Monit* **2015**, 21, 2613–2620. <https://doi.org/10.12659/MSM.895075>.

Watanabe, T.; Hirano, S. Metabolism of Arsenic and Its Toxicological Relevance. *Arch Toxicol* **2013**, 87 (6), 969–979. <https://doi.org/10.1007/s00204-012-0904-5>.

Wongsasuluk, P.; Chotpantarat, S.; Siri Wong, W.; Robson, M. Heavy Metal Contamination and Human Health Risk Assessment in Drinking Water from Shallow Groundwater Wells in an Agricultural Area in Ubon Ratchathani Province, Thailand. *Environ Geochem Health* **2014**, 36 (1), 169–182. <https://doi.org/10.1007/s10653-013-9537-8>.

Wyss-Coray, T.; Mucke, L. Inflammation in Neurodegenerative Disease—A Double-Edged Sword. *Neuron* **2002**, 35 (3), 419–432. [https://doi.org/10.1016/S0896-6273\(02\)00794-8](https://doi.org/10.1016/S0896-6273(02)00794-8).

- Yamasaki, S.; Sakata-Sogawa, K.; Hasegawa, A.; Suzuki, T.; Kabu, K.; Sato, E.; Kurosaki, T.; Yamashita, S.; Tokunaga, M.; Nishida, K.; Hirano, T. Zinc Is a Novel Intracellular Second Messenger. *Journal of Cell Biology* **2007**, *177* (4), 637–645. <https://doi.org/10.1083/jcb.200702081>.
- Yang, Y.-W.; Liou, S.-H.; Hsueh, Y.-M.; Lyu, W.-S.; Liu, C.-S.; Liu, H.-J.; Chung, M.-C.; Hung, P.-H.; Chung, C.-J. Risk of Alzheimer's Disease with Metal Concentrations in Whole Blood and Urine: A Case–Control Study Using Propensity Score Matching. *Toxicology and Applied Pharmacology* **2018**, *356*, 8–14. <https://doi.org/10.1016/j.taap.2018.07.015>.
- Yokel, R. A. Manganese Flux Across the Blood–Brain Barrier. *Neuromol Med* **2009**, *11* (4), 297–310. <https://doi.org/10.1007/s12017-009-8101-2>.
- Yu, C. H.; Dolgova, N. V.; Dmitriev, O. Y. Dynamics of the Metal Binding Domains and Regulation of the Human Copper Transporters ATP7B and ATP7A: MBD Dynamics in Copper Transporters. *IUBMB Life* **2017**, *69* (4), 226–235. <https://doi.org/10.1002/iub.1611>.
- Zamora, P. L.; Rockenbauer, A.; Villamena, F. A. Radical Model of Arsenic(III) Toxicity: Theoretical and EPR Spin Trapping Studies. *Chem. Res. Toxicol.* **2014**, *27* (5), 765–774. <https://doi.org/10.1021/tx4004227>.
- Zatta, P.; Frank, A. Copper Deficiency and Neurological Disorders in Man and Animals. *Brain Research Reviews* **2007**, *54* (1), 19–33. <https://doi.org/10.1016/j.brainresrev.2006.10.001>.
- Zhang, Y.; McDermott, S.; Davis, B.; Hussey, J. High Incidence of Brain and Other Nervous System Cancer Identified in Two Mining Counties, 2001–2015. Spatial and Spatio-temporal Epidemiology 2020, *32*, 100320. <https://doi.org/10.1016/j.sste.2019.100320>.
- Zhao, C. Q.; Young, M. R.; Diwan, B. A.; Coogan, T. P.; Waalkes, M. P. Association of Arsenic-Induced Malignant Transformation with DNA Hypomethylation and Aberrant Gene Expression. *Proceedings of the National Academy of Sciences* 1997, *94* (20), 10907–10912. <https://doi.org/10.1073/pnas.94.20.10907>.
- Zheng, W.; Aschner, M.; Gherzi-Egea, J.-F. Brain Barrier Systems: A New Frontier in Metal Neurotoxicological Research. *Toxicol Appl Pharmacol* **2003**, *192* (1), 1–11.
- Zheng, W.; Chodobski, A. *The Blood-Cerebrospinal Fluid Barrier*; CRC Press, 2005. p. 413–36
- Zheng, W.; Monnot, A. D. Regulation of Brain Iron and Copper Homeostasis by Brain Barrier Systems: Implication in Neurodegenerative Diseases. *Pharmacology & Therapeutics* **2012**, *133* (2), 177–188. <https://doi.org/10.1016/j.pharmthera.2011.10.006>.
- Zhou, Z.; Wang, L.; Song, Z.; Saari, J. T.; McClain, C. J.; Kang, Y. J. Abrogation of Nuclear Factor-KappaB Activation Is Involved in Zinc Inhibition of Lipopolysaccharide-Induced Tumor Necrosis Factor-Alpha Production and Liver Injury. *Am J Pathol* **2004**, *164* (5), 1547–1556. [https://doi.org/10.1016/s0002-9440\(10\)63713-3](https://doi.org/10.1016/s0002-9440(10)63713-3).

Zogzas, C. E.; Mukhopadhyay, S. Inherited Disorders of Manganese Metabolism. In *Neurotoxicity of Metals*; Aschner, M., Costa, L. G., Eds.; Springer International Publishing: Cham, 2017; Vol. 18, pp 35–49. <https://doi.org/10.1007/978-3-319-60189-23>.

Zoni, S.; Bonetti, G.; Lucchini, R. Olfactory Functions at the Intersection between Environmental Exposure to Manganese and Parkinsonism. *Journal of Trace Elements in Medicine and Biology* 2012, 26 (2–3), 179–182. <https://doi.org/10.1016/j.jtemb.2012.04.023>.

10. Appendix A: BCA Assay Dilution Tables and Calculations

Table IX: Standard Mixture Volumes Needed

Final Concentration of BSA (μg/mL)	Volume of Water (μL)	Volume of 500μg/mL BSA (μL)	Volume of K ₂ HPO ₄ Buffer (μL)	Total Standard Solution Volume (μL)
0	90	0	10	100
10	88	2	10	100
25	85	5	10	100
50	80	10	10	100
75	75	15	10	100
100	70	20	10	100
150	60	30	10	100
200	50	40	10	100
250	40	50	10	100
300	30	60	10	100

$$M_1V_1 = M_2V_2 \quad (7)$$

$$V_1 = \frac{M_2V_2}{M_1} = \frac{10 \frac{\mu g}{mL} * 100\mu L}{500 \frac{\mu g}{mL}} = 2 \mu L \text{ of BSA}$$

where BSA is bovine serum albumin stock, M_1 is concentration of diluted BSA stock, M_2 is desired final concentration of BSA, and V_2 is the total volume desired of the standard dilution.

Table X: Dilution Factors to Determine Unknown Protein Concentration

Unknown Dilution Factors	Volume of Water (μL)	Volume of Unknown Solution (μL)	Volume of K ₂ HPO ₄ Buffer (μL)	Total Standard Solution Volume (μL)
1:50	88	2	10	100
1:100	89	1	10	100

$$\frac{1}{50} = 0.02 * 100 \mu L = 2 \mu L \text{ Unknown} \quad (8)$$

$$100 \mu L \text{ total} - 10 \mu L K_2HPO_4 - 2 \mu L \text{ Unknown} = 80 \mu L \text{ water} \quad (9)$$

where unknown is the sample of interest.

11. Appendix B: Sample Protein Concentrations and SDS-PAGE Gel Loading Volumes

Table XI: BCA Assay Values for SDS-PAGE Sample Loading

Sample	Protein Concentration (µg/mL)	Volume needed for 40 µg (mL)
HEK293 Control	8.88E+03	4.50
HEK293 As	1.03E+04	3.87
HEK293 Cu	1.08E+04	3.70
HEK293 Mn	9.69E+03	4.13
HEK293 Zn	7.05E+03	5.67
HEK293 AsCu	3.29E+03	12.14
HEK293 AsMn	5.72E+03	7.00
HEK293 AsZn	1.12E+04	3.56
HEK293 CuMn	6.83E+03	5.86
HEK293 CuZn	8.14E+03	4.92
HEK293 MnZn	4.85E+03	8.25
HEK293 AsCuMnZn	1.28E+04	3.12
BEAS-2B Control	5.46E+03	7.33
BEAS-2B As	5.77E+03	5.98
BEAS-2B Cu	6.01E+03	7.37
BEAS-2B Mn	5.04E+03	9.02
BEAS-2B Zn	4.76E+03	7.62
BEAS-2B AsCu	1.01E+04	3.95
BEAS-2B AsMn	1.00E+04	4.00
BEAS-2B AsZn	9.09E+03	4.40
BEAS-2B CuMn	1.01E+04	3.95
BEAS-2B CuZn	9.23E+03	4.33
BEAS-2B MnZn	1.10E+04	3.63
BEAS-2B AsCuMnZn	6.63E+03	6.03
Meconium Sample 1	4.31E+03	9.29
Meconium Sample 2	6.05E+03	6.61
Meconium Sample 3	6.10E+03	6.56
Meconium Sample 7	7.15E+03	5.59
Meconium Sample 8	6.75E+03	5.93
Meconium Sample 9	1.62E+04	2.47
Meconium Sample 10	1.51E+04	2.66
Meconium Sample 11	1.26E+04	3.19
Meconium Sample 12	6.47E+03	6.19
Meconium Sample 13	6.16E+03	6.49
Meconium Sample 14	5.43E+03	7.36
Meconium Sample 15	1.27E+04	3.16
Meconium Sample 16	1.34E+04	2.98

12. Appendix C: Raw Data Used to Generate Metal Box Plots

Table XII: Raw Arsenic Data Used to Generate Box Plot

Total Dust (mg/kg) ±0.01	Stomach Dust (mg/kg) ±0.01	Intestinal Dust (mg/kg) ±0.01	Total Soil (mg/kg) ±0.01	Stomach Soil (mg/kg) ±0.01	Intestinal Soil (mg/kg) ±0.01
20.00	2.83	8.42	42.00	4.54	28.67
16.97	2.03	3.52	26.92	0.96	19.79
11.49	1.77	2.75	50.45	2.08	41.18
66.30	6.91	23.80	33.86	5.53	18.28
11.49	1.64	4.85	24.45	2.79	14.06
17.45	2.74	8.23	41.33	5.81	32.59
8.98	1.61	4.21	41.96	3.57	30.98
17.48	2.10	5.01	52.40	6.48	41.04

Table XIII: Raw Cadmium Data Used to Generate Box Plot

Total Dust (mg/kg) ±0.01	Stomach Dust (mg/kg) ±0.01	Intestinal Dust (mg/kg) ±0.01	Total Soil (mg/kg) ±0.01	Stomach Soil (mg/kg) ±0.01	Intestinal Soil (mg/kg) ±0.01
2.99	1.21	0.16	2.49	1.46	0.23
BDL	0.59	0.12	3.50	0.81	0.32
BDL	0.77	BDL	2.50	1.16	0.50
BDL	0.33	BDL	2.99	0.86	0.12
BDL	0.58	BDL	3.49	1.88	0.51
BDL	0.80	BDL	2.49	1.72	0.59
BDL	0.02	BDL	BDL	0.83	0.38
BDL	1.00	BDL	BDL	1.61	0.47

Table XIV: Raw Copper Data Used to Generate Box Plot

Total Dust (mg/kg) ±0.01	Stomach Dust (mg/kg) ±0.01	Intestinal Dust (mg/kg) ±0.01	Total Soil (mg/kg) ±0.01	Stomach Soil (mg/kg) ±0.01	Intestinal Soil (mg/kg) ±0.01
736.00	24.81	11.77	793.00	100.33	180.63
1247.01	29.27	2.42	618.15	22.01	83.44
382.12	26.71	2.39	642.36	35.40	139.54
1172.48	46.23	9.57	868.53	53.63	24.59
686.81	29.29	1.19	681.14	24.49	118.08
561.81	42.99	6.83	589.14	17.26	135.09
408.18	5.22	3.38	470.03	20.72	102.50
690.81	29.64	5.37	655.19	66.73	137.11

Table XV: Raw Manganese Data Used to Generate Box Plot

Total Dust (mg/kg) ±0.01	Stomach Dust (mg/kg) ±0.01	Intestinal Dust (mg/kg) ±0.01	Total Soil (mg/kg) ±0.01	Stomach Soil (mg/kg) ±0.01	Intestinal Soil (mg/kg) ±0.01
410.00	48.52	5.83	688.50	98.88	155.23
451.60	31.20	11.04	739.78	72.46	129.51
236.26	35.08	18.49	687.81	89.24	176.32
293.62	19.38	6.72	412.35	51.46	5.42
441.56	22.23	3.90	733.03	213.39	228.39
366.40	40.04	13.71	1025.90	212.24	194.92
169.16	0.92	43.35	562.44	92.24	125.38
318.68	28.99	5.13	661.68	65.19	289.50

Table XVI: Raw Lead Data Used to Generate Box Plot

Total Dust (mg/kg) ±0.01	Stomach Dust (mg/kg) ±0.01	Intestinal Dust (mg/kg) ±0.01	Total Soil (mg/kg) ±0.01	Stomach Soil (mg/kg) ±0.01	Intestinal Soil (mg/kg) ±0.01
99.50	8.20	3.24	158.00	8.18	4.81
105.29	0.03	0.41	156.53	2.89	5.68
60.44	5.10	0.80	252.25	4.58	24.23
259.22	19.18	6.25	121.02	2.42	3.50
74.93	6.97	0.93	170.66	6.30	11.55
85.74	9.74	2.86	320.22	8.62	15.07
31.44	0.40	1.49	106.89	2.19	20.58
108.89	6.27	1.96	823.35	51.69	ADL

Table XVII: Raw Zinc Data Used to Generate Box Plot

Total Dust (mg/kg) ±0.01	Stomach Dust (mg/kg) ±0.01	Intestinal Dust (mg/kg) ±0.01	Total Soil (mg/kg) ±0.01	Stomach Soil (mg/kg) ±0.01	Intestinal Soil (mg/kg) ±0.01
582.00	240.80	20.46	609.00	187.71	35.95
1064.37	334.69	9.85	477.57	52.58	23.03
678.82	337.83	9.91	971.03	222.88	91.74
894.82	263.06	16.51	379.48	42.30	5.36
746.25	217.42	16.97	700.60	227.34	51.93
644.57	282.83	18.96	560.76	215.03	26.39
466.07	10.22	24.21	375.12	116.66	30.91
1029.47	444.02	12.12	780.94	214.65	201.85

13. Appendix D: Average Stomach and Intestinal Digest Metal Concentrations

Table XVIII: Average Stomach Digest Concentrations

Metal	Average Dust Concentration (mg/kg) ±0.01	Average Dust Bioavailability	Average Soil Concentration (mg/kg) ±0.01	Average Soil Bioavailability
Arsenic	2.30	12.14%	3.70	9.63%
Cadmium	0.58	19.85%	1.10	42.54%
Copper	26.00	3.73%	41.00	5.62%
Molybdenum	0.96	---	0.24	---
Manganese	89.00	25.09%	97.00	13.74%
Lead	6.20	5.64%	9.10	2.84%
Zinc	229.00	29.60%	142.00	23.09%

Table XIX: Average Intestinal Digest Concentrations

Metal	Average Dust Concentration (mg/kg) ±0.01	Average Dust Bioavailability	Average Soil Concentration (mg/kg) ±0.01	Average Soil Bioavailability
Arsenic	7.42	38.35%	27.79	71.23%
Cadmium	0.14	BDL	0.41	16.61%
Copper	4.95	0.72%	116.23	17.24%
Molybdenum	2.94	---	8.08	---
Manganese	34.10	12.35%	166.87	24.03%
Lead	2.33	2.26%	11.17	6.82%
Zinc	18.86	2.89%	55.76	8.38%

14. Appendix E: Normalized Western Blot Protein Data

Table XX: As Exposure Normalized Densitometric AS3MT Values in HEK293 Cells

Adj. Volume (Int)	Norm. Factor	Norm. Vol. (Int)	Sample Identification	Percent Expression
2299760	0.339357	780440	Vinculin Control	----
491160	0.339357	166678	AsCuMnZn	37%
700920	1.113451	780440	Vinculin Control	----
150280	1.113451	167329	AsZn	37%
2867000	0.272215	780440	Vinculin Control	----
1027960	0.272215	279825	AsMn	62%
5102200	0.152961	780439	Vinculin Control	----
2937360	0.152961	449302	AsCu	100%
1302320	0.599269	780440	Vinculin Control	----
606960	0.599269	363732	As	81%
780440	1	780440	Vinculin Control	----
449600	1	449600	Control	100%

Table XXI: As Exposure Normalized Densitometric AS3MT Values in BEAS-2B Cells

Adj. Volume (Int)	Norm. Factor	Norm. Vol. (Int)	Sample Identification	Percent Expression
3609872	1.601362	5780712	Vinculin Control	----
421792	1.601362	675441	AsCuMnZn	53%
900060	6.422585	5780712	Vinculin Control	----
152880	6.422585	981884	AsZn	77%
3524724	1.640047	5780712	Vinculin Control	----
896644	1.640047	1470538	AsMn	116%
1278144	4.522739	5780712	Vinculin Control	----
465080	4.522739	2103435	AsCu	166%
7812224	0.739957	5780712	Vinculin Control	----
1504496	0.739957	1113262	As	88%
5780712	1	5780712	Vinculin Control	----
1268232	1	1268232	Control	100%

Table XXII: Cu Exposure Normalized Densitometric CTR1 Values in HEK293 Cells

Adj. Volume (Int)	Norm. Factor	Norm. Vol. (Int)	Sample Identification	Percent Expression
3127460	0.419457	1311835	Vinculin Control	----
1064560	0.419457	446537	AsCuMnZn	41%
5745915	0.228307	1311835	Vinculin Control	----
1496950	0.228307	341764	CuZn	65%
2747780	0.259251	712365	Vinculin Control	----
566195	0.259251	146786	CuMn	31%
3284855	0.179498	589625	Vinculin Control	----
1146950	0.179498	205875	AsCu	54%
1232875	1.064045	1311834	Vinculin Control	----
1763580	1.064045	1876529	Cu	172%
1311835	1	1311835	Vinculin Control	----
1091160	1	1091160	Control	100%

Table XXIII: Cu Exposure Normalized Densitometric CTR1 Values in BEAS-2B Cells

Adj. Volume (Int)	Norm. Factor	Norm. Vol. (Int)	Sample Identification	Percent Expression
386645	1	386645	Vinculin Control	----
1573005	1	1573005	Control	100%
850395	0.454665	386645	Vinculin Control	----
3841810	0.454665	1746737	Cu	111%
322070	1.2005	386644	Vinculin Control	----
1547245	1.2005	1857467	CuAs	118%
929145	0.41613	386645	Vinculin Control	----
2790620	0.41613	1161260	CuMn	74%
368165	1.050195	386645	Vinculin Control	----
1203125	1.050195	1263515	CuZn	80%
478205	0.808534	386645	Vinculin Control	----
1643950	0.808534	1329189	AsCuMnZn	84%

15. Appendix F: Tumor Necrosis Factor ELISA Data

Table XXIV: HEK293 TNF- α ELISA Concentration Data

Sample ID	Avg. Absorbance	pg/mL Sample	ng/mL Sample	normalized
Control	0.0885	343.75	0.34	100%
As	0.0923	640.63	0.64	186%
Cu	0.0945	808.59	0.81	235%
Mn	0.0947	828.13	0.83	241%
Zn	0.1704	6742.19	6.74	1961%
AsCu	0.1121	2187.50	2.19	636%
AsMn	0.0820	---	---	---
AsZn	0.0845	31.25	0.03	9%
CuMn	0.0855	109.38	0.11	32%
CuZn	0.0942	789.06	0.79	230%
MnZn	0.0978	1070.31	1.07	311%
AsCuMnZn	0.1009	1312.50	1.31	382%

Table XXV: BEAS-2B TNF- α ELISA Concentration Data

Sample ID	Avg. Absorbance	pg/mL Sample	ng/mL Sample	normalized
Control	0.1210	2882.81	2.88	100%
As	0.1721	6875.00	6.88	238%
Cu	0.1375	4167.97	4.17	145%
Mn	0.0889	375.00	0.38	13%
Zn	0.0966	976.56	0.98	34%
AsCu	0.0998	1226.56	1.23	43%
AsMn	0.0951	859.38	0.86	30%
AsZn	0.1099	2011.72	2.01	70%
CuMn	0.2489	12871.09	12.87	446%
CuZn	0.1506	5195.31	5.20	180%
MnZn	0.0888	367.19	0.37	13%
AsCuMnZn	0.0821	---	---	---

Table XXVI: Meconium TNF- α ELISA Concentration Data

Sample ID	Avg. Absorbance	Protein Content	pg/mL Sample
1	0.1434	9.2578	92.58
2	0.0885	0.6875	6.88
3	0.0771	---	---
7	0.0791	---	---
8	0.0851	0.1563	1.56
9	0.0846	0.0781	0.78
10	0.0875	0.5313	5.31
11	0.1060	3.4219	34.22
12	0.0940	1.5469	15.47
13	0.0850	0.1406	1.41
14	0.1040	3.1094	31.09
15	0.1108	4.1719	41.72
16	0.1145	4.7500	47.5

16. Appendix G: Interleukin 6 ELISA Data

Table XXVII: HEK293 IL6 ELISA Concentration Data


Sample ID	Avg. Absorbance	pg/mL Sample	ng/mL Sample	normalized
Control	0.1210	2882.81	2.88	100%
As	0.1721	6875.00	6.88	238%
Cu	0.1375	4167.97	4.17	145%
Mn	0.0889	375.00	0.38	13%
Zn	0.0966	976.56	0.98	34%
AsCu	0.0998	1226.56	1.23	43%
AsMn	0.0951	859.38	0.86	30%
AsZn	0.1099	2011.72	2.01	70%
CuMn	0.2489	12871.09	12.87	446%
CuZn	0.1506	5195.31	5.20	180%
MnZn	0.0888	367.19	0.37	13%
AsCuMnZn	0.0821	---	---	---

Table XXVIII: BEAS-2B IL6 ELISA Concentration Data

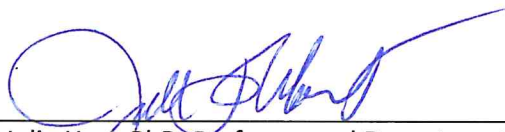
Sample ID	Avg. Absorbance	pg/mL Sample	ng/mL Sample	normalized
Control	0.1473	5635.084	5.64	100%
As	0.1483	5756.530	5.76	102%
Cu	0.1424	5040.000	5.04	89%
Mn	0.1409	4851.759	4.85	86%
Zn	0.1581	6940.627	6.94	123%
AsCu	0.1717	8602.410	8.60	153%
AsMn	0.1731	8768.386	8.77	156%
AsZn	0.1671	8033.639	8.03	143%
CuMn	0.1717	8598.361	8.60	153%
CuZn	0.1568	6782.747	6.78	120%
MnZn	0.1651	7790.747	7.79	138%
AsCuMnZn	0.1578	6910.265	6.91	123%

SIGNATURE PAGE

This is to certify that the thesis prepared by Student Name entitled "Protein Expression in Mammalian Cell Lines after Low-Level Metal Exposure" has been examined and approved for acceptance by the Department of Chemistry and Geochemistry and Department of Industrial Hygiene, Montana Technological University, on this 7th day of May, 2021.



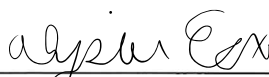
Katie Hailer, PhD, Professor and Department Head
Department of Chemistry and Geochemistry
Chair, Examination Committee



Julie Hart, PhD, Professor and Department Head
Department of Safety, Health and Industrial Hygiene
Member, Examination Committee



Karen Wesenberg, PhD, Instructor III
Department of Chemistry and Geochemistry
Member, Examination Committee



Alysia Cox, PhD, Associate Professor
Department of Chemistry and Geochemistry
Member, Examination Committee